THE CLEVELAND MUSEUM OF NATURAL HISTORY NUMBER 58

KIRTLANDIA®

MARCH 2013

KIRTLANDIA

The Scientific Publication of The Cleveland Museum of Natural History

Michael J. Ryan, Editor

Proofreader: Joseph T. Hannibal

Editorial Assistant: Wendy Wasman

Brief History and Purpose

Kirtlandia, a publication of The Cleveland Museum of Natural History, is named in honor of Jared Potter Kirtland, a noted nineteenth-century naturalist who lived in the Cleveland, Ohio area. It began publication in 1967 and is a continuation of the earlier series *Scientific Publications* volumes 1 to 10 (1928–1950), and new series volumes 1 to 4 (1962–1965).

Supported by the Kirtlandia Society of The Cleveland Museum of Natural History, *Kirtlandia* is devoted to the publication of scientific papers in the various fields of inquiry within the Museum's sphere of interest: Cultural and Physical Anthropology; Archaeology; Botany; Geology; Ornithology; Paleobotany; Invertebrate and Vertebrate Paleontology; Systematics; Ecology; and Invertebrate and Vertebrate Zoology. Issues will vary from single monographs to collections of short papers, review articles, and brief research notes.

Kirtlandia is abstracted in *Biological Abstracts* and indexed in *GeoRef* and *Zoological Record*. An index to *Kirtlandia* numbers 1–52 was published in *Kirtlandia* number 52 (2001).

Kirtlandia No. 58
ISSN 0075-6245

Cover: *Cladoselache* specimen, CMNH 5408, from the Cleveland Member. Specimen is about 62 cm long.

Copies of *Kirtlandia*, and many issues of the *Scientific Publications* series of
The Cleveland Museum of Natural History, are available for sale.
Write to: Library, The Cleveland Museum of Natural History, 1 Wade Oval Drive,
University Circle, Cleveland, Ohio 44106-1767 (library@cmnh.org) for a current price list.

KIRTLANDIA
The Cleveland Museum of Natural History

March 2013 *Number 58:1–4*

A NEW SPECIMEN OF *PORTHOCHELYS* (TESTUDINES: CHELONIOIDEA) FROM THE LATE CRETACEOUS NIOBRARA FORMATION OF KANSAS

MICHAEL DENSMORE
Department of Developmental Biology
Harvard School of Dental Medicine, 188 Longwood Avenue
Boston Massachusetts 02115
Michael_Densmore@hsdm.harvard.edu

AND **DONALD B. BRINKMAN***
Royal Tyrrell Museum of Palaeontology, Box 7500, Drumheller
Alberta, T0J 0Y0, Canada
don.brinkman@gov.ab.ca

ABSTRACT

The second known specimen, a lower jaw, of the cheloniid turtle *Porthochelys* sp. from the Niobrara Formation of Kansas is described. It is similar to *Porthochelys laticeps* and different from all other cheloniids in the Niobrara Formation in having widely angled dentaries with a blunt anterior end and a comparatively deep profile in lateral view. However, it differs from *Porthochelys laticeps* in having a convex triturating surface that is uniformly wide from the symphysis to the coronoid, and a ventral shelf at the symphysis that is barely exposed in dorsal view. These differences suggest that a second species of *Porthochelys* was present in the Niobrara Formation.

Introduction

Porthochelys Williston 1901, a marine turtle from the Niobrara Formation represented by a single specimen, is one of the most enigmatic Late Cretaceous chelonioids. We describe a second specimen of *Porthochelys*, a lower jaw (MCZ 4104). The mandible is comprised of nearly complete dentaries that were collected in the mid to late 1870s by B. F. Mudge in the Niobrara Formation (Late Cretaceous) in Wallace County, KS. It was donated in 1879 to the Boston Society of Natural History (now the Boston Museum of Science) and catalogued as BSNH 10956. It was later transferred to the Harvard Museum of Comparative Zoology where it was catalogued as *Porthochelys laticeps* Williston 1901. Although this specimen can be included in the genus *Porthochelys* on the basis of several characters shared with the type specimen, differences are present that suggest that MCZ 4104 is specifically distinct. The purpose of this paper is to describe MCZ 4104 and compare it with other cheloniids from the Niobrara Formation. Although taxonomically significant features are present that distinguish it from *Porthochelys laticeps* we refrain from erecting a new species for it pending the discovery of new material that can be placed in stratigraphic position within the formation.

Material Examined

For the purposes of describing MCZ 4104, comparison was made with the following specimens: *Toxochelys latiremis*: MCZ 1046, FMNH PF 124, FMNH UR 3, FMNH UR 96; *Toxochelys browni*: UCMP 45199, UCMP 45200, FMNH PR 648, FMNH PR 659, SDSM 482, SDSM 4614, SDSM 54348, SDSM 56190, USMN 13252, USNM 18279; *Ctenochelys procax*: FMNH UC 614; *Ctenochelys acris*: FMNH PR 97, FMNH PR 444, FMNH PR 1047; *Ctenochelys temista*: FMNH 27339, FMNH PR 1047; *Ctenochelys* sp.: FMNH P 27337, FMNH UC 614, AMNH 6137; *Prionochelys galeotergum*: UCMP 34533.

Institutional Abbreviations

AMNH, American Museum of Natural History, New York, NY; **BSNH**, Boston Society of Natural History (now Boston Museum of Science), Boston, MA; **KUVP**, University of Kansas, Museum of Vertebrate Paleontology, Lawrence, KS; **MCZ**, Harvard Museum of Comparative Zoology, Cambridge, MA

Systematic Paleontology

Order TESTUDINES Batsch, 1788
Suborder CRYPTODIRA Cope, 1868
Superfamily CHELONOIOIDEA Baur, 1893
Family CHELONIIDAE Bonaparte, 1832
Genus *Porthochelys* Williston, 1901

Type species
Porthochelys laticeps Williston, 1901.

*Corresponding author

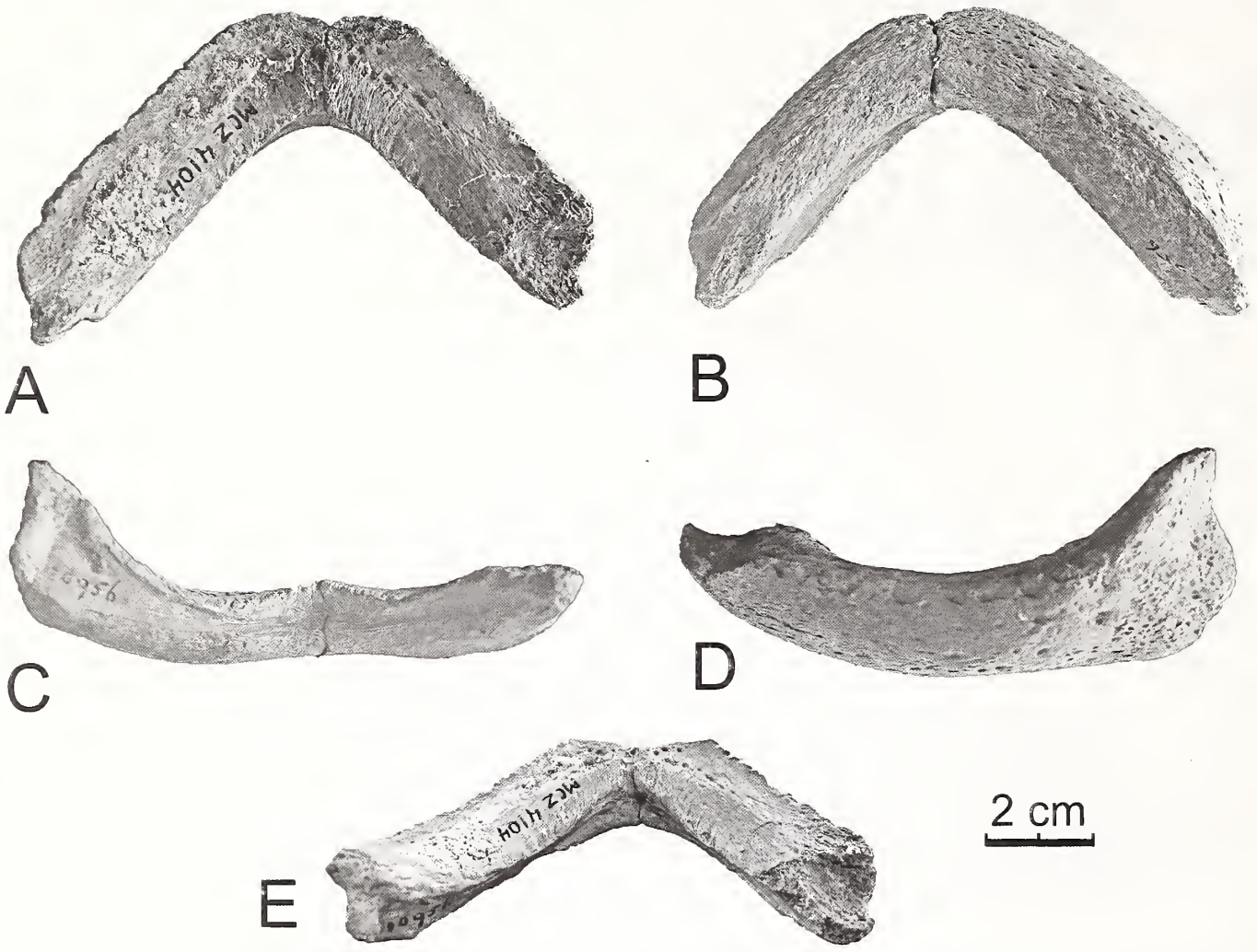

Figure 1. Dentaries of *Porthochelys* sp., MCZ 4104. A, dorsal, B, ventral, C, posterior, D, left lateral view with anterior to the left, and E, dorsoposterior view showing the convex triturating surface and the labial ridge.

Comments

The phylogenetic position of *Porthochelys* has not yet been tested with a cladistics analysis. It is included in the Chelonioidea here because the plastron of *Porthochelys laticeps*, as described by Williston (1901), is chelonioid-like in features that were used by Parham (2005) to distinguish between "macrobaenids" and chelonioids (e.g., the reduced articulation with the bridge and the weak articulation between opposite hyo- and hypoplastron at the midline). As well, the carapace is similar to *Toxochelys* in being circular. However, the phylogenetic position of *Toxochelys* is not resolved. Hirayama (1994) includes *Toxochelys* in the Cheloniidae, while Kear and Lee (2005) conclude that it is basal to the split between cheloniids and protostegids. Pending further study, we include both *Toxochelys* and *Porthochelys* within the Cheloniidae because their plastron is generally similar to that of *Ctenochelys* and different from the plastron of protostegids in that the bridge is narrower and the mid-ventral plastral fenestrae are smaller.

Porthochelys sp.
Figure 1

Referred material

MCZ 4101, anterior portion of mandible consisting of both nearly complete dentaries.

Distribution

Smoky Hill Chalk, Niobrara Formation, upper Coniacian to Lower Campanian. According to the original records, MCZ 4104 was collected in Wallace County in the mid to late 1870s. However, Wallace County was split into two counties, Wallace and St. John counties in 1881, and St. John County was changed to Logan County in 1885 (Elias, 1931). The Smoky Hill Chalk exposures are primarily in what is now Logan County and most of the fossils collected by Mudge and others were likely from these exposures (Bennett, 2000). However, since the exact locality of the specimen is unknown and the Smoky Hill Chalk was deposited over an approximately five million year period, uncertainty regarding the age of the specimen remains.

Description

MCZ 4104 consists of both dentaries (Fig. 1). Both are missing a small portion of the anterior tips, and the posterior portion of the right dentary is also missing. The dentaries are robust, blunt, and broad, forming an angle of approximately 90°. The overall length of the conjoined dentaries measured along the midline is 6 cm. The length of the left dentary measured along its long axis is 7 cm. The width between the ends of the dentaries is 10.5 cm.

Table 1. Comparison of dentaries from Cheloniidae of the Niobrara Formation.

	Porthochelys laticeps	*MCZ 4104*	*Toxochelys latiremis*	*Ctenochelys stenopora*	*Ctenochelys procax*	*Prionochelys galeotergum*
Size	Large, robust	Large, robust	Large, gracile	Large, gracile	Large, gracile	Large, gracile
Rami angle	Wide (90°)	Wide (90°)	Narrow (60°)	Narrow (60°)	Narrow (60°)	Narrow (60°)
Coronoid contact	Rises sharply	Rises sharply	Shallow	Shallow	Shallow	Shallow
Triturating surface width	Wide posteriorly, narrower at symphysis	Uniformly wide	Narrow posteriorly, wider at symphysis	Wide at symphysis, narrowing posteriorly;	Wide at symphysis, narrowing posteriorly	Wide at symphysis, narrowing posteriorly
Tip	Blunt	Blunt	Pointed	Pointed	Pointed	Pointed
Depth	Thick	Thick	Thin	Thin	Thin	Thin
Triturating surface	Flat	Convex	Flat	Flat	Flat	Flat
Symphysial Ridge	Present	Present	Absent	Present	Present	Present
Symphysis: visibility of ventral shelf in dorsal view	Highly visible	Not visible	Visible	Not visible	Not visible	Not visible

Thus, this specimen is slightly larger than *Porthochelys laticeps*, which is 9 cm across the posterior end of the dentary. The symphysis is short and bears a small sagittal ridge. The ventral shelf is barely visible in dorsal view posterior to the triturating surface (Fig. 1A). A low labial ridge is present but a distinct lingual ridge is absent. The triturating surface of the left dentary is partially obscured by adhering matrix, but this surface is fully exposed on the right dentary. The surface is relatively narrow with a uniform width of 2 cm for most of its length. The triturating surface is unusual for chelononiids in being convex as a result of the presence of a wide ridge extending from the symphysis along the center of the triturating surface to the point where the dentary rises to meet the coronoid (Fig. 1E).

In medial view, the *sulcus cartilaginis meckeli* is deep and narrow anteriorly, becoming broader and shallower posteriorly. The ventral surfaces are convex. The lateral side is ornamented with small foramina that extend almost to the posterior margin, suggesting the dentary was almost entirely covered by a beak.

Discussion

In the latest review of turtles of the Niobrara Formation (Zangerl, 1953), seven non-protostegid chelonioids are recognized in the formation: *Porthochelys laticeps*, *Toxochelys latiremis* Cope, 1873, *Ctenochelys stenopora* (Hay, 1905), *Ctenochelys procax* (Hay, 1905), and *Prionochelys galeotergum* Zangerl, 1953, *Lophochelys natatrix* Zangerl, 1953, and *Cynocerus incisivus* Cope 1872. The validity of *Lophochelys* was questioned by Hirayama (1997), who suggested that it was a grouping of juveniles of other taxa. In an earlier paper, Hirayama (1994) includes the holotype specimen of *Lophochelys natatrix* in a list of specimens of *Ctenochelys stenopora*. We follow Hirayama (1994, 1997) in considering *Lophochelys natatrix* to be a juvenile individual of *Ctenochelys stenopora*. *Cynocerus incisivus* Cope 1872, which is only represented by caudal vertebrae, is considered a *nomen vanum* since cheloniids cannot be distinguished on the basis of caudal vertebrae. All of the five cheloniids from the Niobrara Formation are represented by dentaries.

Differenees between the dentary of the cheloniids present in the Niobrara Formation and that of MCZ 4104 are listed in Table 1. MCZ 4104 is referred to *Porthochelys* because it shares three characters with *Porthochelys laticeps* that distinguish them from all other members of the Cheloniidae in the Niobrara Formation (Fig. 2, Table 1). One of these is the shape of the jaw as seen in dorsal view. The rami of the lower jaw are widely angled, the anterior end of the jaw is blunt, and the dentary has a comparatively deep profile in lateral view. In the mandibles of *Toxochelys*, *Ctenochelys*, and *Prionochelys* the angle formed by the dentaries is only 60° while in MCZ 1046 and the type specimen it is nearly 90°. Secondly, MCZ 4104 and the type specimen of *Porthochelys* also differ from *Toxochelys*, *Ctenochelys*, and *Prionochelys* in that the triturating surface rises sharply at the posterior end of the dentary towards the coronoid. The third feature distinguishing MCZ 4104 from the remaining cheloniids is the shape of the triturating surface. The triturating surface of MCZ 4104 and the type specimen of *Porthochelys* are similar to that of *Ctenochelys* and *Prionochelys* and different from *Toxochelys latiremis* in being relatively broad, and differ from *Ctenochelys* and *Prionochelys* in that the surfaces are wide posteriorly. In *Ctenochelys* and *Prionochelys* the triturating surface narrows posteriorly.

Specimen MCZ 4104 differs from the type specimen of *Porthochelys laticeps* in three characters that are of potential taxonomic significance. Firstly, the presence of a convex triturating surface. In *Porthochelys laticeps*, this surface is distinctly concave (Williston, 1901), the typical condition for basal cheloniids. Secondly, the triturating surface in MCZ 4104 is uniformly wide from the symphysis to the coronoid contact, but is relatively narrower at the symphysis than at the coronoid in the type specimen of *P. laticeps*. Thirdly, the structure of the symphysis as seen in dorsal view; in MCZ 4104 the ventral shelf is barely visible in dorsal view but it is prominently exposed in *P. laticeps*. Although the three described differences may represent autapomorphies that could support a new taxon, we refrain from erecting a species at this time, and thus refer the dentary to *Porthochelys* sp.

With the recognition of a second species of *Porthochelys* the number of cheloniids present in the Niobrara Formation is increased to six. However, since the exact locality from which the jaw was collected is not known, the age of the specimen relative to the type specimen of *Porthochelys laticeps* is uncertain. The type specimen of *Porthochelys laticeps* was collected along the Saline River in Trego County, KS, relatively low in the chalk (Late Coniacian). Since the Smoky Hill Member extends from the upper Coniacian to the lower Campanian there may be a considerable difference in the age of the two specimens. Exposures in Logan County, tend to be stratigraphically higher in the formation (Bennett, 2000), so it is likely that *Porthochelys* sp. is younger than *Porthochelys laticeps*. However, additional specimens that can be placed in stratigraphic context are required to firmly establish whether or not these species represent successive species of the

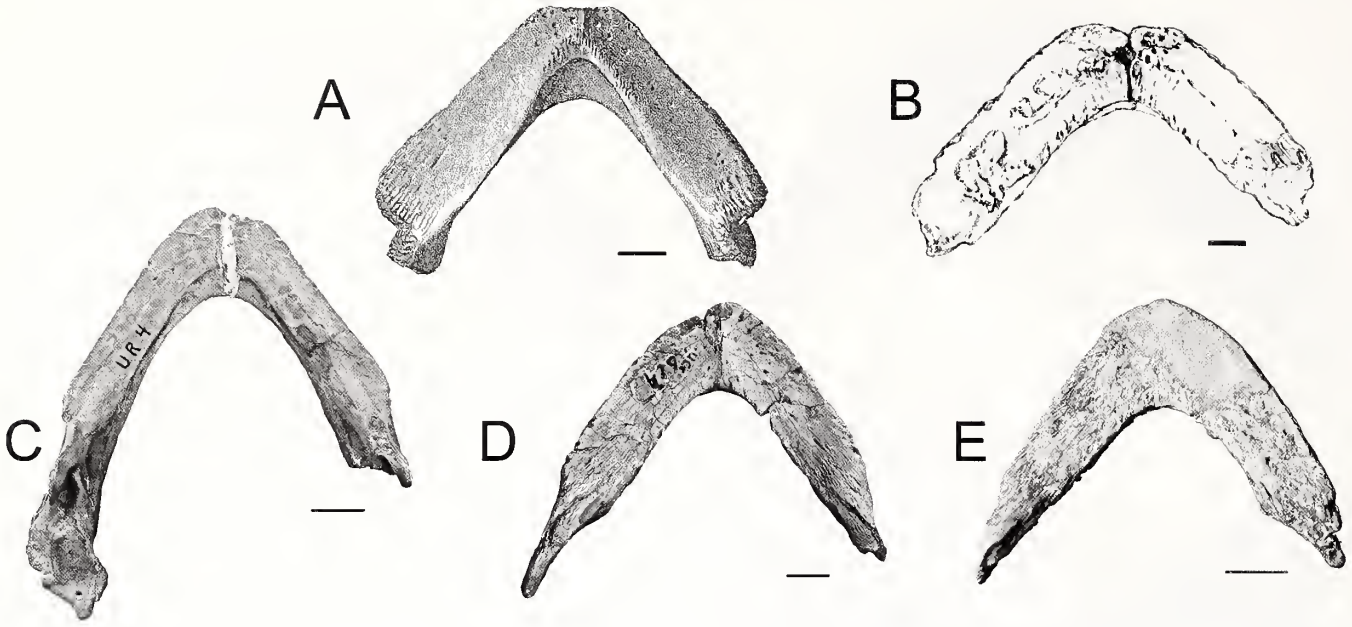

Figure 2. Comparison of specimen MCZ 4104 with dentaries of cheloniids from the Niobrara Formation. A, *Porthochelys laticeps*, type specimen, from Williston (1901). B, *Porthochelys* sp., MCZ 4014, drawing in dorsal view. C, *Toxochelys latiremis*, subadult, FMNH UR 4. D, *Ctenochelys procax*, FMNH UC 614. E, *Prionochelys galeotergum*, UCMP 34533. All in dorsal view. Scale bar equals 1 cm.

genus *Porthochelys* and to determine the stratigraphic range of these species.

Acknowledgments

We thank the late Dr. Farish Jenkins Jr. and the Harvard Museum of Comparative Zoology for access to specimens from their collections. Jennifer Cundiff (MCZ) was very helpful in locating specimens and obtaining permissions. We also thank Barbara Hershey, Rebecca Melius and Emma Dill of the Boston Museum of Science for information from and access to their files from the Boston Society of Natural History. The drawing of MCZ4104 in Figure 2 was produced by Karen Adams. We would also like to thank Andreas Matzke, then at Tubingen University, who provided photographs of many of the cheloniid dentaries used for comparison. Jim Parham and Mike Everhart read earlier versions of this manuscript and made suggestions that led to its improvement. Their efforts are greatly appreciated.

References

Batsch, A. J. G. C. 1788. Versuch einer Anleitung, zur Kennnish und Geschichte der Thiere und Mineralien. Akademische Buchhandlung, Jena. 528.

Baur, G. 1893. Notes on the classification of the Cryptodira. American Naturalist, 27:672–675.

Bennett, S. C. 2000. Inferring stratigraphic position of fossil vertebrates from the Niobrara Chalk of western Kansas. Kansas Geological Survey, Current Research in Earth Sciences, Bulletin 244, part 1. http://www.kgs.ku.edu/Current/2000/bennett/bennett1.html.

Bonaparte, C. L. 1832. Saggio d'una distribuzione metodica degli animali vertrati a sangue freddo. Antonio Boulzalcr, Roma. 86.

Brinkman, D. B., M. Hart, H. Jamniczky, and M. Colbert. 2006. *Nichollsemys baieri gen, et sp. nov*, a primitive chelonioid turtle from the Late Campanian of North America. Paludicola, 5:111–124.

Cope, E. D. 1868. On the origin of genera. Proceedings of the Academy of Natural Sciences, Philadelphia, 20:242–300.

Cope, E. D. 1872. *Cyanocerus incisivus*. Proceedings of the American Philosophical Society, 12:308.

Cope, E. D. 1873. *Toxochelys latiremis*. Proceedings of the Academy of Natural Sciences, Philadelphia, 1873:10.

Elias, M. K. 1931. The geology of Wallace County, Kansas. Kansas Geological Survey, Bulletin 18, 254.

Hay, O. P. 1905. A Revision of the species of the family of the fossil turtles called Toxochelyidae with descriptions of two new species of *Toxochelys* and a new species of *Porthochelys*. Bulletin of the American Museum of Natural History, 21:177–185.

Hirayama, R. 1994. Phylogenetic systematics of chelonioid sea turtles. Island Arc, 3:270–284.

Hirayama, R. 1997. Distribution and diversity of Cretaceous chelonioids, p. 225–241. *In* J. M. Callaway and E. L. Nicholls (eds.), Ancient Marine Reptiles. Academic Press, San Diego, California.

Kear, B. P., and M. L. Lee. 2006. A primitive protostegid from Australia and early sea turtle evolution. Biology Letters, 22:116–119.

Nicholls, E. L. 1988. New material of *Toxochelys latiremis* Cope, and a revision of the genus *Toxochelys* (Testudines, Chelonioidea). Journal of Vertebrate Paleontology, 8:181–187.

Parham, J. F. 2005. A reassessment of the referral of sea turtle skulls to the genus *Osteopygis* (Late Cretaceous, New Jersey, USA). Journal of Vertebrate Paleontology, 25:71–77.

Williston, S. W. 1901. A New Turtle from the Kansas Cretaceous. Kansas Academy of Science, Transactions, 17:195–199, pl. 18–22.

Zangerl, R. 1953. The vertebrate fauna of the Selma Formation of Alabama. Part 4. The turtles of the family Toxochelyidae. Fieldiana, Geology Memoirs, 3:137–277.

KIRTLANDIA
The Cleveland Museum of Natural History

March 2013 *Number 58:5–37*

THE POSTCRANIAL SKELETON OF *STYRACOSAURUS ALBERTENSIS*

ROBERT HOLMES*
Department of Biological Sciences, CW 405 Biological Sciences Building, Edmonton, Alberta T6G 2E9, Canada
holmes1@ualberta.ca

AND **MICHAEL J. RYAN**
Department of Vertebrae Paleontology
Cleveland Museum of Natural History, 1 Wade Oval Drive
University Circle, Cleveland, Ohio 44106, U.S.A.
mryan@cmnh.org

ABSTRACT

Recently discovered material of *Styracosaurus albertensis* (Dinosauria, Ceratopsidae) in combination with the partial holotype skeleton from Dinosaur Provincial Park, Alberta, permits a comprehensive description of the postcranial skeleton of this taxon for the first time. Although this study generally supports the commonly held view that the postcranial skeleton of ceratopsids is structurally conservative, a survey of what is known about the structural diversity in the ceratopsid postcranial skeleton suggests that morphological variation of potential phylogenetic significance exists. This variation includes presacral vertebral counts (both total numbers and distribution amongst the cervical, dorsal, and sacral components of the column), patterns of intervertebral fusion, as well as morphology of the cervical ribs sacrum, pelvis, scapula, and humerus.

Introduction

The holotype skull of the centrosaurine ceratopsid *Styracosaurus albertensis* (CMN 344) was collected in 1913 by C.H. Sternberg and described later the same year (Lambe, 1913), but for reasons explained elsewhere (Holmes et al., 2005), the postcranial skeleton was not collected until 1935. The postcranial skeleton was eventually reunited with the skull as a display mount in the fossil gallery of the National Museum of Natural Sciences (now the Canadian Museum of Nature) in Ottawa, but in the intervening years, it was never described. Contemporary mounting techniques that used a heavy welded supporting steel armature rendered much of the skeleton inaccessible and made a detailed description impractical. However, in 2003, the skeletal mount was disassembled and conserved, providing for the first time unfettered access to its anatomy.

Although the postcranial skeleton of CMN 344 is reasonably well preserved, it is incomplete. The tail is represented by only seven proximal vertebrae. Most of the elements of the epipodials, mani, and pedes were not recovered, and the sacrum, left ilium, and both pubes are missing (Holmes et al., 2005). This is unfortunate, as *Styracosaurus* is relatively rare compared with most other ceratopsids from the Dinosaur Park Formation of southern Alberta. The only other described postcranial skeleton attributed to this genus (*Styracosaurus* "*parksi*," Brown and Schlaikjer, 1937) is associated with a very incomplete skull, and its identity is in question (Ryan et al., 2007). In 1989, a second articulated *Styracosaurus* skeleton (TMP 1989.097.001) was collected from Dinosaur Provincial Park (DPP). Although this individual is slightly smaller than the type and apparently not fully mature, its parietal bears the parietal spikes diagnostic of *Styracosaurus* (Ryan et al., 2007). Many of the preserved elements of the postcranial skeleton, including several presacral vertebrae, ribs, right pectoral girdle and humerus, and right pubis, right ilium, and rear propodials and epipodials overlap with those of the type, thus providing useful corroboration of its identification. It also includes complete ilia, right hind foot, and tail, thus providing much new anatomical information not preserved in the holotype. Between the two specimens, virtually every part of the skeleton except the manus is preserved.

More recently, another partial skeleton (TMP 2009.080.001), that includes most of the skull and a limited number of disarticulated postcranial elements has been collected. This specimen provides anatomical corroboration and a few features not preserved or exposed in the other *Styracosaurus* skeletons.

Institutional Abbreviations

AMNH, American Museum of Natural History; **CMN**, Canadian Museum of Nature (formerly the National Museum

*Corresponding author

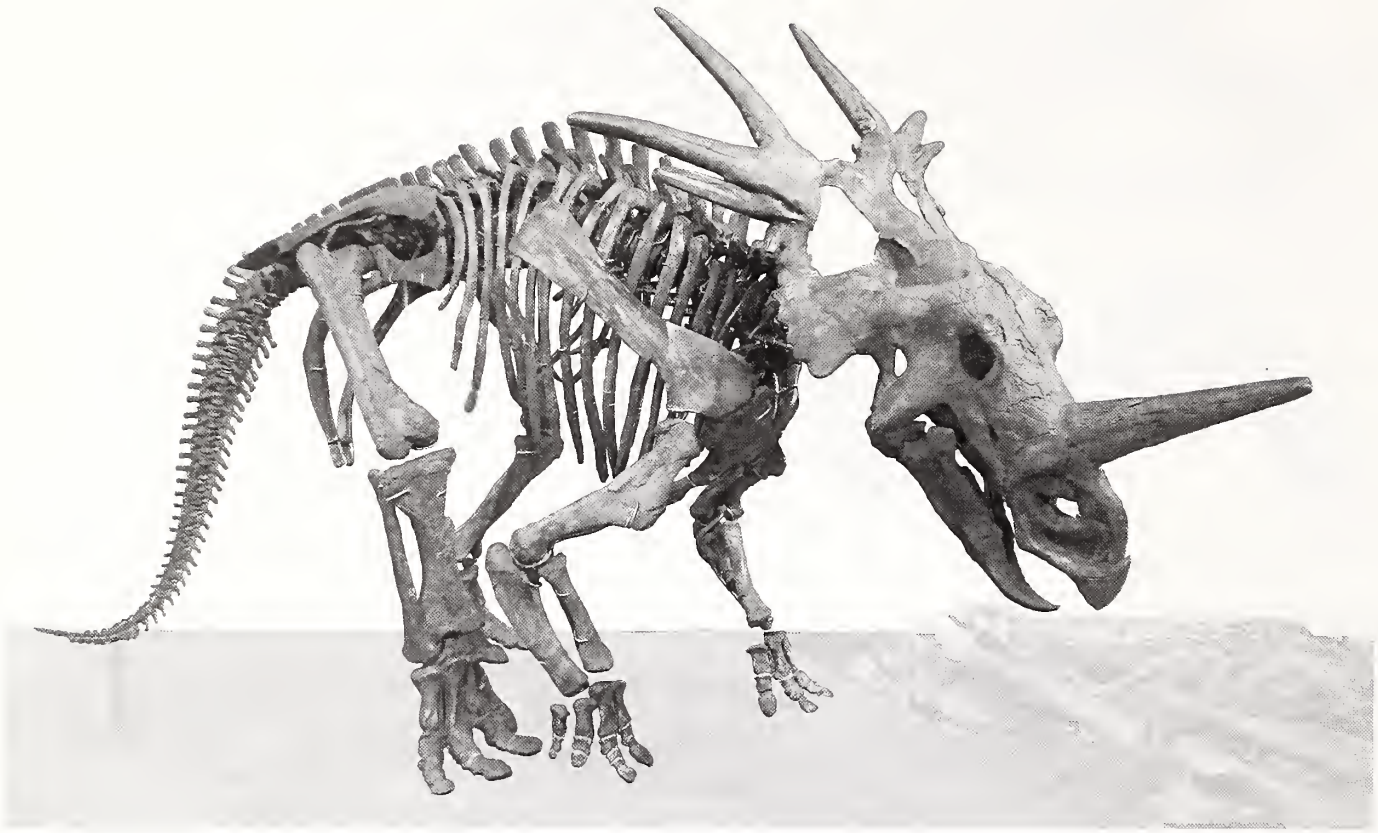

Figure 1. *Styracosaurus albertensis*, CMN 344. Mount of skeleton on exhibit at the Canadian Museum of Nature (Ottawa). Photograph taken February, 2012.

of Canada), Ottawa; **NHMUK**, Natural History Museum, London; **NSM**, National Museum of Nature and Science (formerly National Science Museum), Tokyo; **ROM**, Royal Ontario Museum, Toronto; **TMP**, Tyrrell Museum of Paleontology; **USNM**, United States National Museum, Washington.

Geology

CMN 344 was collected from the southeast quarter of section 1, TP21, R11 (Sternberg, 1950) at the extreme eastern end of what is now DPP. It occurs in the upper Dinosaur Park Formation close to prairie level in this part of the Park (708.9 masl; Currie and

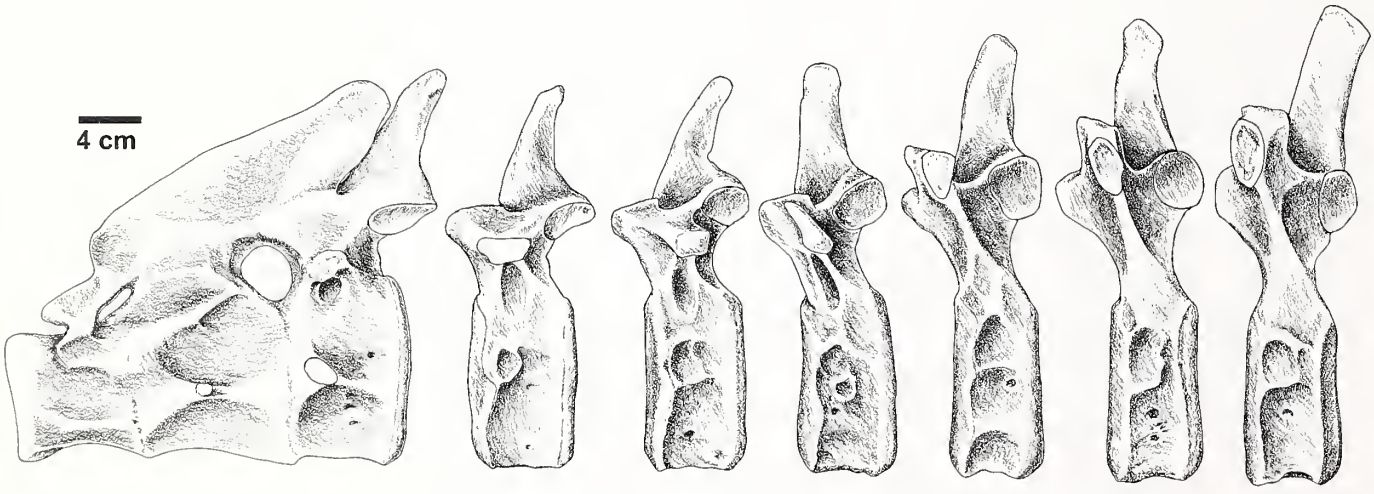

Figure 2. *Styracosaurus albertensis*, CMN 344. Cervical vertebrae (C1–C9) in left lateral view. Scale bar equals 4 cm.

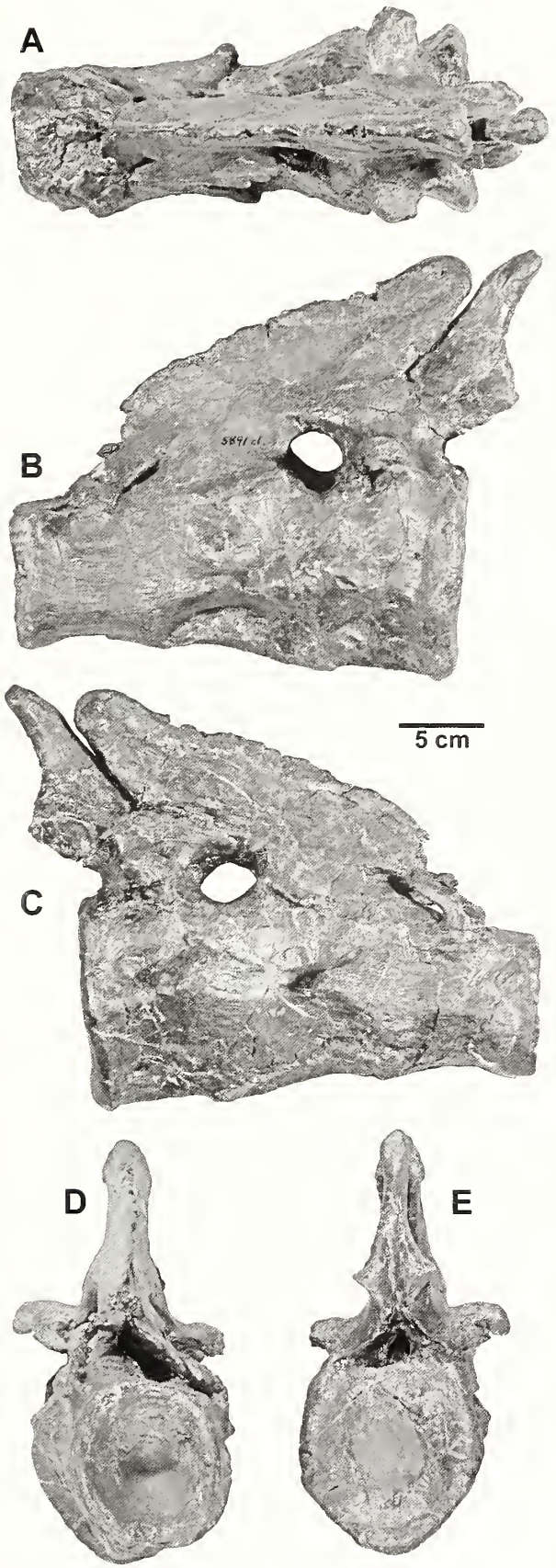

Figure 3. *Styracosaurus albertensis*, CMN 344, syncervical. A, dorsal, B, left lateral, C, right lateral, D, anterior, and E, posterior views. Scale bar equals 5 cm.

Russell, 2005), 43 m above the contact with the Oldman Formation. This places it in Dinosaur Park faunal zone 2, which is characterized by the presence of the centrosaurine ceratopsid *Styracosaurus* and the lambeosaurine *Lambeosaurus* (Ryan and Evans, 2005; Ryan, et al., 2012).

TMP 1989.097.001 was discovered at Sage Creek, near Onefour, southeastern Alberta (12, 545,414 E; 451,340 N [WGS 84]) in sediments of the Dinosaur Park Formation, less than 10 m below the Lethbridge Coal Zone (Ryan et al., 2007).

TMP 2009.080.001 was collected from Dinosaur Provincial Park, UTM 12; 461,295; 5,617,724—NAD83. The elevation was not recorded, but the field notes indicate that it occurred high in section.

Materials and Methods

Specimens examined

CMN 344—Comprises a largely complete skull with partial frill (Ryan et al, 2007), complete presacral vertebral column and partial caudal series, a set of ribs missing only the pair associated with the axis of the syncervical, right scapulocoracoid, left scapula, right sternal plate, both humeri, ulnae, and radii, right metacarpus I, left metacarpus IV, left terminal manual phalanges I and II, right ilium, both ischia, femora, tibiae, left fibula, and left metacarpus II (Figures 1–23; Table 1).

TMP 1989.097.001—Comprises a partial skull (Ryan et al., 2007) and a mostly articulated postcranial skeleton including a partial presacral vertebral column scattered ribs, a complete tail, right scapulocoracoid, a partly exposed left scapulocoracoid, both humeri, a complete pelvis (although the sacrum is not exposed), both femora, right tibia and fibula, and the compete right metatarsus and pes (Figures 24–35; Table 1).

TMP 2009.080.001—Comprises a large, virtually complete skull and associated cervical vertebrae, sacrum, and scapula.

Methods

Although the type postcranial skeleton was collected in 1935, a comprehensive description has been hampered by its use as a display mount at the Victoria Memorial Museum Building in Ottawa. When the old Earth Sciences gallery was dismantled in the early 2000's, this material was rendered accessible to study for the first time. Following disassembly of the display mount, the elements were conserved and made available for study for several months before a new mount was constructed (Figure 1). This made it possible to determine the extent of reconstruction, and eliminated the risk that plaster elements, fabricated to replace missing bones, might be included in the description. Individual elements were photographed from as many perspectives as practical. Many of these images were published in Holmes et al. (2005). As the vertebrae and ribs were particularly prone to distortion, an attempt was made to reconstruct their original shapes. These reconstructions are included in this paper.

Description

Vertebral column

A syncervical, eighteen separate presacral vertebrae, and seven caudal vertebrae are preserved in CMN 344 (Figures 1–16). The incomplete presacral vertebral column of TMP 1989.097.001 comprises a syncervical, five other cervicals, and eight dorsal vertebrae (Figures 24–27). The caudal series of the latter specimen is complete and articulated (Figures 28–30).

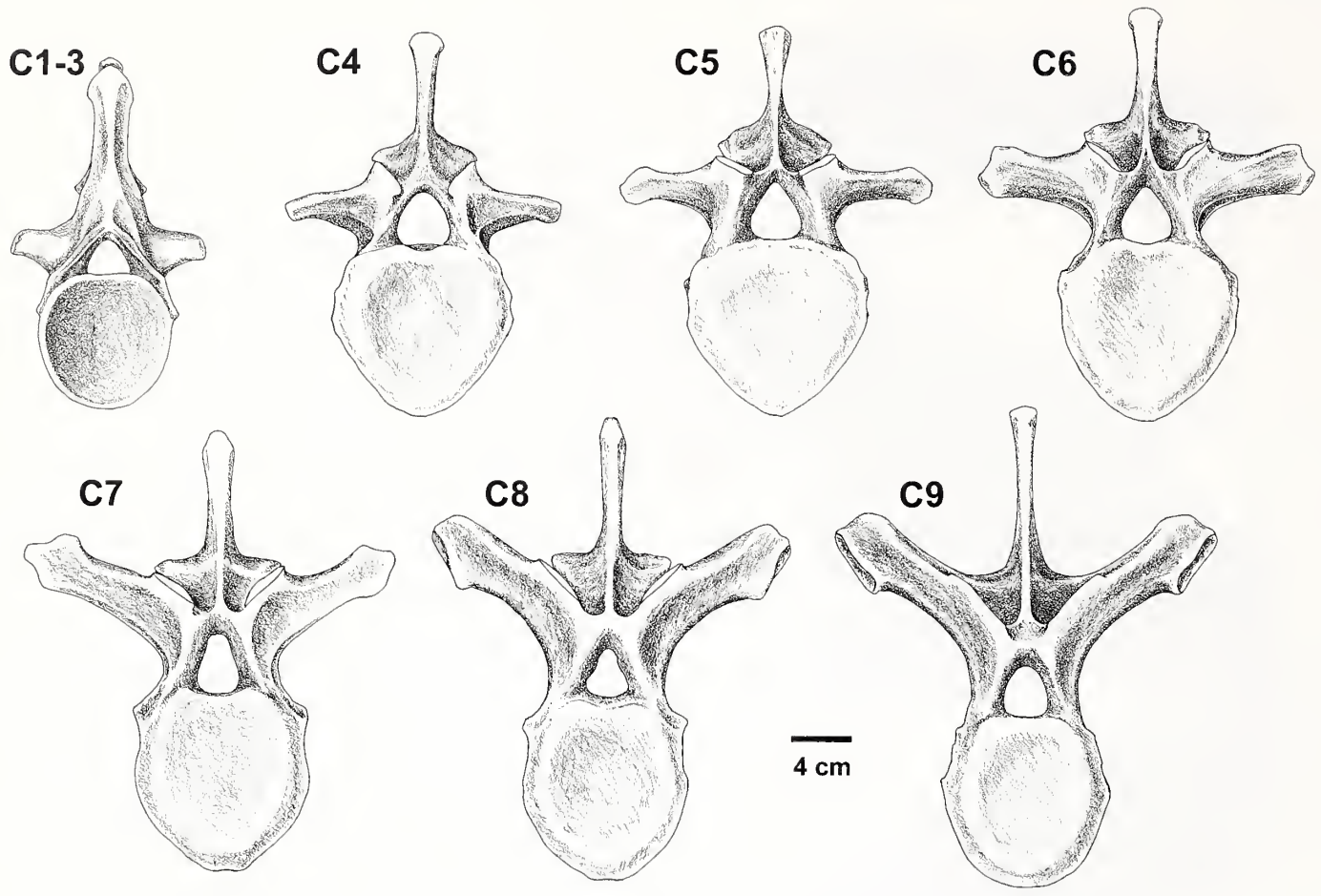

Figure 4. *Styracosaurus albertensis*, CMN 344. Cervical vertebrae (C1–C9) in anterior view. Scale bar equals 4 cm.

The presaeral count of CMN 344 (nine cervical and 12 dorsal vertebrae), which matches that of *Centrosaurus* (Brown, 1917), is considered to be typical for ceratopsids (Dodson et al., 2004). In the original display mount, an additional vertebra, fabricated entirely in plaster, was inserted between the last cervical and first dorsal vertebrae. The reasons for this addition are uncertain, since there is no evidence that any presacral vertebrae are missing. However, C. M. Sternberg, who supervised the mounting of this specimen, may have used a well preserved, articulated postcranial skeleton (CMN 8547), usually attributed to the chasmosaurine *Anchiceratops*, as a guide. This skeleton is unusual in possessing supernumerary presacral vertebrae (Mallon and Holmes, 2010), and it is possible that this misled Sternberg into assuming that at least one presacral vertebra was missing from CMN 344.

As in other ceratopsids, the three anterior cervical vertebrae are co-ossified to form a syncervical (see Campione and Holmes, 2006; Tsuihiji and Makovicky, 2007). The anterior surface of the centrum of the syncervical bears a deep, circular cotyle to receive the occipital condyle. The posterior end of the syncervical bears an essentially flat, heart-shaped facet for articulation with the centrum of the first free cervical vertebra (Figures 2, 4–6). The most anterior (atlantal) neural arch is paired. Each half arises from the dorsal surface of the compound centrum at the midpoint of the first constriction and dorsally fuses indistinguishably with the lateral surface of the second, much more robust (axial) arch. No remnants of zygapophyses persist. There is no evidence of diapophyses or parapophyses to indicate the presence of an atlantal rib. A small, slit-like canal for passage of the spinal nerve separates the bases of these arches. Both the centra and zygapophyses of the second and third segments of the syncervical are co-ossified. Immediately ventral to these zygapophyses, a large circular nerve foramen pierces the bone. Each centrum bears a short parapophyseal process at mid-height. The tapered third neural spine, similar to those on more posterior cervical vertebrae, projects posterodorsally. Immediately ventral to the base of the short transverse process, the lateral wall of the arch of the third syncervical vertebra bears a deep pocket. Although superficially resembling a foramen, it does not pierce the laminar bone surface. A similar feature has been described on cervical vertebrae of *Chasmosaurus* (CMN 2245, NHMUK R4948 [Maidment and Barrett, 2011]) and *Vagaceratops* (CMN 41357, RH, pers. obs., August, 2012), but they apparently do not occur in all individuals, and when they do, the number of vertebrae showing the feature varies, and so their significance is uncertain.

The six vertebrae immediately posterior to the syncervical (Figures 2, 4–6) bear parapophyses on the lateral surfaces of their centra and are therefore considered here to be cervicals (see below). The first free cervical (C4) bears a parapophyseal facet at mid-height on the centrum. This facet becomes progressively more dorsal in position toward the posterior end of the cervical series, and in the last cervical (C9), occupies the anterolateral quadrant of the lateral surface of the centrum. The anterior facets

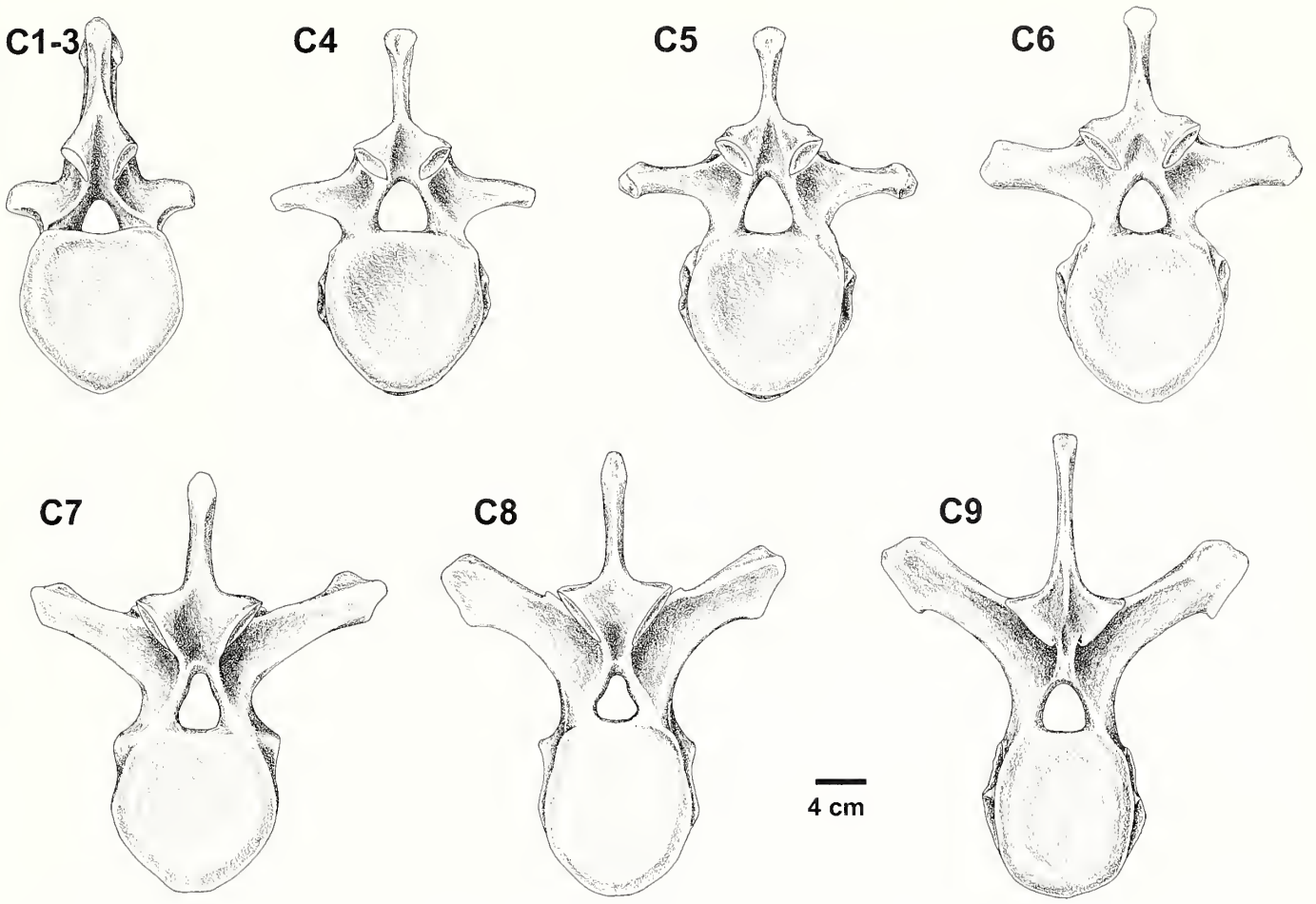

Figure 5. *Styracosaurus albertensis*, CMN 344. Cervical vertebrae (C1–C9) in posterior view. Scale bar equals 4 cm.

of the cervical centra are nearly flat, bearing only a lightly raised rim and very shallow central depression. The posterior facets are slightly more concave, but otherwise similar to the anterior facets. The centra of the more anterior cervicals are distinctly heart-shaped in outline, in contrast to the quasi-circular outline seen in the vertebrae of *Centrosaurus* (Lull, 1933) and *Triceratops* (Ostrom and Wellnhofer, 1986). Although the centra maintain approximately the same height throughout the cervical series, they become anteroposteriorly shorter, a trend also observed in *Centrosaurus* (Brown, 1917) and transversely narrower towards the posterior end of the series, with the anterior surfaces of the eighth and ninth cervicals presenting quasi-circular and dorso-ventrally elongate oval outlines, respectively.

The neural arch pedicels of the last vertebral unit of the syncervical and first three free cervicals (i.e., C4–C6) each bears on its lateral surface a deep circular pit resembling those on the third vertebra of the syncervical. The distinctly triangular neural canals are large in comparison to those of the dorsal vertebrae, indicating that spinal tissue associated with the brachial plexus was accommodated in this part of the column (Giffen, 1995). The prezygapophyses of the first free cervical vertebra (C4) form a relatively steep angle of approximately 45° with the frontal plane, suggesting that axial rotation relative to the syncervical was restricted. However, its postzygapophyses form a much lower angle of about 25° with the frontal plane, matching closely the inclination of the prezygapophyses of the next (second free) cervical. This angle gradually increases toward the posterior end of the cervical region, reaching a maximum of about 50° in the most posterior (ninth) cervical. The articular surfaces of prezygapophyses of the cervical vertebrae are distinctly convex, and match closely with the complementary concave facets on the postzygapophyses. Although this configuration of the articular surfaces would have permitted lateral and dorsoventral flexion, it would have strongly resisted any axial rotation of the neck. In the first free cervical, the transverse processes are directed laterally and slightly ventrally, in contrast to the condition in *Triceratops* cervical vertebrae, in which they are directed dorsolaterally (Hatcher et al., 1907; Ostrom and Wellnhofer, 1986). However, in at least one specimen of *Chasmosaurus*, the orientation matches that of CMN 344 (Maidment and Barrett, 2011). Orientation of the transverse processes of this vertebra has not been described in centrosaurines, but published figures (Brown, 1917: plate xxxvii; Lull, 1933: fig. 8) suggest a lateral or slightly ventrolateral orientation. This process is directed laterally in the second free cervical, slightly dorsally in the third, and gradually attain a dorsolateral orientation in more posterior cervicals, forming an angle of about 40° with the frontal plane in the last (ninth) cervical, much as described for *Chasmosaurus* (Maidment and Barrett, 2011: fig. 17). The diapophyseal surfaces face laterally in the anterior vertebrae, but gradually become reoriented to face

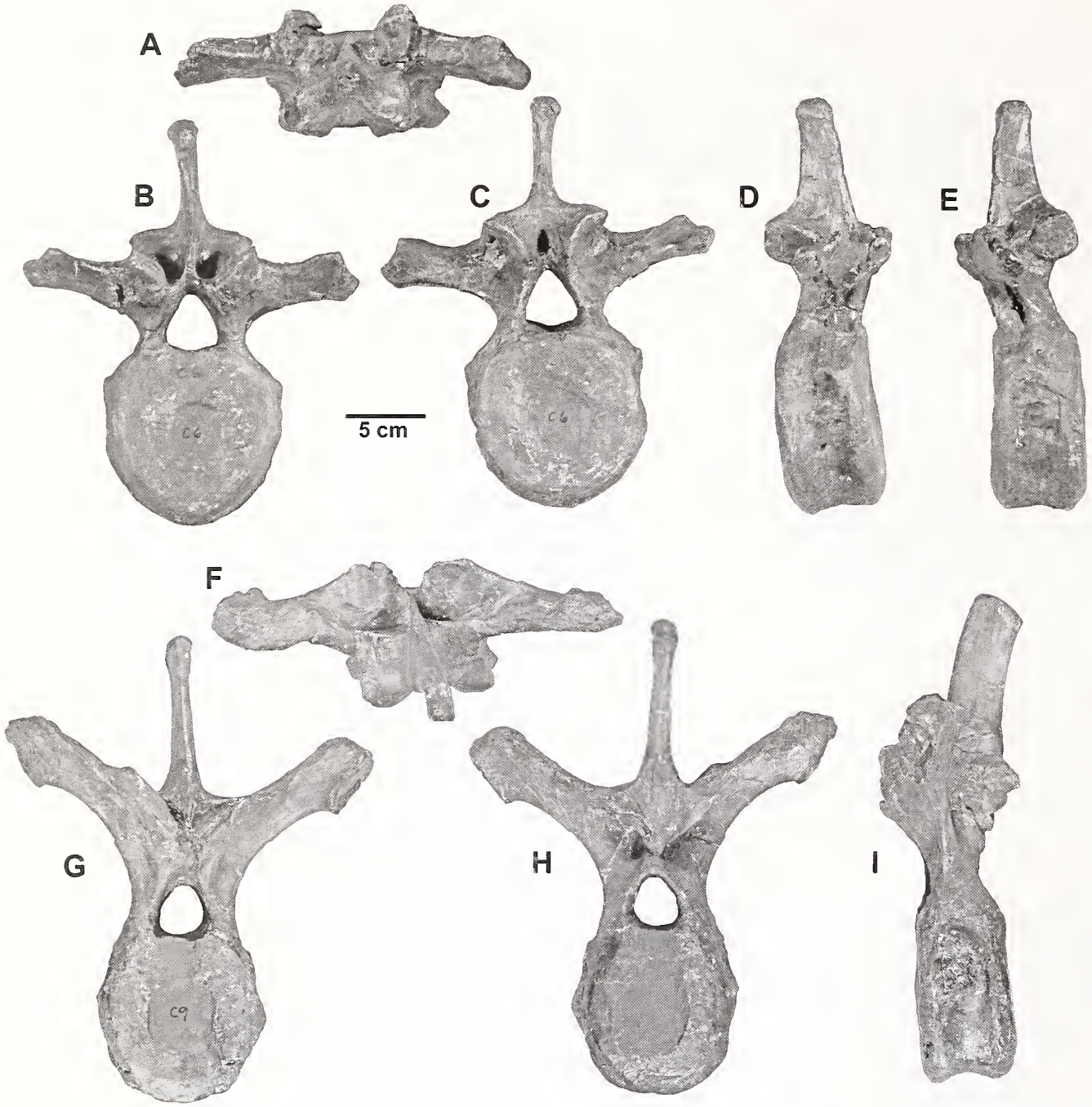

Figure 6. *Styracosaurus albertensis*, CMN 344, cervical vertebrae. Cervical vertebra 6 in, A, dorsal, B. anterior, C, posterior, D, right lateral, and E, left lateral views. Cervical vertebra 9 in F, dorsal, G. anterior, H, posterior, and I, left lateral views. Scale bar equals 5 cm.

ventrolaterally at the posterior end of the cervical series. The neural spines of C4 to C6 are approximately the same height, but from C7 to C9 they become progressively slightly longer. Anterior and posterior margins of the spines converge dorsally. Each spine flares at its dorsal tip to form a prominent knob that is thicker posteriorly than it is anteriorly. This morphology becomes less pronounced in the posterior part of the cervical series, where the spines gradually become more flattened, upright, and rectangular in outline.

The tenth vertebra is characterized by an abrupt shift of the parapophysis from the lateral surface of the centrum to the base of the neural arch (Figure 7). This is generally taken to mark the beginning of the dorsal series (e.g., Brown, 1917; Sternberg, 1951; Dodson et al., 2004; but see Ostrom and Wellnhofer, 1986 for an alternate interpretation). The centrum is slightly taller but narrower than that of the last cervical, appearing as a dorsally elongate oval in anterior view (Figure 8). The neural canal, although retaining its triangular outline, is distinctly smaller than in any cervical vertebra, indicating that the bulk of the brachial plexus exited the spinal cord anterior to this point (Giffen, 1995). The transverse processes are more elongate, and the diapophyseal surfaces face more laterally than in the last cervical vertebra. The

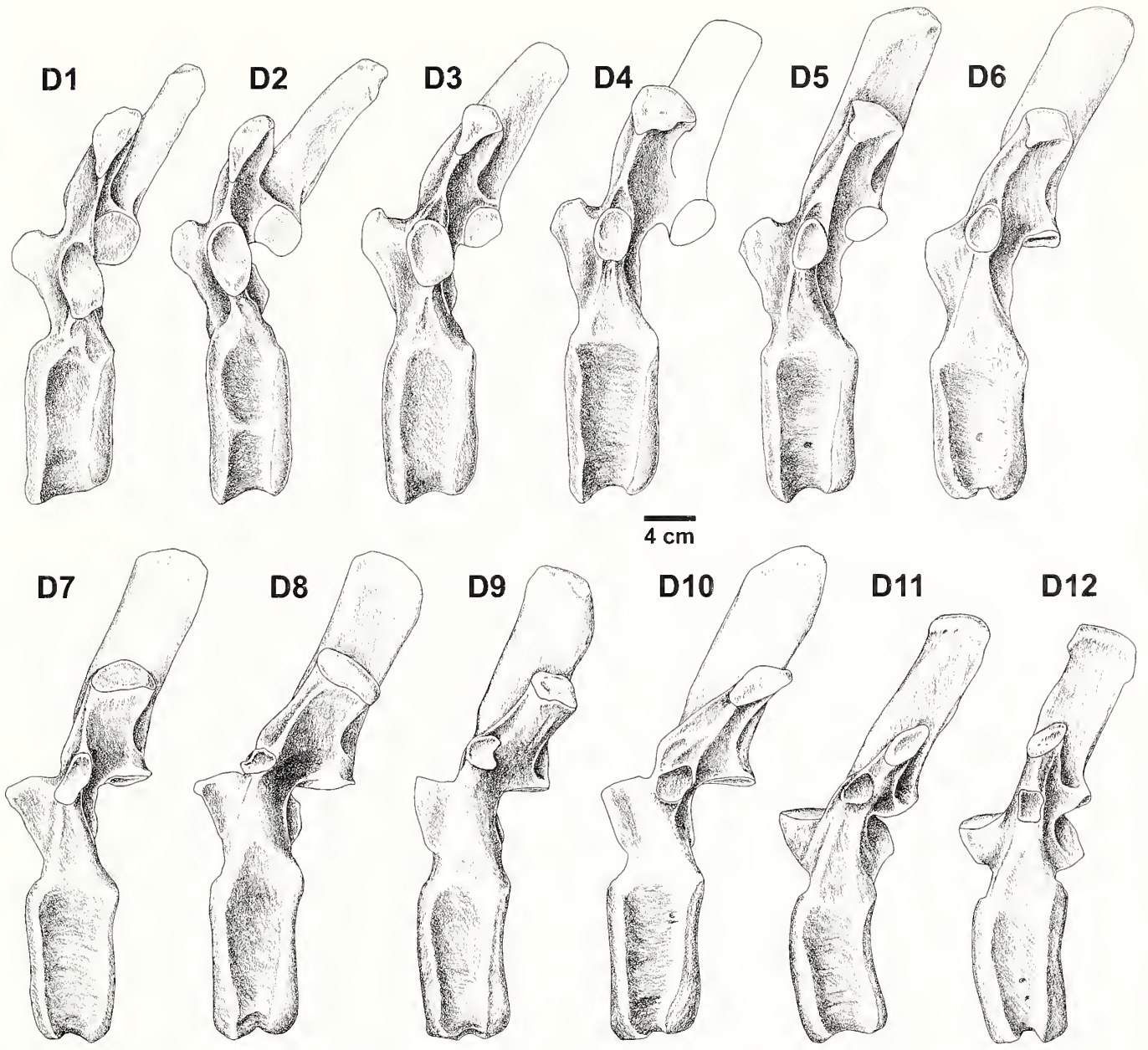

Figure 7. *Styracosaurus albertensis*, CMN 344. Dorsal vertebrae (D1–D12) in left lateral view. Scale bar equals 4 cm.

neural spines lean more posteriorly, but are otherwise similar to that of the last cervical vertebra.

The dorsal vertebral series (Figures 7–12) shows some clear anteroposterior trends. The centrum, exhibiting a dorsally elongate oval outline in the first four vertebrae, becomes slightly wider ventrally in the fifth dorsal vertebra and becomes slightly pear-shaped towards the posterior end of the series. A similar trend occurs in *Triceratops* (Hatcher et al., 1907; Ostrom and Wellnhofer, 1986), but not in *Centrosaurus*, in which the dorsal centra are more circular in outline throughout the column (Lull, 1933). The zygapophyses, sharply angled (45° to the frontal plane) in the first dorsal vertebra, gradually rotate to a more horizontal orientation (about 25° in the last dorsal vertebra). Prezygapophyses become larger, approaching the midline, and in the seventh dorsal vertebra, fuse to form a single dorsally-facing concave articular surface (Figure 9), although a remnant of the cleft is variably retained on the anterior surface of the conjoined prezygapophyses. This cleft reopens in the last (12th) dorsal vertebra. It has been suggested (Maidment and Barrett, 2011) that this median fusion of zygapophyses is an ontogenetic feature, presumably only occurring in older individuals. Articular facets of the prezygapophyses of the posterior dorsal vertebrae vary from a gentle cup shape (dorsal vertebrae 7, 8, 10) to gently convex (dorsal vertebrae 9, 11, 12). In most of the dorsal vertebrae (probably all, but preservation is not good enough to be sure), the pedicels of the postzygapophyses fuse to form a sharp, median, posteriorly projecting keel (Figures 10–12). The keel of the 11th dorsal vertebra is particularly well developed, and extends posteriorly to insert into deep slots between the prezygapophyses of the 12th dorsal vertebra. An equally prominent keel on the 12th

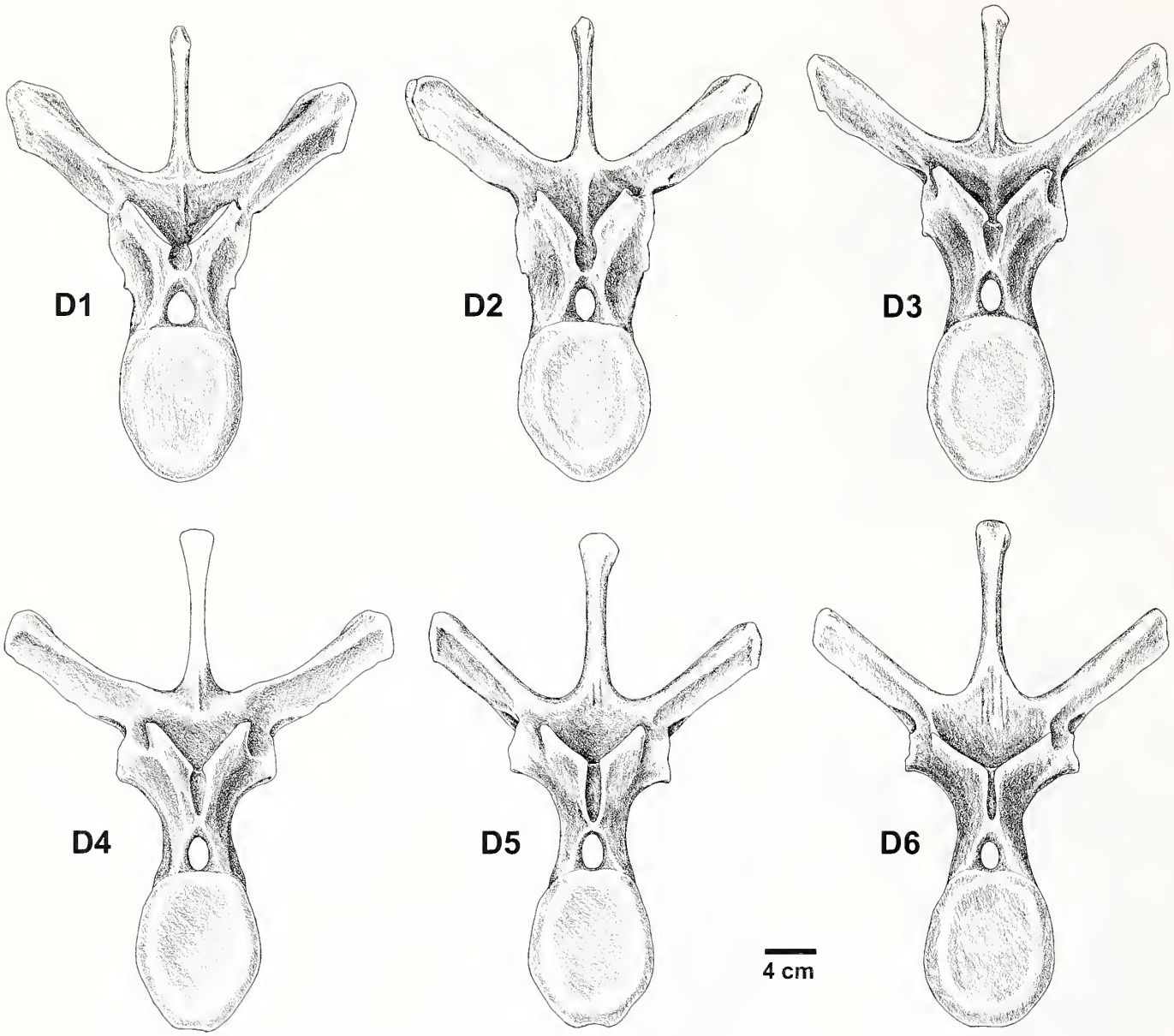

Figure 8. *Styracosaurus albertensis*, CMN 344. Dorsal vertebrae (D1–D6) in anterior view. Scale bar equals 4 cm.

dorsal vertebra presumably inserted between the prezygapophyses of the first dorsosacral vertebra, although the latter is not preserved. The postzygapophyses of the 12th dorsal vertebra face posteriorly as well as dorsally.

The parapophyseal facet is borne on the lateral surface of the neural arch pedicel on the first few dorsal vertebrae. It gradually migrates dorsolaterally onto the ventral surface of the transverse process in more posterior vertebrae, and in the last few dorsal vertebrae is located at least one-third of the distance between the base and tip of the process. This facet is largest in the anterior dorsal vertebrae, and becomes smaller toward the posterior end of the dorsal series, reflecting the reduced size of the capitulum of the posterior ribs. Neural spines become both taller and anteroposteriorly broader until about the fifth or sixth dorsal. These proportions are maintained to the 10th dorsal vertebra, after which there is a modest decrease in dimensions. Although the neural canal of the first dorsal vertebra is triangular in outline, in all subsequent dorsals, it is oval. Although variable in size, it appears to be smallest at or near the middle of the dorsal series. There is no evidence that the 12th dorsal vertebra had begun to fuse to the sacrum. In this, it resembles Brown's (1917) *Centrosaurus* specimen, but not Lull's (1933) specimen, in which the 12th dorsal has fused to the front of the sacrum to become a dorsosacral. However, it is clear that the latter vertebra is homologous to the last (12th) dorsal vertebra of CMN 344, as its associated ribs (Lull, 1933, fig. 18) closely resemble those associated with the 12th dorsal vertebra of CMN 344, and the 11th dorsal vertebra of Lull's specimen (Lull, 1933, fig 16) is very similar to the 11th dorsal vertebra of CMN 344. Lull's specimen has a second dorsosacral vertebra that lacks ribs. Its distally expanded diapophyses fuse to the ilium. This morphology is not present in the most posterior dorsal vertebrae of CMN 344.

Seven caudal vertebrae (Figures 13–16) are preserved in CMN 344. The two largest, lacking facets for reception of chevrons,

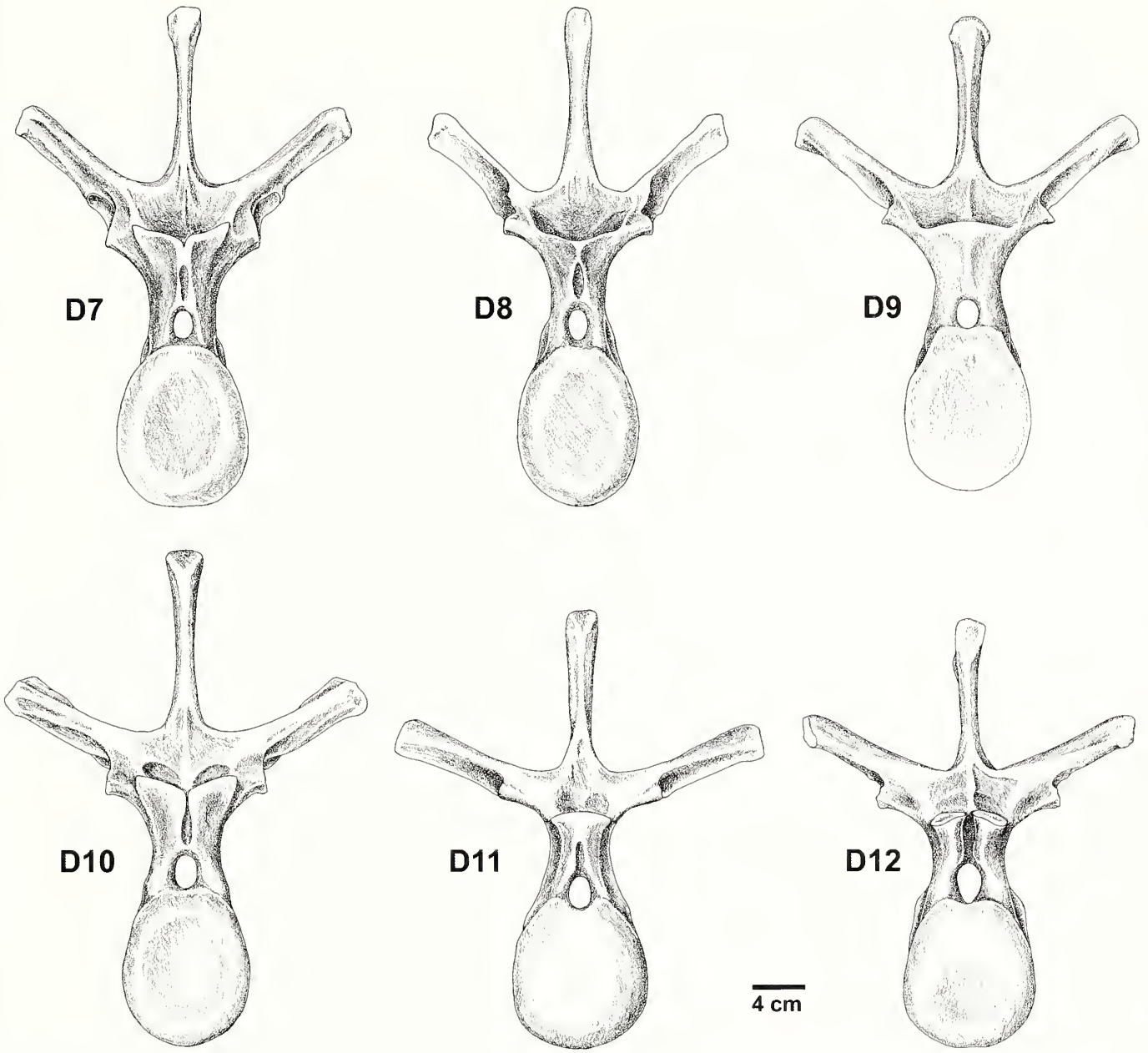

Figure 9. *Styracosaurus albertensis*, CMN 344. Dorsal vertebrae (D7–D12) in anterior view. Scale bar equals 4 cm.

probably represent the first and second caudal vertebrae. Their transverse processes project anteriorly as well as laterally. A third vertebra, extensively restored in plaster (see Holmes et al., 2005, plate 10), was inserted immediately behind the second in the original mount. Since its true morphology cannot be established, it will not be described or illustrated here. All of the remaining vertebrae bear facets for chevrons. In *Centrosaurus* and cf. *Anchiceratops* (CMN 8547), the first chevron articulated between the third and fourth caudal vertebrae (Brown, 1917; Mallon and Holmes, 2010), suggesting that no vertebrae are missing from the preserved series described here. All are approximately the same size and exhibit similar morphology, and can be assembled into a series that plausibly represents the fourth to eighth caudals. Viewed laterally, the centra of most of the caudal vertebrae are slightly longer dorsally than ventrally, forcing the base of the tail to a distinct ventral curvature, much as observed in *Triceratops* (Larson and Ott, 2004).

A complete tail is preserved in articulation with the sacrum in TMP 1989.097.001. As much matrix as practical was removed from the 17 proximal caudal vertebrae, but otherwise they were left in articulation as preserved (Figure 28). The 28 distal caudal vertebrae have been removed from the matrix, and many of them have been separated (Figure 29). The angle of articulation of the proximal caudal vertebrae confirms the observation, based on the partial tail of CMN 344 that the tail curved ventrally immediately posterior to the sacrum.

Of the 45 caudal vertebrae, only the first 20 bear transverse processes, as compared with 25 in *Brachyceratops* (Gilmore, 1917), 23 in *Centrosaurus* (Brown, 1917), 22 in cf. *Anchiceratops* (Mallon and Holmes, 2010), and 19 in *Pentaceratops* (Wiman,

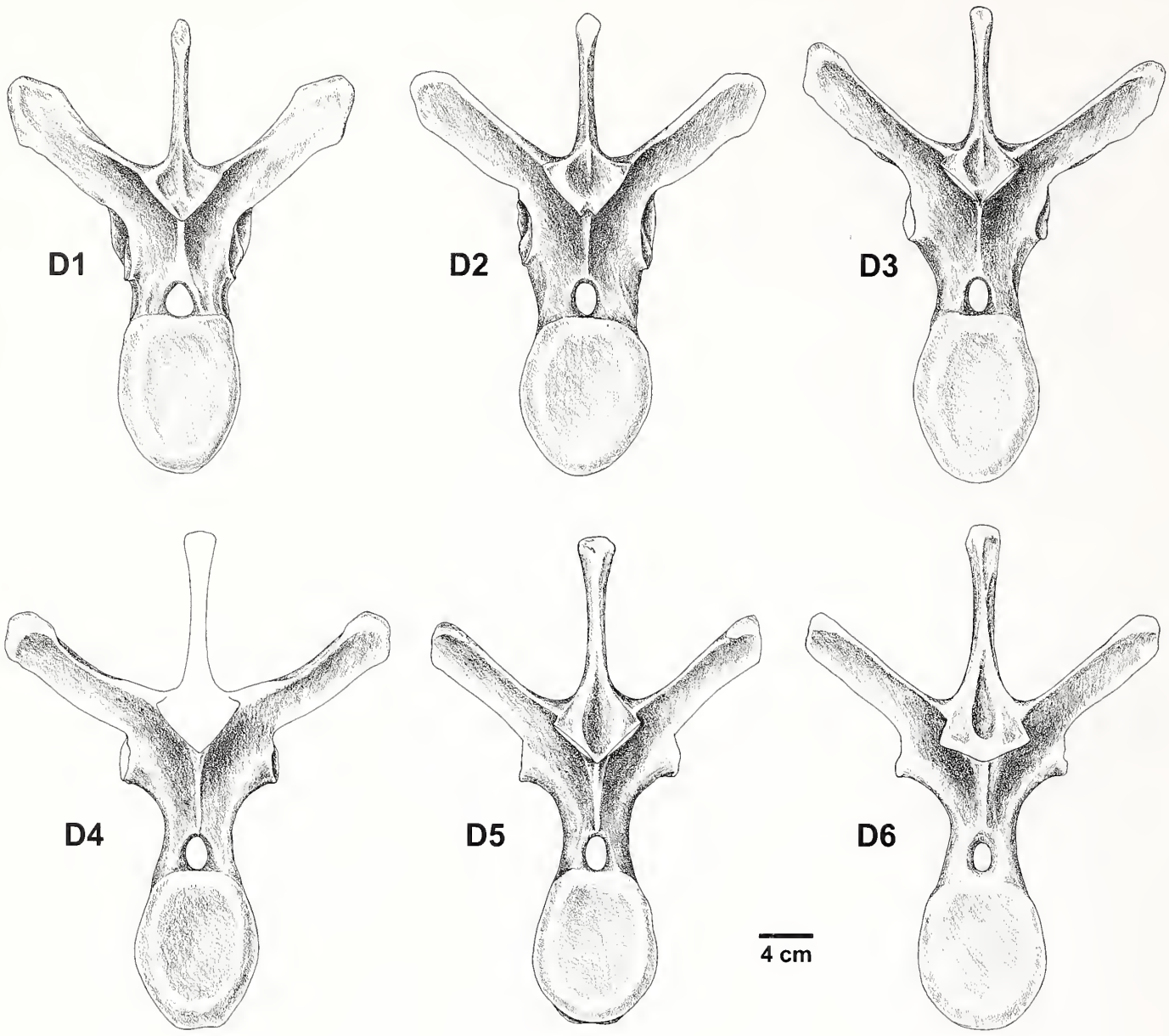

Figure 10. *Styracosaurus albertensis*, CMN 344. Dorsal vertebrae (D1–D6) in posterior view. Scale bar equals 4 cm.

1930). The transverse processes of the first three caudal vertebrae are incomplete. However, it is clear that the process of the first caudal vertebra is directed strongly anteriorly, that of the second, anterolaterally, and that of the third, directly laterally, as are those of all more posterior caudal vertebrae. A similar trend is also seen in CMN 344, although the anterior deflection of the transverse processes of the first caudal vertebra is not as pronounced. Although the processes gradually diminish in size anteroposteriorly, their disappearance in the 21st caudal is abrupt (Figure 30). Four vertebrae (27–30) are pathological—extensive co-ossification has occurred, and their anatomy has been obscured by considerable secondary bone growth (Figure 29). Although well developed prezygapophyseal processes are present as far posteriorly as the 36th caudal, the most posterior postzygapophyseal processes appear to occur between the 26th and 27th caudal (or possibly between 27 and 28—secondary bone growth in the pathological section of the tail makes it difficult to tell). This indicates that the last several prezygapophyseal processes were not functional (Figure 30). The most posterior neural arches are not preserved, but broken stumps indicate that they were present on all caudals except the last two (44 and 45). These latter vertebrae, each about half of the length of the 43rd caudal, are co-ossified, although the separation between the two elements is clearly marked by a raised ridge on the ventral and lateral surfaces of the compound element.

The most anterior preserved chevron is located between caudal vertebrae four and five, although there may have been one between caudals three and four—the ventral aspects of the centra are not well enough exposed to confirm the presence of facets for its reception. Chevrons are preserved as far posteriorly as the 17th caudal. Although their distal ends are not generally well preserved, there appears to be little or no lateral compression or

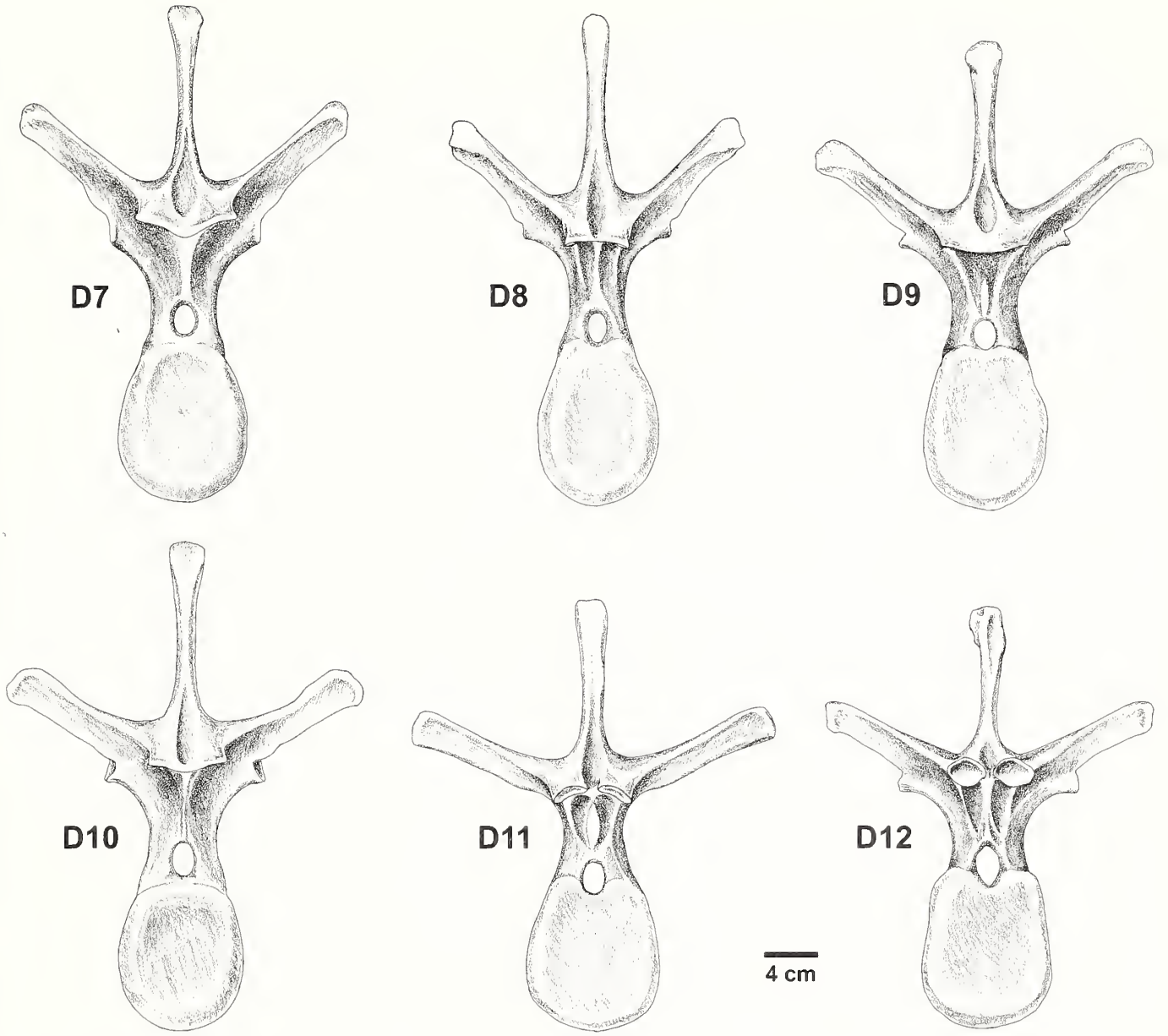

Figure 11. *Styracosaurus albertensis*, CMN 344. Dorsal vertebrae (D7–D12) in posterior view. Scale bar equals 4 cm.

anteroposterior expansion to form a blade. Bevels preserved on the ventral rims of the centra indicate that chevrons were present as far back as caudal vertebra 32.

The total count of 45 caudal vertebrae compares closely with that of other centrosaurines with complete tails; *Centrosaurus* has 46 (Brown, 1917), and *Brachyceratops*, 47 (Gilmore, 1917); but this number is distinctly higher than in chasmosaurines in which the count can be established or estimated: 39 in *Anchiceratops* (Mallon and Holmes, 2010), at least 30 in *Pentaceratops* (Wiman, 1930), and approximately 40 in *Chasmosaurus*—(CMN 2245, RH, pers. obs., August, 2012).

Sacrum

The synsacrum is not preserved in CMN 344, and although present in TMP 1989.097.001, it is obscured by the right ilium and ossified tendons (Figure 24). However, a partial synsacrum is preserved in TMP 2009.080.001. Co-ossification is advanced, but there appear to be two dorsosacral vertebrae present, as the portion of the sacral bar immediately anterior to the first sacral vertebra is nearly twice as long as the first sacral centrum (Figure 31). As in *Triceratops* (Hatcher et al., 1907) and *Chasmosaurus* (Maidment and Barrett, 2011), the broad base of the large first sacral rib originates from the posterolateral part of the second dorsosacral as well as from the lateral surface of the centrum of the first sacral vertebra. The midventral surface of the first two sacral vertebrae and anterior half of the third bear a shallow, indistinct longitudinal groove (Figure 31). The ventral surfaces of the fourth sacral and the first two preserved caudosacrals actually bear a low midventral keel. Maidment and Barrett (2011) have suggested that a midventral, longitudinal

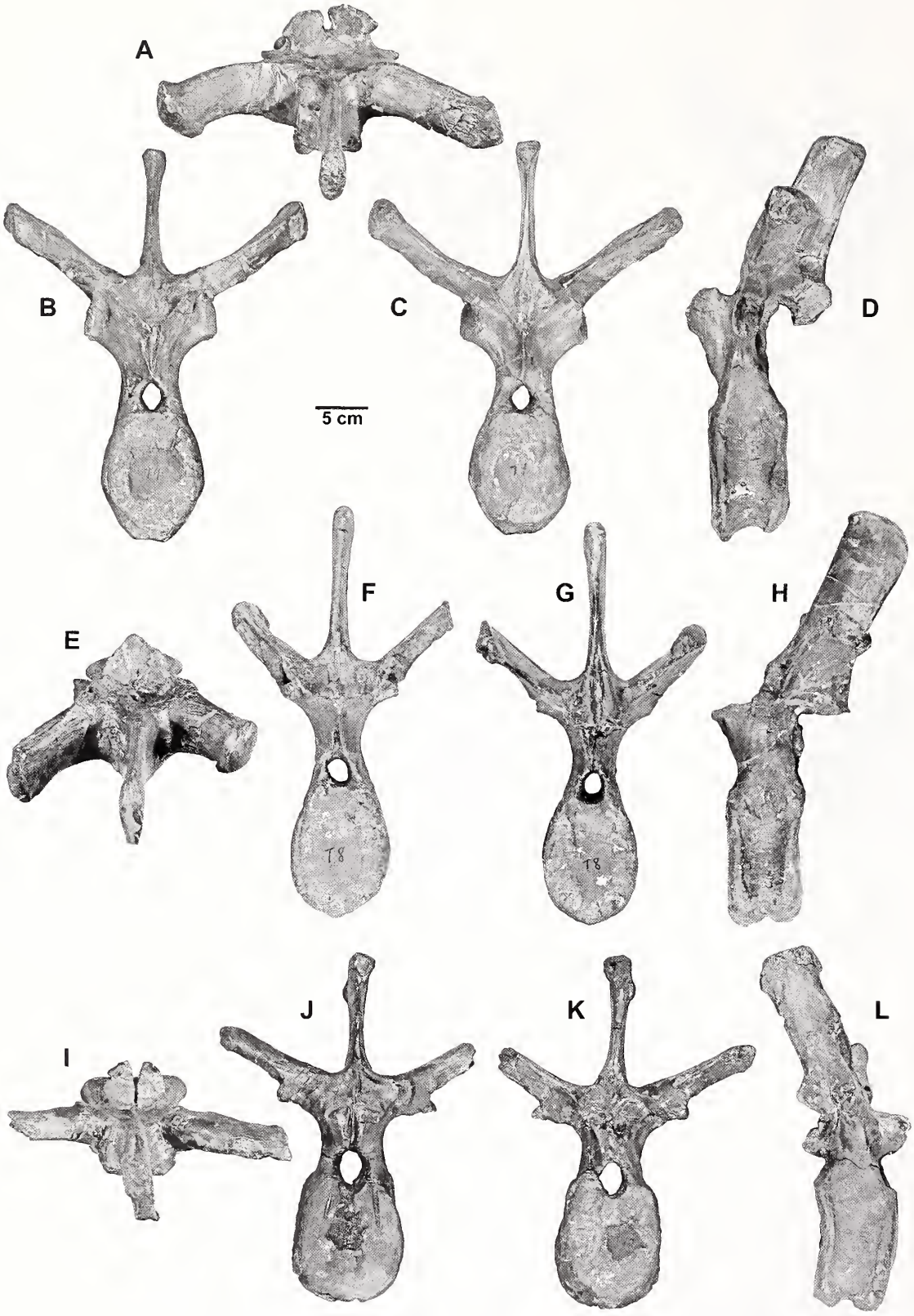

Figure 12. *Styracosaurus albertensis*, CMN 344, dorsal vertebrae. Dorsal vertebra 4 in A, dorsal, B, anterior, C, posterior, and D, left lateral views. Dorsal vertebra 8 in E, dorsal, F. anterior, G, posterior, and H, left lateral views. Dorsal vertebra 12 in I, dorsal, J, anterior, K, posterior, and L, right lateral views. Scale bar equals 5 cm.

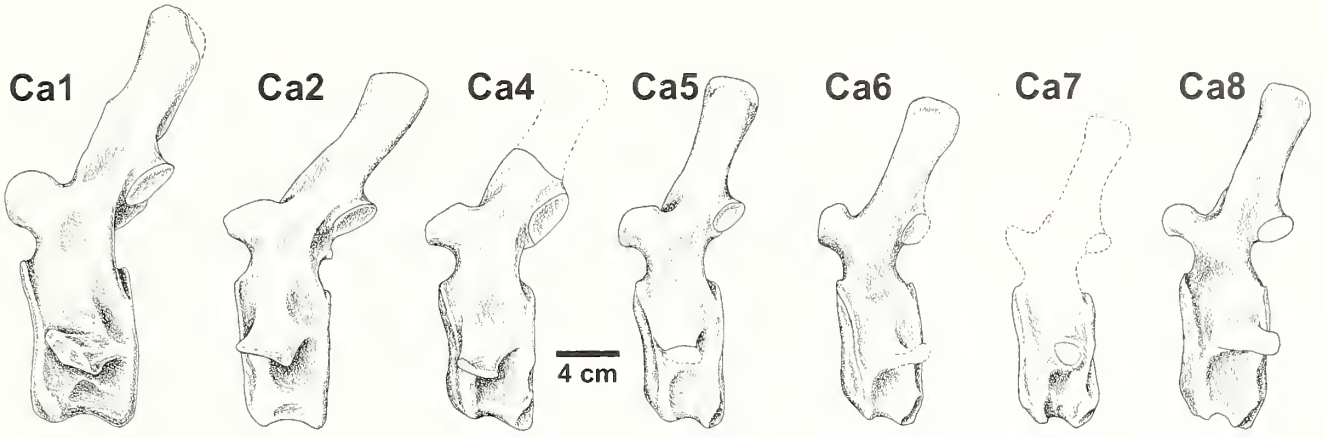

Figure 13. *Styracosaurus albertensis* CMN 344. Caudal vertebrae (1, 2, 4–8) in left lateral view. Scale bar equals 4 cm.

groove, present in the sacrum of all ceratopsids, is conspicuous in chasmosaurines, but is poorly developed in centrosaurines. This specimen supports their hypothesis.

Ribs (Holmes et al., 2005, plates 13–19; Figures 17, 24, 25, 32, and 33 of this paper)

The ribcage of CMN 344 is largely complete (see Holmes et al., 2005 for details). Several ribs, disarticulated from their vertebrae, are preserved in TMP 1989.097.001. As in other ceratopsids, the atlantal segment of the syncervical lacks ribs. The axial segments bear diapophyses and parapopophyses, but neither axial rib is preserved. The rib associated with the last syncervical segment (third cervical) comprises a broad, flat lamina connecting the dorsal tuberculum and ventral capitulum, and a short shaft. As in *Centrosaurus* (Brown, 1917), a short triangular spine projects from the anterior edge of this lamina. A distinct neck is lacking. The flattened, laterally convex shaft of the next rib (associated with the first free, or fourth, cervical vertebra) expands distally to form a rounded crest dorsally and a longer, triangular spine ventrally. The rib associated with the fifth cervical vertebra is similar to that of the fourth, although the ventral spine-like process of the shaft turns gently laterally toward its tip. This effect is more pronounced in the sixth rib, which is otherwise very similar to the fifth.

The tuberculum and capitulum become more widely separated in more posterior cervical ribs as the connecting lamina becomes progressively reduced. All ribs turn sharply ventrally at their necks, so that their straight shafts project directly posteroven-

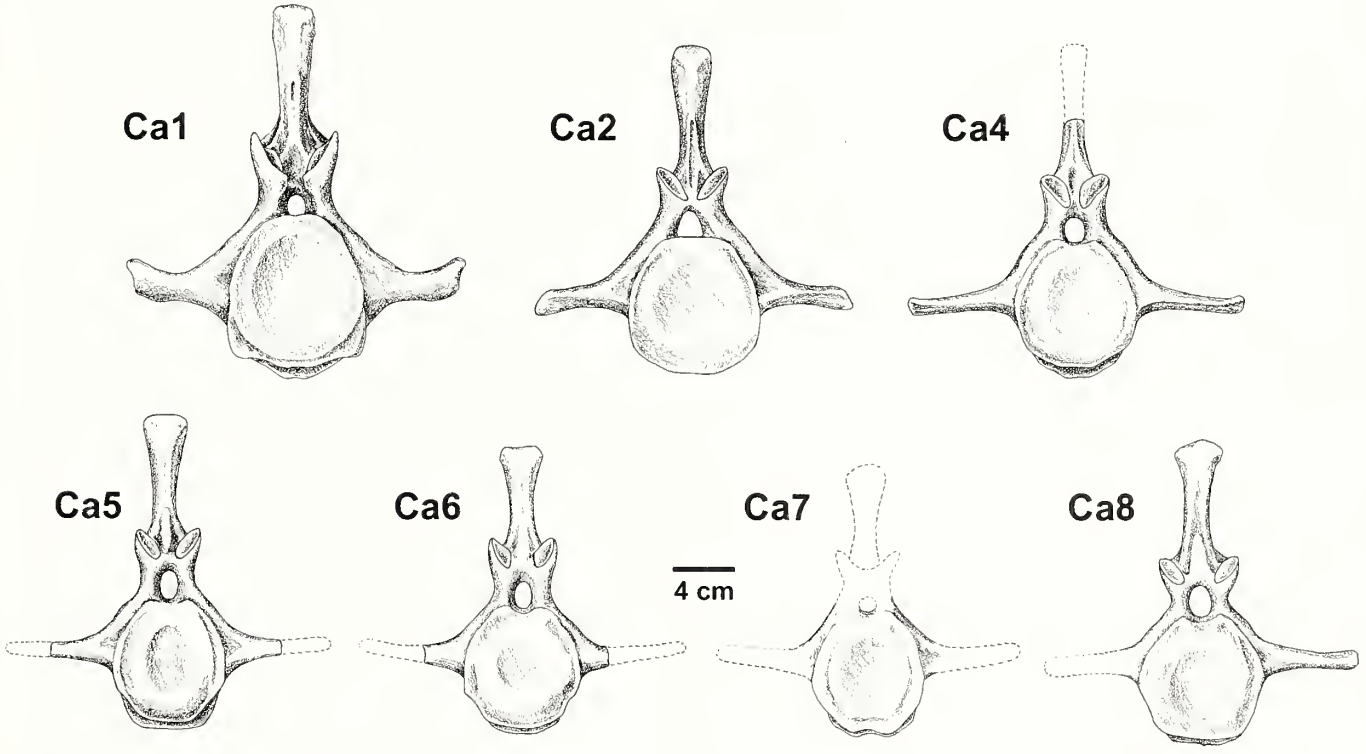

Figure 14. *Styracosaurus albertensis* CMN 344. Caudal vertebrae (1, 2, 4–8) in anterior view. Scale bar equals 4 cm.

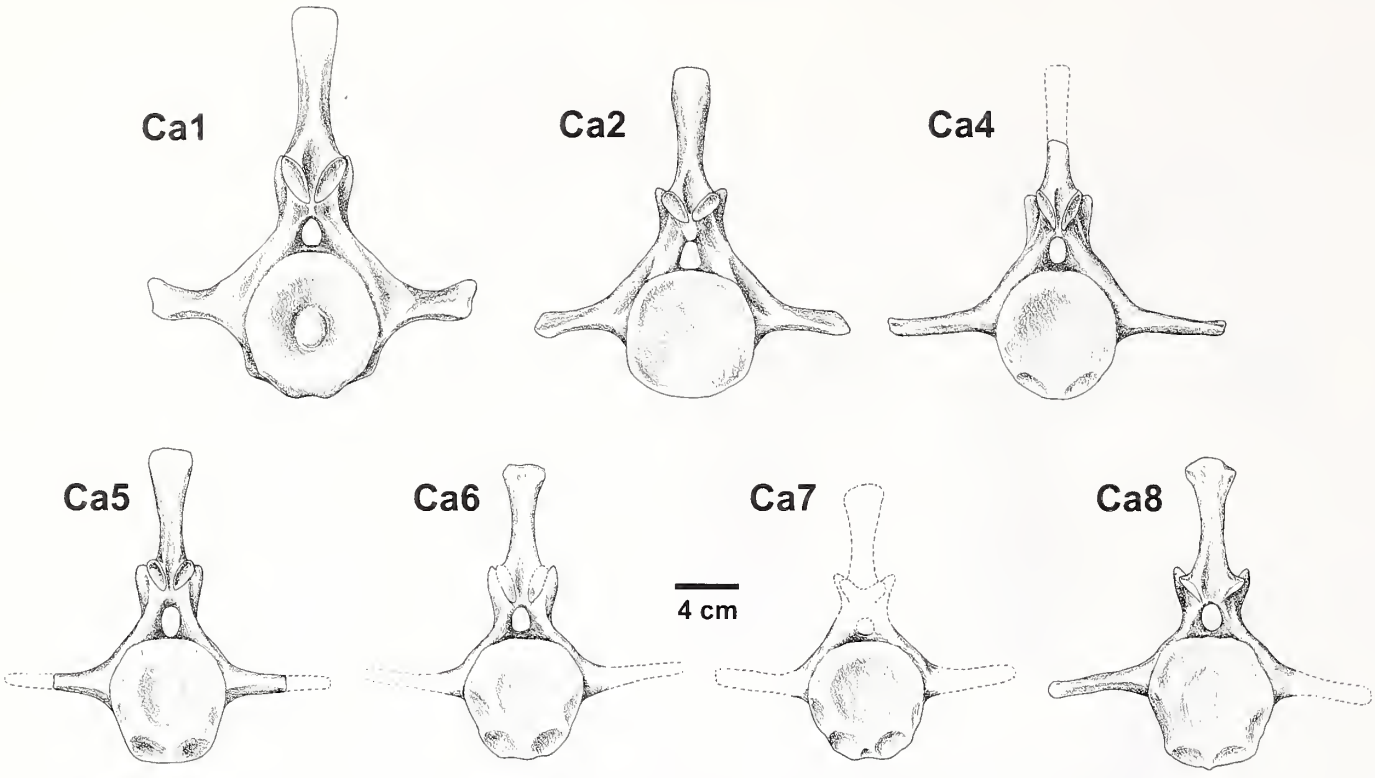

Figure 15. *Styracosaurus albertensis* CMN 344. Caudal vertebrae (1, 2, 4–8) in posterior view. Scale bar equals 4 cm.

trally. The shafts become longer toward the posterior end of the series. The ribs associated with the second, third and fourth free cervical vertebrae (i.e., C5 to C8) attenuate to a point ventrally, indicating a lack of cartilaginous costal extensions. However, the end of the last cervical rib expands both anteroposteriorly and mediolaterally, suggesting that it may have continued in cartilage to the sternum.

The rib associated with the first dorsal vertebra is distinct from that of the last cervical in having a much shorter capitular shaft that correlates with the abrupt dorsal migration of the parapophysis from the centrum of the vertebra to the lateral surface of the neural arch pedicel. Both capitular and tubercular shafts are extremely broad and spatulate. Its slightly flattened shaft, the most massive of the whole presacral series, is distinctly more curved than any of the cervical vertebrae ribs, although the more distal portion of the shaft is almost straight. Its expanded, rugose termination indicates continuation in cartilage.

A number of trends are apparent in the thoracic rib series. The tubercular shaft becomes further reduced posterior to the first thoracic rib, and by the fourth thoracic, it is essentially absent. In more posterior thoracic ribs, the tubercular facet occupies a triangular notch on the dorsal surface of the angle of the rib. Both tubercula and capitula become less massive, with the shape of their articular facets gradually changing from an elongate, flattened oval to quasi-circular in outline. The shaft of the first thoracic rib is essentially straight distal to the angle, but the more posterior ribs gradually develop more curvature. Beginning at the seventh thoracic rib, the shaft begins to twist relative to the plane of the proximal articulations, causing the rib to curve posteriorly as well as ventrolaterally. This trend continues until the 11th thoracic rib, in which the shaft forms a tight, posteroventromedial arc. On the inside of this arc, the rib shaft bears a flattened facet that may have provided articulation with the anterior margin of the prepubic process, as suggested by Sternberg (1927) for *Chasmosaurus*. The 12th thoracic rib, in contrast, is much shorter, essentially straight, and projects laterally and slightly anteriorly. A very similar rib, associated with the first dorsosacral (12th postcervical) has been described in *Centrosaurus* (Lull 1933, fig. 18). It articulates with (but does not fuse to) the parapophysis of the vertebra, and lies along the internal surface of the anterior iliac process.

The stout shafts of the second and third thoracic ribs, as in the first, are oval in cross section and are expanded it their distal ends for articulation with sternal ribs. However, more posterior thoracic ribs gradually become more flattened, and their rounded, spatulate ends show no evidence of cartilaginous extensions. None of the thoracic ribs bear facets to accommodate the scapula like those observed in *Triceratops* (Kozisek and Derstler, 2004; Larson and Ott, 2004).

Although many of the ribs show considerable distortion, a sufficient number have retained their original shape, allowing the ribcage to be reconstructed with considerable confidence (Figures 32 and 33). In general, the inferred body cross-section resembles that reconstructed by Lehman (1989) for *Agujaceratops* (*Chasmosaurus*) *mariscalensis*. Anteriorly, the chest is narrow but dorsoventrally deep, comprising relatively straight, ventrally directed rib shafts that are swept back at an angle of about 35° from the vertical. Only the first three thoracic ribs are expanded distally. All others taper distally, providing no evidence for presence of costal cartilages. Therefore, even if the last pair of cervical ribs is included, there is evidence for no more than four pairs of 'true' ribs that connected to the sternum. Brown (1917)

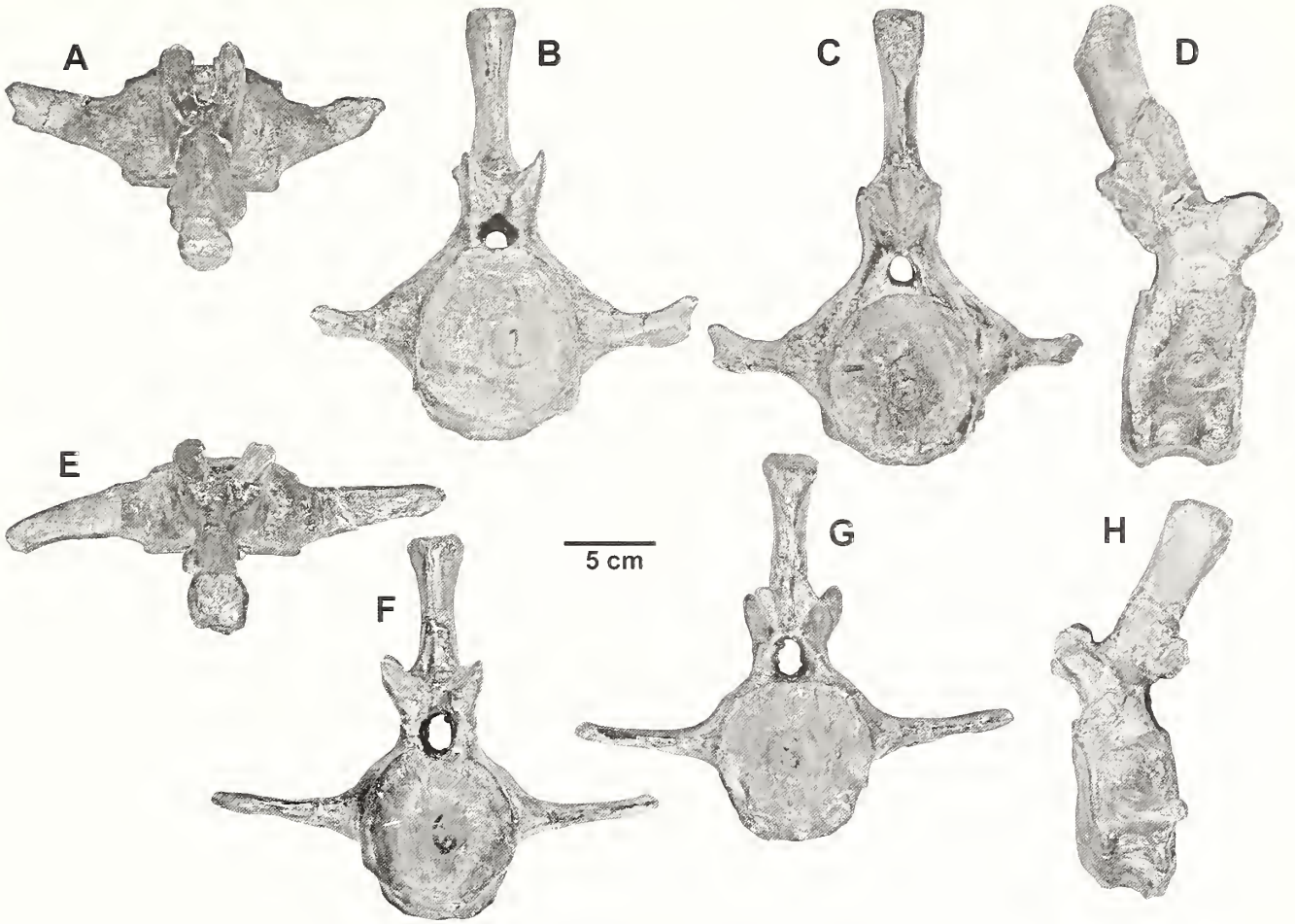

Figure 16. *Styracosaurus albertensis*, CMN 344, caudal vertebrae. Caudal vertebra 1 in A, dorsal, B, anterior, C, posterior, and D, right lateral views. Caudal vertebra 6 in, E, dorsal, F, anterior, G, posterior, and H, left lateral views. Scale bar equals 5 cm.

hypothesized the presence of up to 11 pairs of 'true' ribs in *Centrosaurus* based on what he took to be scars for individual costal cartilages on the posterior margin of the sternal plate. However, we have never observed distinct costal cartilage scars on any ceratopsid sternal plate, so cannot confirm such a high rib count. Ribs become longer until the fourth thoracic, then become shorter again, at first gradually, and then more rapidly after the 10th thoracic. Posteriorly, the rib shafts become more broadly curved and vertically oriented. Beginning at about the ninth thoracic, their necks arch dorsolaterally from the diapophyseal–capitular articulation, thus raising the dorsal wall of the body cavity, before turning laterally and then ventrolaterally to form a broad, but dorsoventrally shallow posterior thorax. The elevated ventral wall of the abdomen suggested by the shape of these ribs presumably accommodated anterior excursion of the hind limb.

Pectoral girdle and limb

Both scapulae, the right coracoid, and the right sternal plate are well preserved in CMN 344 (figure 18f; Holmes et al. 2005, plates 20–22). Only the right scapulocoracoid and humerus, and partial left scapulocoracoid and humerus are preserved in TMP 1989.097.001 (Figures 24, 25, 34). The coracoid is pierced on its lateral surface by a conspicuous coracoid foramen. Medially, the foramen opens into a distinct groove that leads to its common suture with the scapula (Holmes et al., 2005, plate 20). The supracoracoideus scar is not conspicuously developed. The prominent, laterally turning acromial process of the scapula is restricted to a short portion of the anterior scapular margin immediately distal to its suture with the coracoid (Figure 18; Holmes et al., 2005, plate 20).

Both humeri of CMN 344 are somewhat crushed, but complete (Figure 19; Holmes et al., 2005, plate 23). The dorsally arched, deltopectoral crest is mueh less extensive proximally than in most chasmosaurs (e.g., CMN 2280, ROM 843 [RH, pers. obs., August, 2012], NHMUK R4948, *Triceratops* [Hatcher et al. 1907, figs. 65–66]), and the insertional area for the pectoralis is less extensive and does not extend as far distally. Both ulnae and radii are preserved (Figure 20; Holmes et al., 2005, plates 24 and 25). As in other ceratopsids, the epipodium is distinctly shorter than the propodium, with the radius being about 65% of the length of the humerus. Only four distal elements can be accounted for: the first metacarpal of the right forelimb, and fourth metacarpal, and first and second distal phalanges of the left forelimb (Holmes et al., 2005, plate 30).

In contrast to the condition seen in *Triceratops* (Kozisek and Derstler, 2004; Larson et al., 2004), the ribs lack facets on their lateral surfaces to accommodate the scapular blade. As a consequence, it is impossible to position the scapula precisely, although its gently curvature conforms best to the relatively

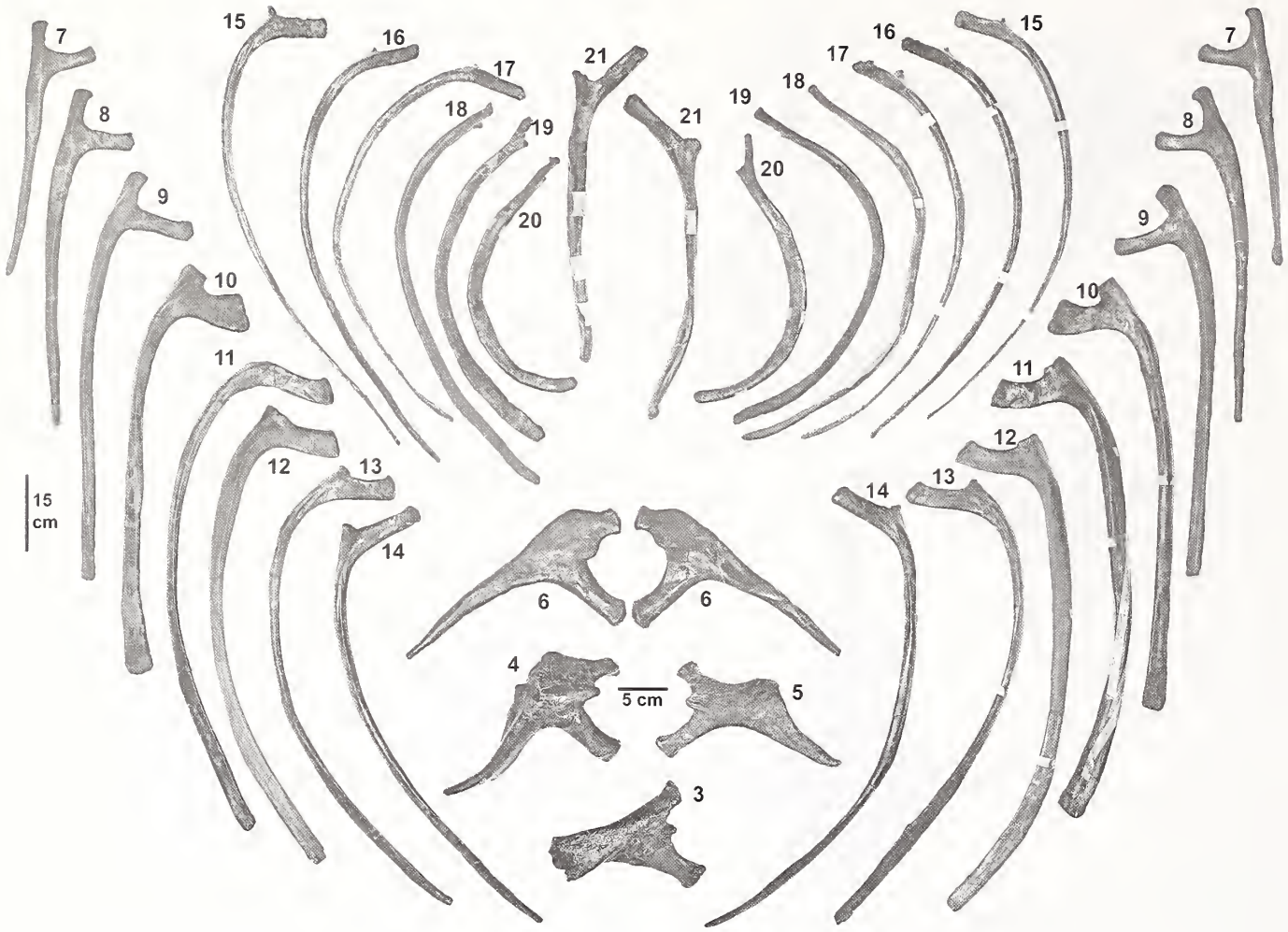

Figure 17. *Styracosaurus albertensis*, CMN 344, ribs in anterior view. 3–9, ribs associated with cervicals 3–9; 10–21, ribs associated with thoracic vertebrae 10–21. Scale bar for ribs 3–6 equals 5 cm. Scale bar for ribs 7–21 equals 15 cm.

straight ribs of the anterior-most thoracic region (Figure 1). With the scapulocoracoid in this position, the articulated humerus projects posterolaterally at an angle of about 30° parasagittally and slightly ventrally, much as hypothesized for other ceratopsids by Dodson and Farlow (1997) and as reconstructed for *Vagaceratops* (*Chasmosaurus*) *irvinensis* (Thompson and Holmes, 2007).

Pelvic girdle and rear limb

Of the pelvic girdle, only the right ilium and right and left ischia (Figure 21; Holmes et al., 2005, plates 26 and 27) are preserved in CMN 344. The entire right half, and much of the left half, of the pelvis is exposed in TMP 1989.097.001 (Figure 24). The anterior (preacetabular) blade of the right ilium is depressed and rotated so that its dorsal surface faces slightly laterally, and its gently curved posterior blade is rotated so that its ventrolateral surface faces essentially laterally. Otherwise, the proportions of the bone resemble those of the type as well as those described for the ilia of *Centrosaurus* (Brown, 1917) and cf. *Anchiceratops* (Mallon and Holmes, 2010).

The gently curved ischia resembles those of other centrosaurines (Brown, 1917; Gilmore, 1917; Lull, 1933), and protoceratopsids (Brown and Schlaikjer, 1940, 1942; You and Dodson, 2004), more than the distinctly strongly curved ischia seen in chasmosaurines (e.g., Hatcher et al., 1907, fig. 60; Wiman, 1930:plate 4; Lehman, 1989, fig. 19; Mallon and Holmes, 2010). Although the posterior process of the right pubis could not be identified in TMP 1989.097.001, the prepubic process is complete, and appears to be in its natural position. It projects almost directly anteriorly, much as in Dodson et al. (2004, fig. 23.5) rather than anteroventrally, as sometimes depicted (e.g., Brown, 1917, plate XIII), and its hatchet-shaped anterior end appears to articulate with the curved shaft of a posterior thoracic rib, probably that associated with the 11th dorsal vertebra.

Both femora, although crushed, are complete in CMN 344 (Figure 22; Holmes et al., 2005, plate 28) and TMP 1989.097.001 (Figures 24, 34). The shafts of both femora of TMP 1989.097.001 appear thicker than in CMN 344 and other ceratopsids in general, but this may be the result of crushing. Otherwise, the femora closely resemble those described for other ceratopsids such as *Chasmosaurus* (Maidment and Barrett, 2011), *Triceratops* (Hatcher et al. 1907, fig. 71, and *Centrosaurus* (as "*Monoclonius*", Hatcher et al. 1907, fig. 86), although they (in particular those of CMN 344) appear to be somewhat more graeile. Whether this is the result of postmortem distortion, ontogeny, or represents a true morphological distinction is unclear.

Preserved epipodials in CMN 344 include the left fibula and both right and left tibiae (Figure 23; Holmes et al., 2005, plate

Figure 18. *Styracosaurus albertensis*, CMN 344, pectoral girdle. Right scapula with articulated coracoid in A, lateral view, B, posterior, and C, medial views. Right sternal plate in D, dorsal, E, medial, and F, lateral views. Scale bar equals 5 cm.

29), and in TMP 1989.097.001, the right tibia and fibula only. They do not differ in any obvious way from the epipodials of other ceratopsids.

The left second metatarsus is the only element of either tarsus, metatarsus and pedal elements to be preserved in CMN 344 (Holmes et al., 2005, plate 30). A virtually complete right metatarsus and pes is preserved in TMP 1989.097.001 (Figure 35). As in other ceratopsids as far as known, the medial (first) metatarsal is the shortest of the functional metatarsals (although this element seems unusually short, being less than 50% of the third metatarsal, as compared with 57% in *Centrosaurus* [Brown, 1917] and 56% in *Brachyceratops* [Gilmore, 1917]), and the third metatarsal is the longest. The second is slightly shorter than the third, as is the fourth. The latter appears to be less robust than the others, especially distally, although this could be the result of crushing. The vestigial fifth metatarsal is present, but is broken into two pieces.

As in other ceratopsids, the phalangeal formula of the pes is 2,3,4,5,0. The first (proximal) phalanx of the first digit is the longest of the proximal phalanges. In ceratopsids, as far as is known, each phalanx of second through fourth digits is shorter than its equivalent in the digit immediately medial (Dodson et al., 2004). As a result, the third digit is only slightly longer than the second digit, and the fourth digit is actually shorter than the third despite a pre-to-post axial increase in phalangeal count. This trend is more pronounced in *Styracosaurus*, in which these digits are virtually the same length (Figure 35). As a result, the digits are distinctly shorter than in *Centrosaurus*. In the latter, the length of each digit exceeds that of its corresponding metacarpal (Brown, 1917, plate xxii; Lull, 1933, fig. 29). In TMP 1989.097.001, this is

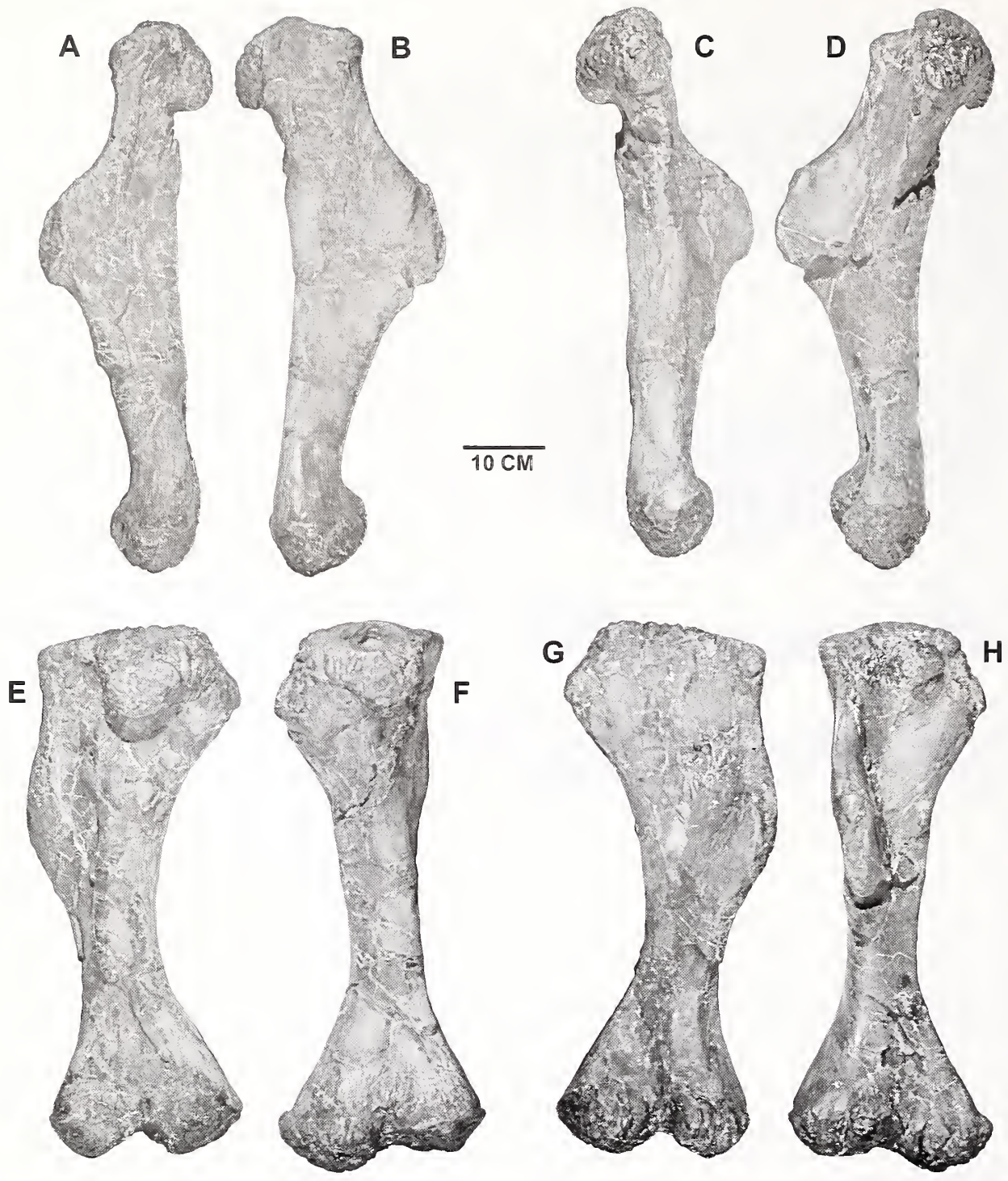

Figure 19. *Styracosaurus albertensis*, CMN 344, humeri. Left humerus in A, anterior; C, posterior; E, dorsal; and G, ventral views. Right humerus in B, anterior, D, posterior; F, dorsal, and H, ventral views. Scale bar equals 10 cm.

true of only the first and fourth digits (although even in these cases, the digits are shorter relative to their corresponding metacarpals than is the case in *Centrosaurus*). The second and third digits of TMP 1989.097.001 are actually shorter than their corresponding metacarpals. The distal ends of the terminal phalanges (unguals) of the first to third digit are highly eroded. The cause of this deformity is uncertain, but outward appearances are consistent with bone resorption. A similar morphology has been observed in *Pachyrhinosaurus* (TMP 2002.076.001, MR, pers. obs.) and large ankylosaurs (R. Sissons, pers. comm.).

Discussion

Although an enormous amount of ceratopsid material has been collected from the Upper Cretaceous deposits of North America, articulated, reasonably complete skeletons are rare. Consequently, the postcranial skeletons of most ceratopsid taxa have not been

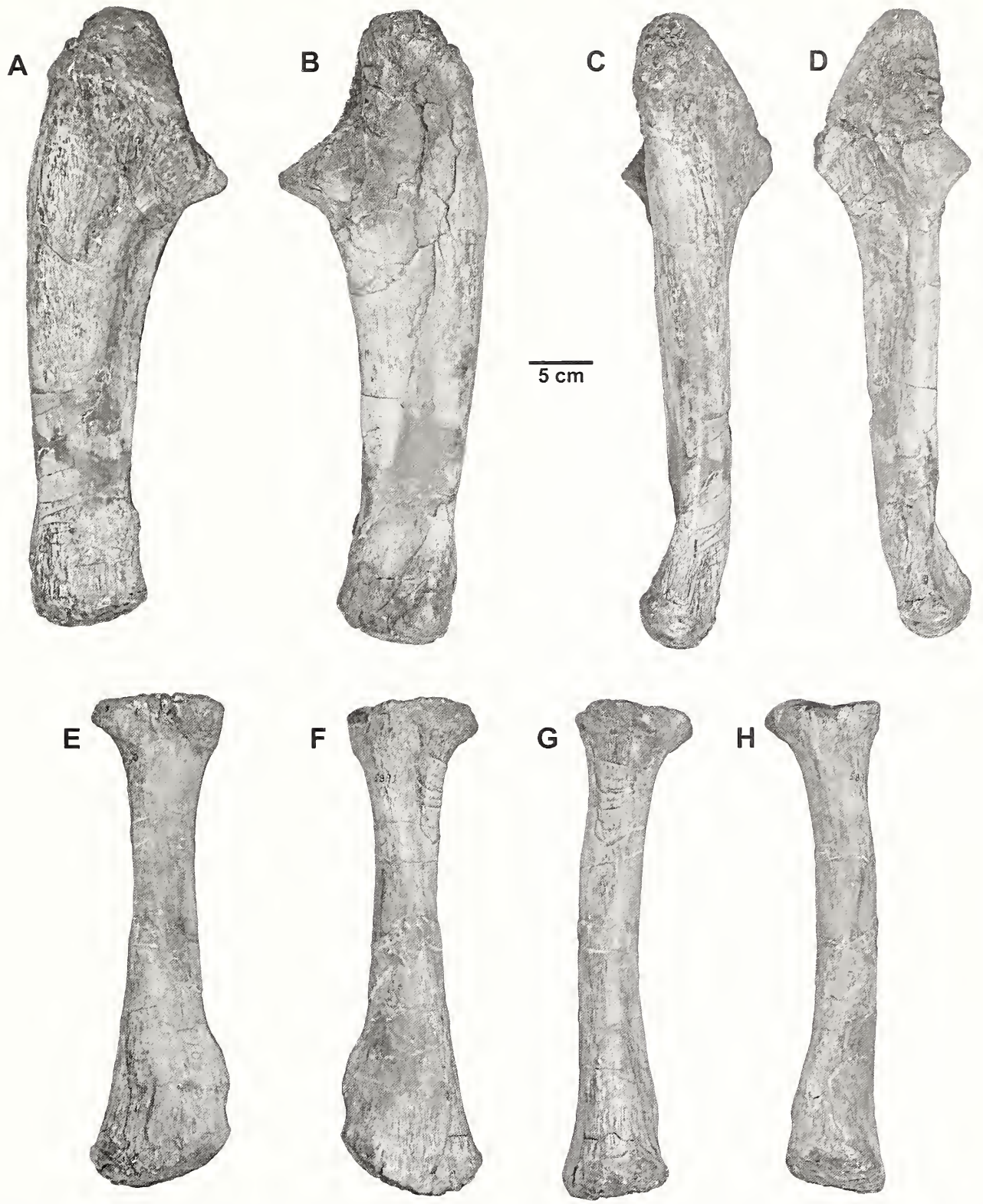

Figure 20. *Styracosaurus albertensis*, CMN 344. Right ulna in A, anterior, B, posterior, C, lateral, and D, medial views. Left radius in E, anterior, F, posterior, G, lateral, and F, medial views. Scale bar equals 5 cm.

described in sufficient detail to provide characters of phylogenetic utility (Maidment and Barrett, 2011). Notable exceptions are the centrosaurine *Centrosaurus* (Brown, 1917; Lull, 1933) and the chasmosaurine cf. *Anchiceratops* (Mallon and Holmes, 2010). In other taxa, skeletons originally described as complete or nearly so (e.g., Sternberg, 1927 for *Chasmosaurus*) have often turned out, under closer examination, to be much less complete than originally assumed (e.g., Mallon and Holmes, 2006), or, if

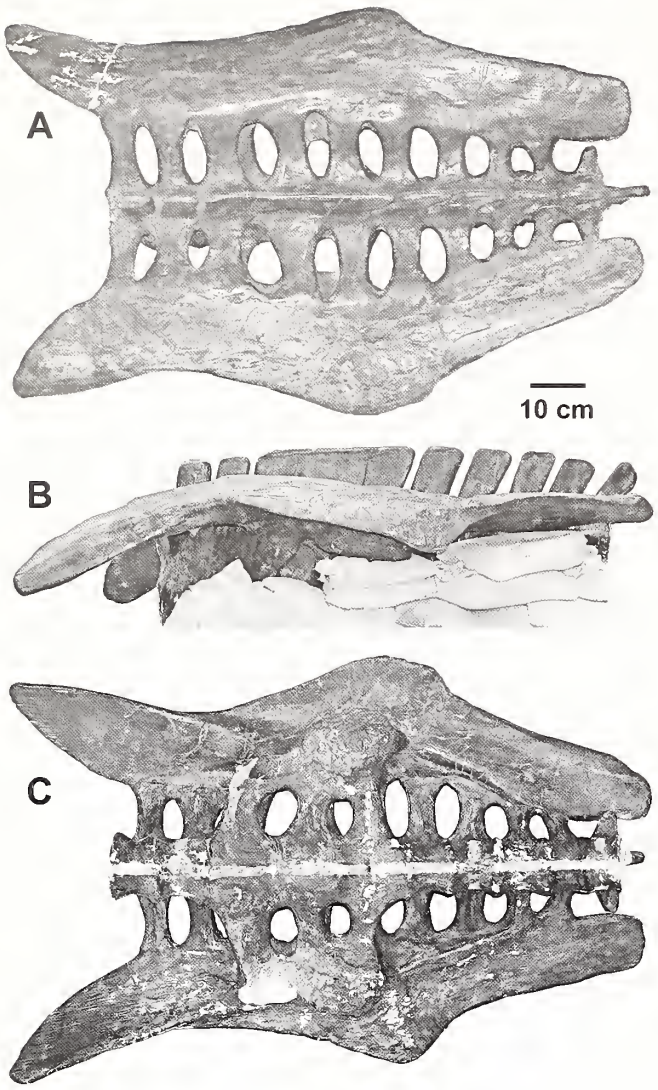

Figure 21. *Styracosaurus albertensis*, CMN 344, pelvic girdle. A, dorsal, B, left Lateral, and C, ventral views. Only the right ilium is preserved; the remainder is reconstructed in plaster. Scale bar equals 10 cm.

comprising a good percentage of the whole animal, still leave large gaps in our knowledge of the skeletal anatomy of these taxa. As a result, little is known about morphological diversity, whether rooted in intraspecific variation (including ontogenetic features and sexual dimorphism) or representing taxonomic distinctions, in the postcranial skeleton of ceratopsids. Consequently, phylogenetic analyses of the family still rest overwhelmingly on cranial characters (e.g., Dodson et al., 2004; Currie et al., 2009; Sampson et al., 2010). It is generally assumed that ceratopsids exhibit little or no inter-specific or inter-generic variability in postcranial anatomy. Although a recent morphometric study (Chinnery, 2004) generally supports this conclusion, it also indicates that some inter-subfamily differences do exist. Moreover, (Maidment and Barrett, 2011) have argued that there may be sufficient variation in discrete postcranial anatomical features to provide phylogenetically significant data. As such, a description of the postcranial skeleton of *Styracosaurus* is not only an important contribution to our understanding of ceratopsid anatomy, but also may contribute to the resolution of the phylogenetic relationships within the family. Although the results of this study do tend to support the contention that ceratopsids are quite conservative in their postcranial anatomy, comparison with the few ceratopsids for which we have significant data, in particular *Centrosaurus* and cf. *Anchiceratops* (CMN 8547), does suggest a few potentially important anatomical features that should be examined closely as more articulated skeletons are discovered.

Variation in the ceratopsid postcranial skeleton

In almost all ceratopsids, the syncervical (cervical bar) is formed by the fusion of the atlas, axis, and third cervical (Campione and Holmes, 2006; Tsuihiji and Makovicky, 2007). However, in at least one specimen (cf. *Anchiceratops*—see Mallon and Holmes, 2010), the fourth cervical vertebra fuses to the posterior end of the bar. However, it should be noted that this is essentially an extension of the process of co-ossification of the first three cervicals to form the syncervical, exhibited by all ceratopsids and at least some basal ceratopsians (Brown and Schlaikjer, 1940, 1942), and is likely an ontogenetic feature rather than one of taxonomic significance. The presence of a syncervical is almost certainly correlated with another characteristic of the family, specifically the very large head. Co-ossification of the cervical vertebrae to form a syncervical (and in the case of cf. *Anchiceratops*, the inclusion of the fourth cervical vertebra as well) presumably augmented the weight-bearing function of the cervical column.

The anterior free cervical vertebrae of both CMN 344 and TMP 1989.097.001 bear a deep pocket on the lateral surface of the centrum immediately under the base of the transverse process. The significance of this feature is uncertain. It has not been described for *Centrosaurus* (Brown, 1917; Lull, 1933), although it is present on the fourth and sixth cervicals (on the right side only) of one specimen of *Centrosaurus* (ROM 767, RH pers. obs. August, 2012). It has been described in some of the cervical vertebrae of one specimen of *Chasmosaurus* (Maidment and Barrett, 2011), but is completely absent from the well preserved cervical series in other well preserved *Chasmosaurus* specimens (CMN 2280, ROM 839, 843, RH pers. obs., August, 2012). Thus, it appears most likely that this character varies intraspecifically in ceratopsids, and is of no taxonomic significance.

Even allowing for postmortem distortion, the shapes of the vertebral centra appear to vary subtly from taxon to taxon. For example, the centra of the anterior cervicals are heart shaped in *Styracosaurus*, unlike *Triceratops*, in which they are circular to dorsally oval. This feature is hard to quantify, but vertebral centrum shape may still prove to be a valid feature to distinguish the vertebrae of various ceratopsid taxa.

Styracosaurus and *Centrosaurus* both show a progressive decrease in centrum length throughout the cervical series. In at least one specimen of *Chasmosaurus* (NHMUK R4948), both dimensions remain sub-equal throughout the cervical series (Maidment and Barrett, 2011, fig. 17), suggesting the possibility that this might represent a distinction between the two subfamilies. However, in another specimen of *Chasmosaurus* (CMN 2280), there is a subtle, but clear anteroposterior reduction in centrum length in the cervical column. This also appears to be the case in at least one specimen of *Triceratops* (Ostrom and Wellnhofer, 1986, plates 2–4). This may simply be an intraspecifically variable character and of no taxonomic significance in ceratopsids, but more complete, well preserved cervical columns are required to resolve this.

Figure 22. *Styracosaurus albertensis*, CMN 344, femora. Left femur in A, Anterior, C, posterior, E, lateral, and G, medial views. Left femur in B, anterior, D, posterior, F, lateral, and H, medial views. Scale bar equals 10 cm.

The number of cervical vertebrae is also known to vary within ceratopsids, although much of the apparent variability recorded in the literature can be traced to differing interpretations of syncervical structure and definitions of what constitutes a cervical vertebra. The syncervical has been hypothesized to have been derived by the fusion of either three or four vertebrae (see, e.g., Hatcher et al., 1907; Brown, 1917; Ostrom and Wellnhofer, 1986; Dodson et al., 2004). However, it now appears almost certain that

Figure 23. *Styracosaurus albertensis*, CMN 344. Left tibia in A, anterior; C, posterior, and E, lateral views. Right tibia in B, anterior, D, posterior, and F, lateral views. Left fibula in G, anterior, H, posterior, and I, medial views. Scale bar equals 10 cm.

it comprised only three vertebrae (Campione and Holmes, 2006; Tsuihiji and Makovicky, 2007), effeetively reducing the cervical count by one vertebra. Identification of the transition point between the cervical and dorsal columns has also proved to be contentious. Most authors define a ceratopsid cervical vertebra as possessing the lower rib facet (parapophysis) on the lateral surface of its centrum (e.g., Brown, 1917). They identify the transition to the first dorsal vertebra at the point where there is an abrupt shift of the parapophysis from the side of the centrum to the underside of the transverse process. A more subjective definition of this transition is associated with a gradual increase in the size and orientation of the neural spine and transverse processes (e.g., Hatcher et al., 1907; Ostrom and Wellnhofer, 1986) as well as enlargement of the neural canal and larger and more ventrally directed ribs associated with the transitional vertebrae (Lull, 1933). The unstated assumption appears to be that the enlarged neural canal for accommodation of the brachial plexus, as well as the presence of ribs long enough to have articulated with the sternum (and therefore contributed to the formation of the rib cage) indicate that these vertebrae should be considered to be part of the thoracic column. However, it has been demonstrated (Giffen, 1995) that in a wide variety of tetrapods, the brachial

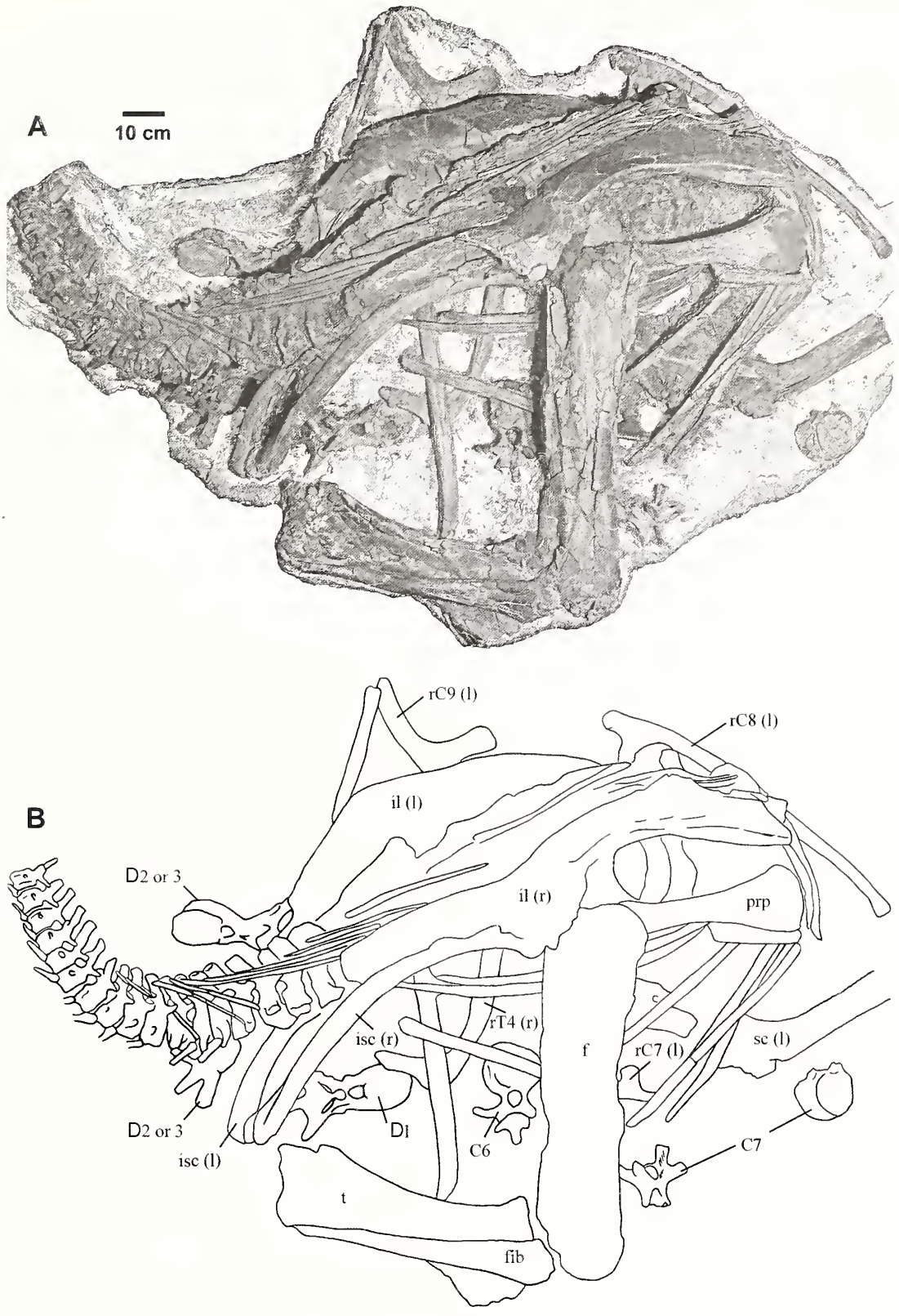

Figure 24. *Styracosaurus albertensis*, TMP 1989.097.001, pelvis, right rear limb, proximal caudal region, disarticulated vertebrae and ribs. A, photograph of specimen. B, outline drawing of specimen. Scale bar equals 10 cm.

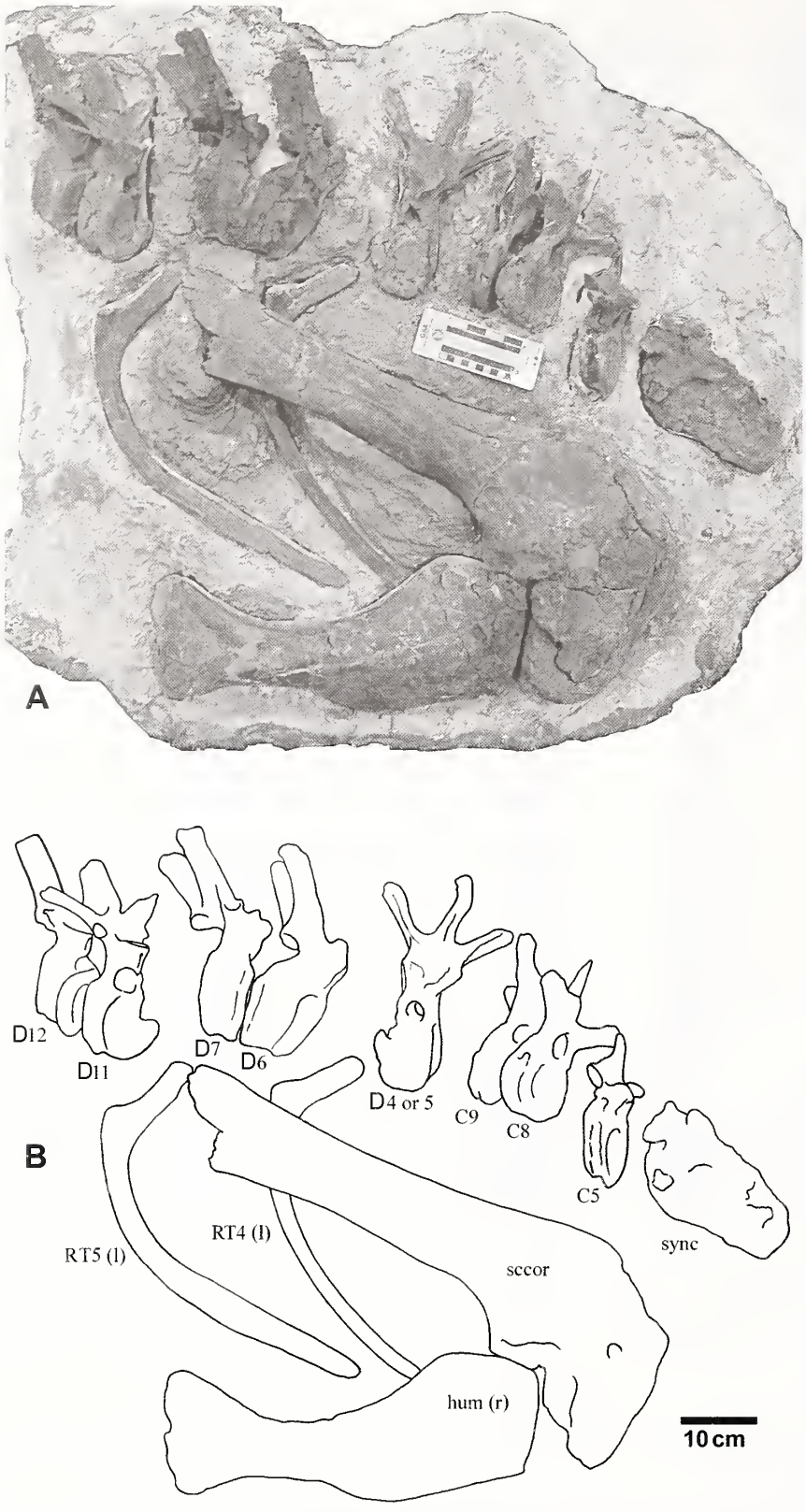

Figure 25. *Styracosaurus albertensis*, TMP 1989.097.001, partial vertebral column, right pectoral girdle, and limb. A, photograph of specimen as mounted. B, outline drawing of specimen. Scale bar equals 10 cm.

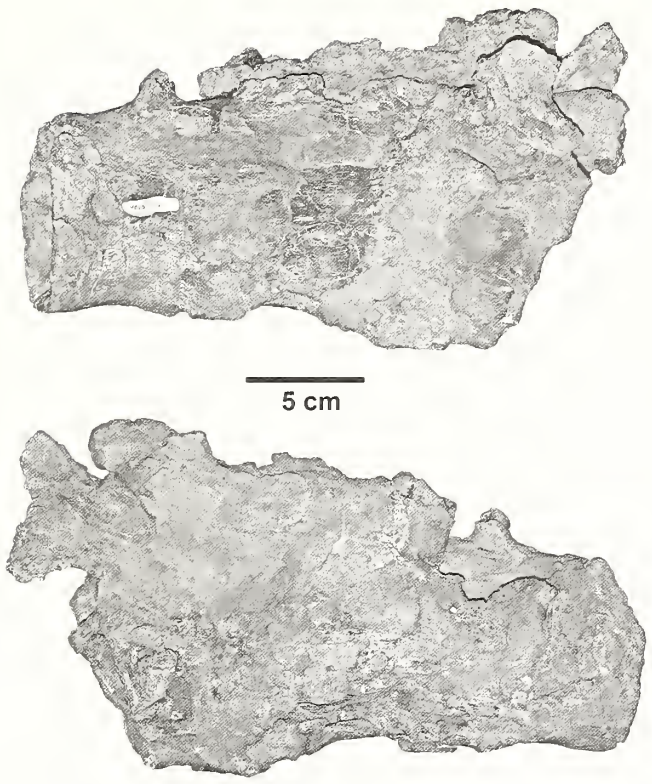

Figure 26. *Styracosaurus albertensis*, TMP 1989.097.001, syncervical. A, left lateral, and B, right lateral views.

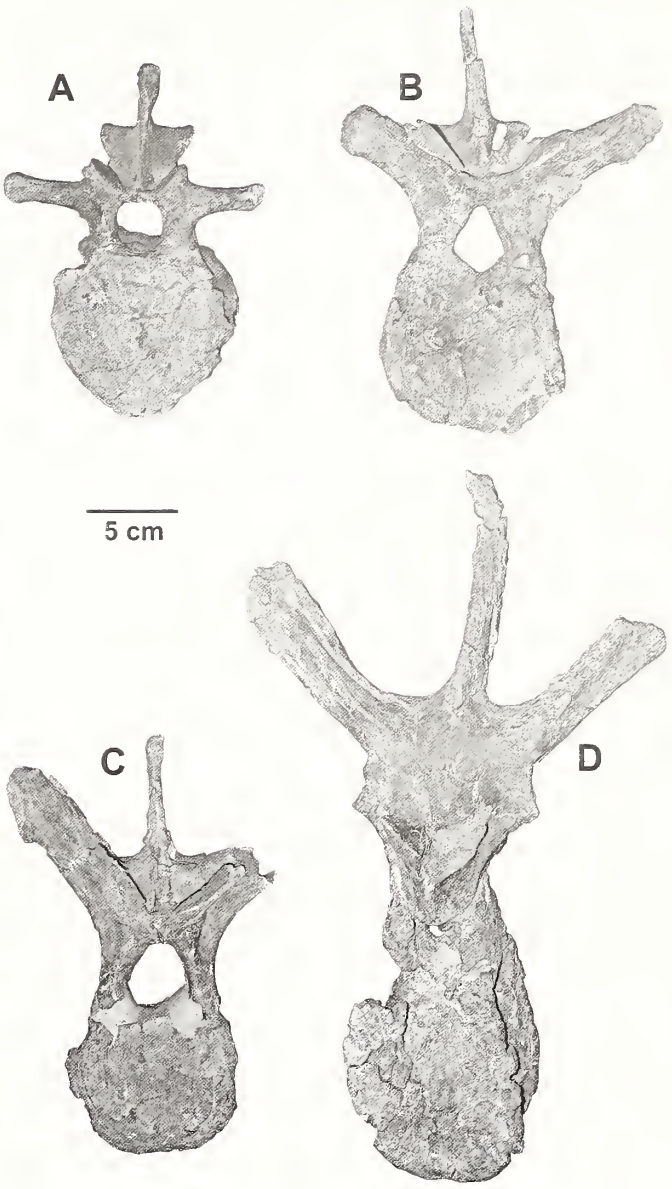

Figure 27. *Styracosaurus albertensis* TMP 1989.097.001. Vertebrae in anterior views. A, C5. B, C8. C, C9. D, D4 or 5. Scale bar equals 5 cm.

plexus is primarily associated with the posterior cervicals, with only relatively minor contributions from the most anterior few dorsal segments. Nevertheless, the ribs of the ninth vertebra (last cervical sensu Brown 1917, or second dorsal sensu Lull, 1933; Ostrom and Wellnhofer, 1986) appear to have had cartilaginous connections to the sternum, suggesting that it might be more properly considered, at least functionally, as part of the dorsal series. However, it must be remembered that the shoulder girdle of ceratopsid dinosaurs was located quite far forward on the body, and almost certainly encroached on the neck region (Figure 1). We suggest that the forward migration of the pectoral girdle is a specialization of the larger, quadrupedal ceratopsids. Why this should have occurred is uncertain, but it may have evolved to help support the large (and heavy) head characteristic of these animals. During the process, it 'captured' two ribs (and their associated vertebrae) whose homologies lie with the posterior cervical region. Although these ribs are modified to serve as part of the thoracic cage (being elongate, although only the more posterior has established a connection with the sternum for support), they both retain the diagnostic cervical rib articulation.

If it is accepted that the syncervical is tripartite, and that the transition from the cervical to thoracic region is marked by an abrupt transition of the parapophysis from the lateral surface of the centrum to the underside of the transverse process, then most ceratopsids have nine cervical and 12 dorsal vertebrae. This is true of *Centrosaurus* (Brown, 1917; Lull, 1933) and *Chasmosaurus* (CMN 2245, 2280, Mallon and Holmes, 2006; ROM 843, RH pers. obs., August, 2012, contra Maidment and Barrett, 2011). The type specimen of *Styracosaurus* exhibits these cervical and dorsal counts, but because the sacrum is not preserved, the number of dorsosacrals is unknown. TMP 1989.097.001 is incomplete, comprising one less cervical and four fewer dorsal vertebrae, but each of the preserved presacral vertebrae can be confidently matched to its homologue in the type (CMN 344). The absence of any vertebrae showing morphology distinct from any of the type vertebrae suggests that it is unlikely that any of the vertebrae of the latter are missing, and a total of 21 presacrals is the true count for *Styracosaurus*. However, some variation in vertebral numbers is known to exist within ceratopsids. At least one specimen of cf. *Anchiceratops* (CMN 8547) has 10 cervicals rather than nine, and the thorax comprises 13 (rather than 12) vertebrae, for a total of 23 presacral vertebrae (Mallon and Holmes, 2010).

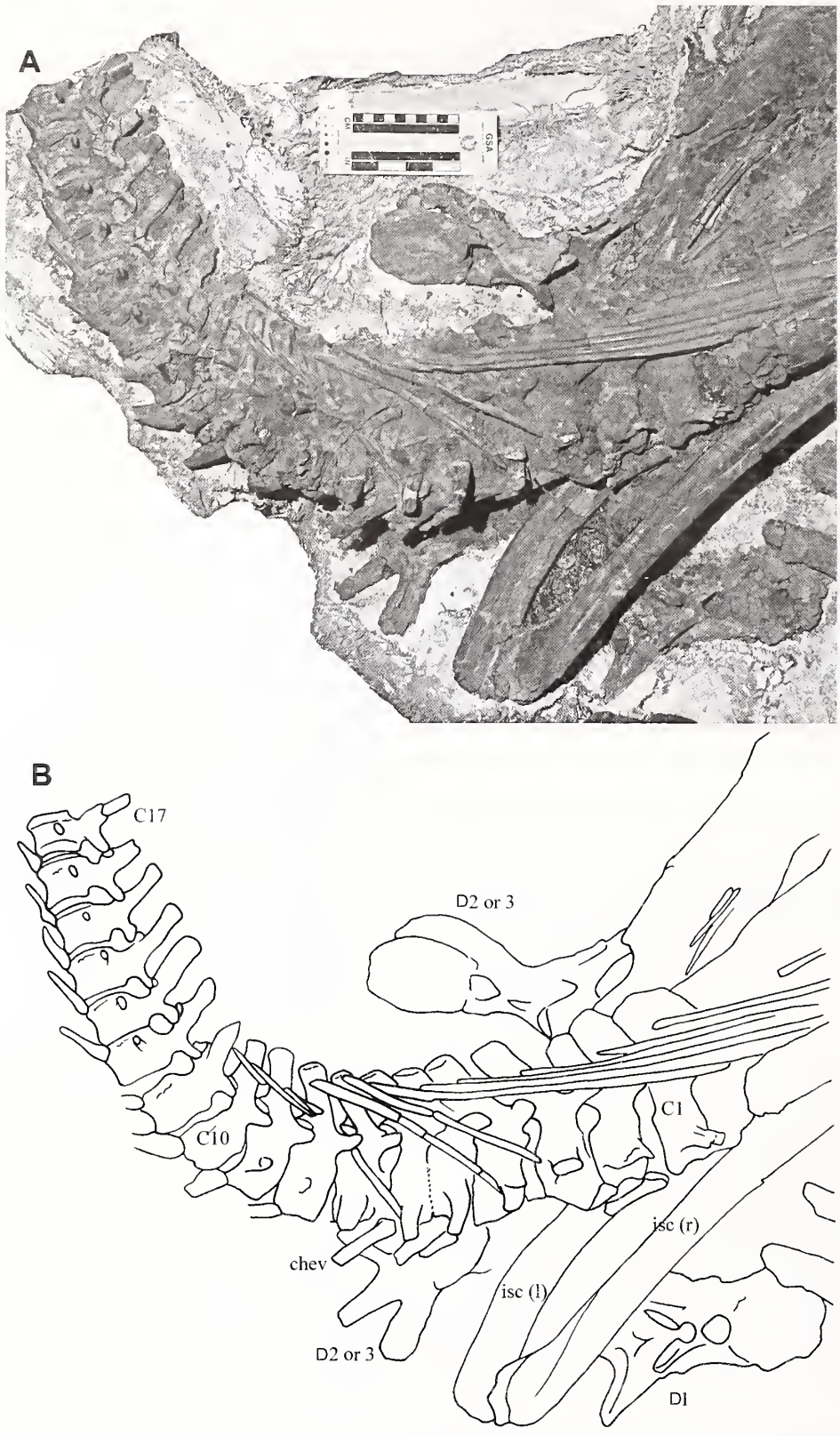

Figure 28. *Styracosaurus albertensis* TMP 1989.097.001. Articulated proximal portion of the tail. A, photograph of the specimen. B, outline drawing of the specimen.

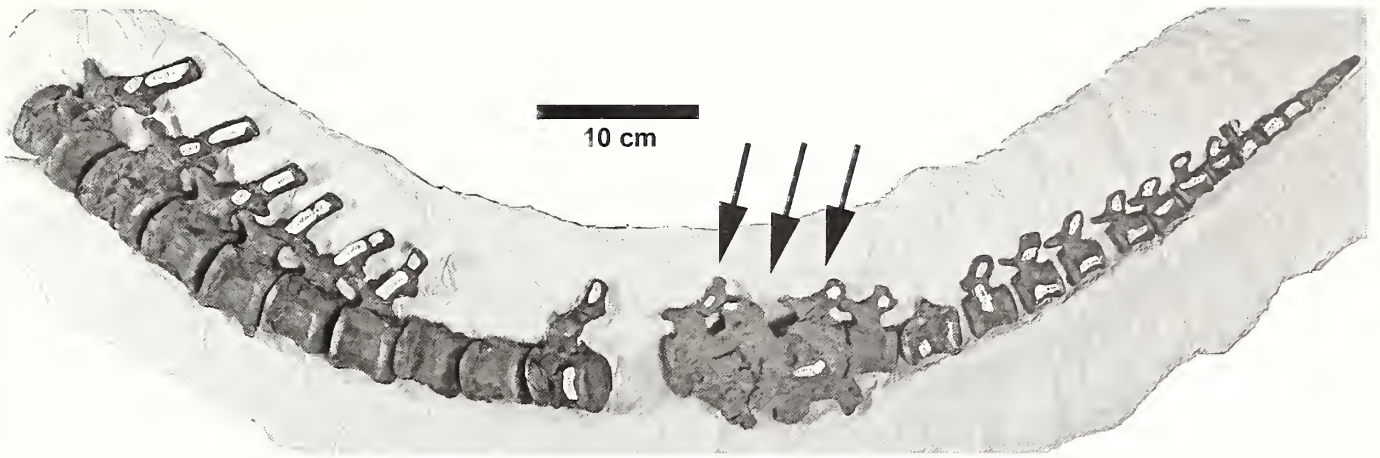

Figure 29. *Styracosaurus albertensis*, TMP 1989.097.001, caudal vertebrae 18–45 in left lateral view. Arrows indicate region of pathological vertebrae. Scale bar equals 10 cm.

The sacrum of ceratopsids comprises four co-ossified vertebrae. A variable number of vertebrae, usually referred to as dorsosacrals, co-ossified to the front of the sacrum. Together with the sacrum and a variable number of caudal vertebrae that fused to the posterior end of the sacrum, they comprise the sacral bar. Most commonly, ceratopsids have one dorsosacral between the 12th dorsal vertebra and the first sacral vertebra. This condition has been reported in *Centrosaurus* (Brown, 1917: plate XIIB; Lull, 1933, fig. 18). The same count occurs in some specimens of *Chasmosaurus* (CMN 2245 contra Maidment and Barrett, 2011). This is precisely the same count seen in the basal ceratopsians *Protoceratops* (Brown and Schlaikjer, 1940), *Montanoceratops* (Brown and Schlaikjer, 1942), and possibly *Leptoceratops* (CMN 8889, RH, pers. obs., August, 2012), suggesting that this is most likely the primitive count for ceratopsids. However, it should be noted that although *Leptoceratops* (CMN 8889) possesses a single dorsosacral bearing a roughened posterior centrum articulation that suggests incomplete co-ossification with the element posterior to it, the sacrum is not preserved. Therefore, it is uncertain whether it articulated with the first sacral vertebra, or a second (unpreserved) dorsosacral. The type of *Styracosaurus* shares these cervical and dorsal counts, but the sacrum is not preserved, and the number of dorsosacrals is unknown.

Dorsosacrals are most parsimoniously homologized with posterior dorsal vertebrae that were incorporated at some point in the ontogeny of the individual into the sacral bar. In at least one specimen of *Centrosaurus* (Lull, 1933), the last (12th) dorsal vertebra had begun to fuse to the front of the synsacrum at the time of death, effectively becoming a second dorsosacral. Essentially the same condition has been described in *Pentaceratops* (Wiman, 1930; Lehman, 1998, fig. 6). However, the number of dorsosacrals appears to vary from individual to individual (or possibly taxon to taxon). This could plausibly be accounted for by progressive incorporation of posterior dorsal vertebrae into the sacral bar during growth, except that the increase in the number of dorsosacrals is not always compensated for by a corresponding reduction in the number of dorsal vertebrae. *Vagaceratops* (=*Chasmosaurus*) *irvinensis* (CMN 41357) has two dorsosacrals fused to the front of the sacral bar (RH, pers. obs., February,

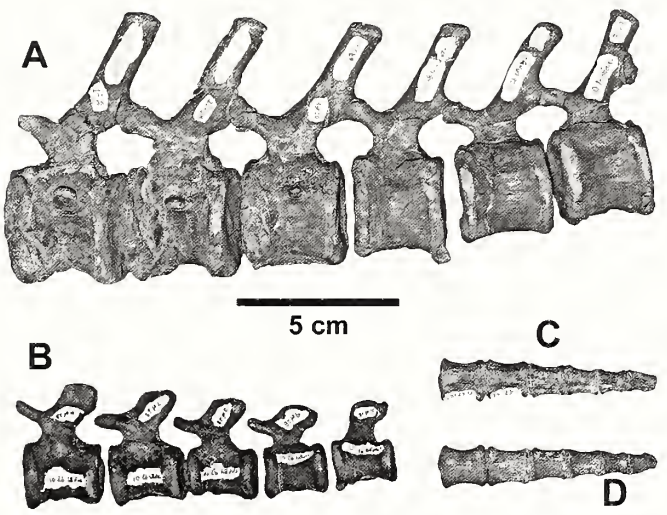

Figure 30. *Styracosaurus albertensis*, TMP 1989.097.001, caudal vertebrae. A, Ca18–23 in left lateral view. B, Ca33–37 in left lateral view. Terminal six (Ca40–45) in C, dorsal and D, ventral views. Scale bar equals 5 cm.

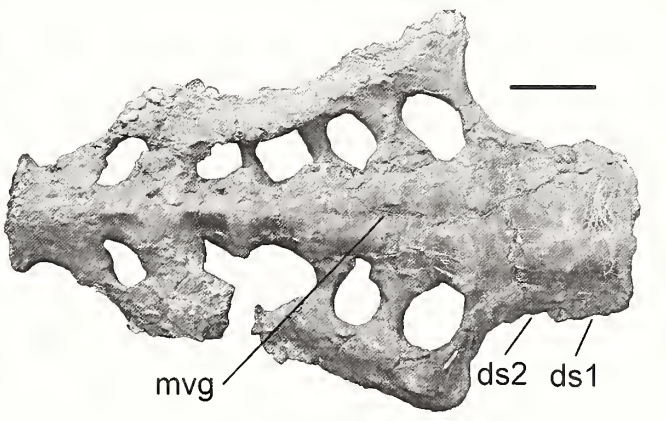

Figure 31. *Styracosaurus albertensis*. TMP 2009.080.001. Ventral view of synsacrum. Scale bar equals 10 cm.

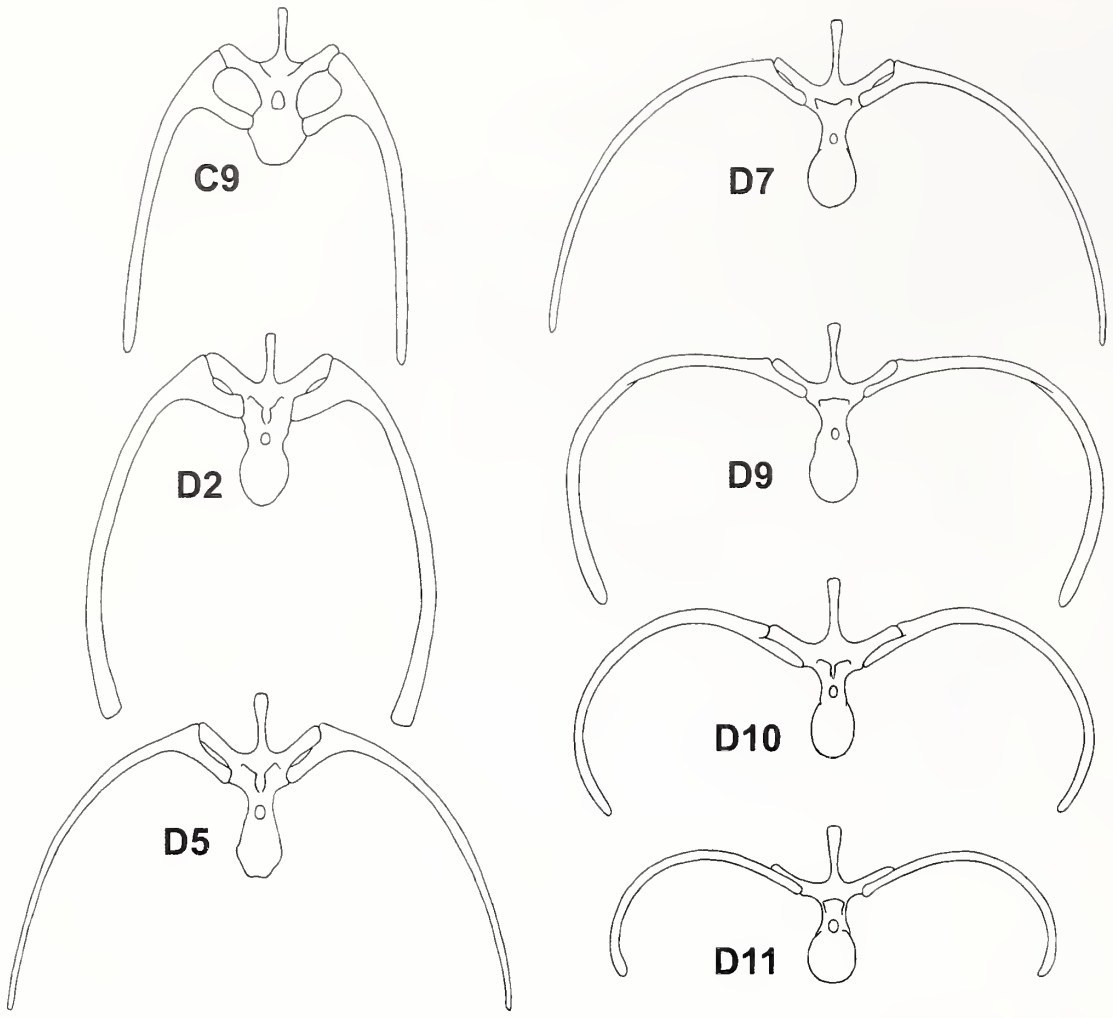

Figure 32. *Styracosaurus albertensis*. Vertebrae and associated ribs from selected points in the presacral column in anterior view.

2012). The more anterior vertebra (13th postcervical) bears a pair of flat, laterally and slightly anteriorly projecting ribs fused to the ends of the diapophyses. Very similar (although unfused) ribs have been described in association with the 12th postcervical rib in *Centrosaurus* (Lull, 1933). In the latter taxon, they lie along the inner surface of the ilium (the ilium is not preserved in CMN 41357). In one specimen of *Chasmosaurus* (ROM 843), there are two dorsosacrals between the last (12th) dorsal and first sacral vertebrae. The first bears a pair of flat, anterolaterally directed ribs that articulate throughout most of their lengths with the dorsomedial edge of the ilium. The rib, which bears no capitulum, is fused to the end of the transverse process, but the suture is still visible. The more posterior dorsosacral bears dorsoventrally flattened, distally expanded transverse processes that articulate with the ilium. No separate rib is evident. This specimen is unusual in that the last dorsal (12th) vertebra fused to the anterior end of the sacral bar before death (so is functionally a dorsosacral), leaving only 11 free dorsal vertebrae. However, a cast of the specimen, on display at the Royal Ontario Museum has a dorsal series comprising 12 free vertebrae in addition to the three vertebrae fused to the anterior end of the sacrum. Close examination of the cast revealed that two of the vertebrae (probably representing D8 or D9) in the mount are exact duplicates (RH, pers. obs., August, 2012)—apparently an extra vertebra was cast during the preparation of the mount and added to the vertebral column, presumably because the technicians believed that one had been lost. This appears to be the source of the unusually high presacral + dorsosacral count reported for this specimen (Maidment and Barrett, 2011).

Triceratops is problematic (Ostrom and Wellnhofer, 1986). Hatcher (1907) appears to suggest that there are two dorsosacrals in USNM 4842 (Hatcher, 1907, figs. 53, 54), but equivocates. However, in the recently described *Triceratops* specimen (NSM PV 20379), 21 presacral vertebrae are identified (Fujiwara, 2009, fig. 2), but the rib associated with the last (his 'p21') looks more like the rib associated with the 11th dorsal vertebra of other ceratopsids (note its anterior curvature and articulation with the pubis) and the rib associated with 's1' (the 22nd presacral) is directed strongly anteriorly and appears to lie along the medial surface of the ilium, much like that of the 21st presacral rib of *Styracosaurus*, suggesting that NSM PV 20379 has one vertebra more than the usual 22 presacrals + one dorsosacral.

A major difficulty in assessing the significance of dorsosacral count is that in many ceratopsid specimens the sacrum is not preserved, or is obscured by the ilium so that the precise location of the first sacral vertebra cannot be established. Without being

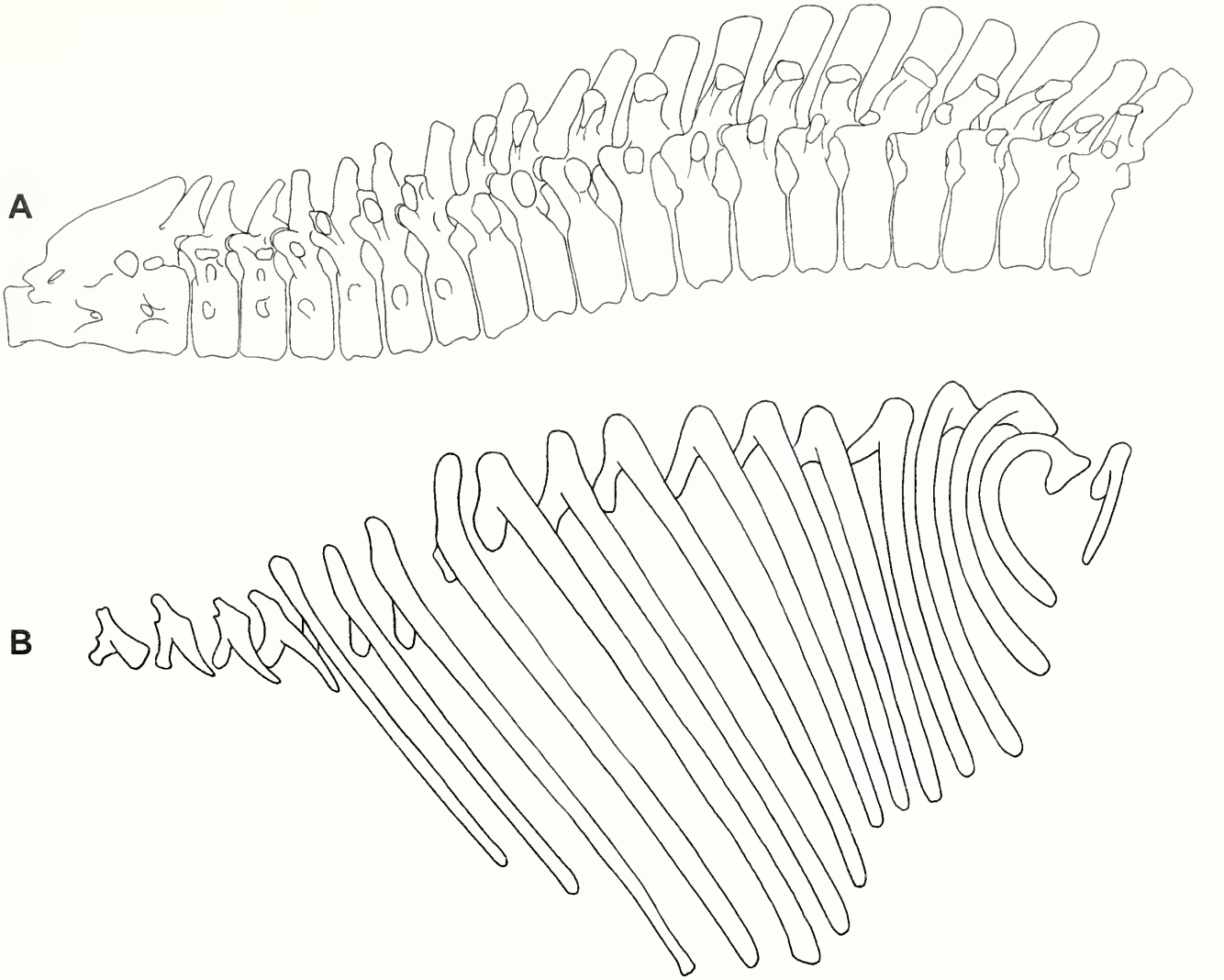

Figure 33. *Styracosaurus albertensis*. A, presacral column in left lateral view, B, set of ribs (C3 to D12) in left lateral view drawn to the same scale as vertebrae in A.

able to establish the position of the sacral vertebrae, it is not possible to distinguish dorsosacrals from late fusing posterior dorsal vertebrae. Such is the case in *Styracosaurus*. The sacrum is not preserved in the type (CMN 344). Although the pelvis and sacrum of TMP 1989.097.001 appear to be complete, the sacral ribs are obscured by the ilia. The only known sacrum that can be unambiguously identified as pertaining to *Styracosaurus* (TMP 2009.080.001, Figure 31) includes two putative dorsosacrals, but as most of the disarticulated presacral column is not preserved in this specimen, it is impossible to determine whether this is in addition to the regular 21 presacrals (i.e., homologous to the dorsosacral of most other ceratopsids), or represents a fusion of the last (presumably 21st) dorsal vertebra to the sacral bar, as occurs in one specimen of *Centrosaurus* (Lull, 1933).

Although it is reasonable to assume that the number of proximal caudal vertebrae that become incorporated into the sacral bar as caudosacrals also varies with age and/or taxon, data are even scarcer than they are for dorsosacrals. In one specimen of *Centrosaurus* (Lull, 1933), there are five caudosacrals fused to the sacrum, but the transverse processes of the most posterior vertebra do not contact the ilium. *Pentaceratops* is described as having four caudosacrals (Wiman, 1930, plate V), as is *Triceratops* (USNM 4842—see Hatcher et al., 1907, fig. 53, 55) although, as described for *Pentaceratops*, the transverse processes of the most posterior vertebra are short and do not contact the ilium. *Chasmosaurus* (ROM 843) has four caudosacrals (Maidment and Barrett, 2011), but again, the anterolaterally-directed transverse processes more closely resemble those of the proximal caudal vertebrae, and do not articulate with the ilium.

Very few ceratopsids have complete tails. Available data suggest that chasmosaurines had shorter tails than centrosaurines, although the possibility of intra-generic, or even intra-specific variation within ceratopsians (e.g., Hone, 2012) renders this generalization potentially problematic. Nevertheless, it is known that *Pentaceratops* has perhaps a few more than 30 caudal vertebrae (Wiman, 1930). The most complete *Chasmosaurus* tail (CMN 2245) has only 21 vertebrae (see Mallon and Holmes, 2006, fig. 3; pers. obs., March, 2011), but judging from the size of the most distal element, the complete tail could not have comprised more than 40 vertebrae. At least one specimen of cf. *Anchiceratops*

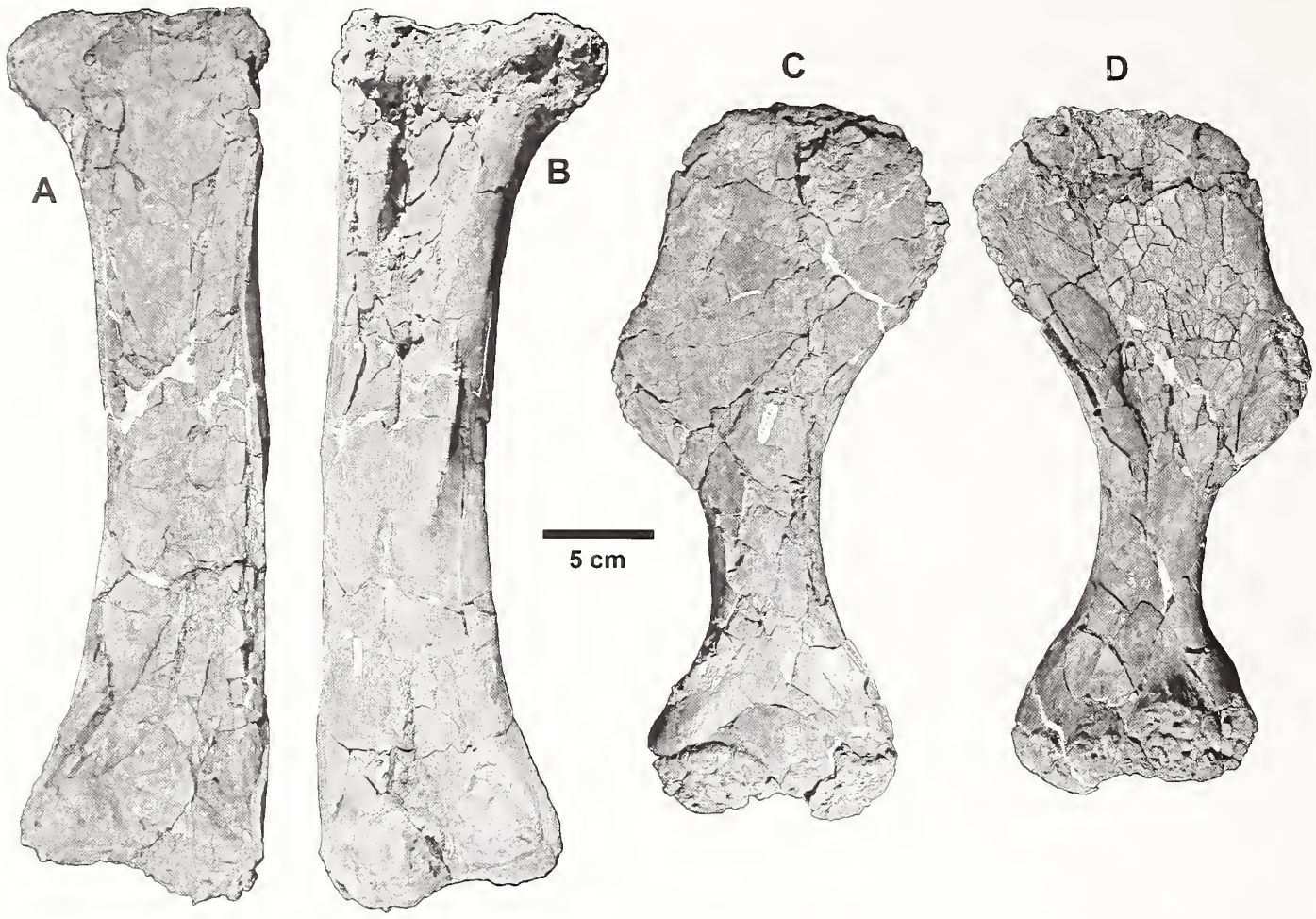

Figure 34. *Styracosaurus albertensis*, TMP 1989.097.001. Left femur in A, dorsal and B, ventral views. Humerus in C, dorsal and D, ventral views. Scale bar equals 5 cm.

(CMN 8547) has 39 caudal vertebrae (Mallon and Holmes, 2010), but this may be related to the combination of a posterior migration of the pelvis, in effect 'creating' one extra cervical and one extra dorsal vertebra, and the incorporation of two extra vertebrae into the synsacrum (see above), essentially removing two more segments from the tail of this individual. Even so, the caudal count would be very close to that reconstructed for *Chasmosaurus*. Centrosaurines, as far as is known, have higher counts, with 46 in *Centrosaurus* (Brown, 1917), 45 in *Styracosaurus*, and 47 in *Brachyceratops* (Gilmore, 1917).

The first four cervical ribs of *Styracosaurus* (C3 to C6) are quite short. The fifth (C7) is considerably longer, being at least two-thirds the length of the longest thoracic rib. The ribs at C8 and C9 become gradually longer. This resembles the situation in *Centrosaurus* (Brown, 1917), but is distinct from that in *Triceratops*, where the ribs on C7 are also short (Hatcher et al., 1907; Ostrom and Wellnhofer, 1986), and so there is an abrupt increase in rib length at the eighth cervical vertebra. In cf. *Anchiceratops*, the seventh cervical rib shows the same morphology as the more anterior ribs in having a short, upturned, spine-like shaft. The eighth rib has a more conventional posteroventrally directed shaft, but it is still quite short. The ninth cervical rib is much longer (its shaft is about 2/3 the length of the longest trunk ribs) and stouter, and the tenth (last) cervical rib is as long as the longest trunk ribs. These differences between the ribs of cf. *Anchiceratops* and those of other ceratopsids is presumably correlated to the possession of an extra cervical vertebra in this taxon.

Maidment and Barrett (2011) have suggested that the morphology of the acromial process of the scapula differs in the two subfamilies, with the process being larger and more conspicuous in chasmosaurines. In *Styracosaurus*, the process is actually quite prominent, curving laterally from its base, albeit restricted to the proximal end of the seapula, as pointed out by Maidment and Barrett (2011). Essentially the same morphology is seen in *Centrosaurus* (AMNH 5351, RH pers. obs., August, 2012). In at least some specimens of *Chasmosaurus* (CMN 2245, NHMUK R4948), the process is very indistinct, and appears to be represented by a low, but much longer crest that sweeps farther distally on the anterior edge of the scapula. However, in the chasmosaurine *Triceratops*, the process is quite distinct (Hatcher et al., 1907, fig.64), suggesting that relative size and shape of the process may be an ontogenetic or allometric feature.

The form of the humerus may differ between the two subfamilies as well (Chinnery, 2004; Maidment and Barrett, 2011). Two features mentioned by the latter authors, the relative size of the triceps fossa and the size and position of the foramen that possibly marks the insertion of the latissimus dorsi, were

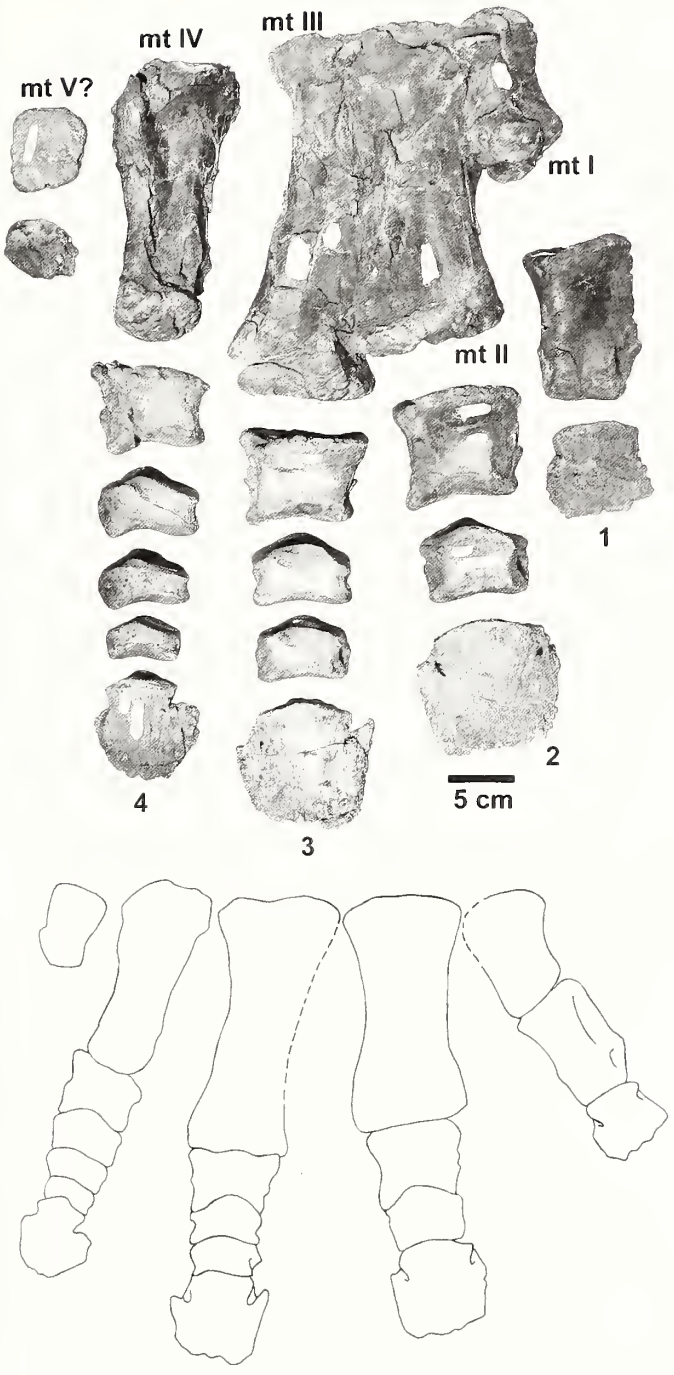

Figure 35. *Styracosaurus albertensis*, TMP 1989.097.001, right pes in dorsal view. Exploded (upper) and articulated (lower). Scale bar equals 5 cm.

difficult for us to assess in most of the specimens we examined as a result of crushing and/or poor preservation. However, the morphology of the proximal humeral head is more often preserved, and we confirm Maidment and Barrett's (2011) observation that the anterior margin of the deltopectoral crest is arched distinctly dorsally in all centrosaurines examined, and that in chasmosaurines (e.g., CMN 2245, 2280, ROM 843), this arching is much less pronounced. In addition, the deltopectoral crest of chasmosaurines is distinctly rectangular in outline, much more massive, and the insertion for the pectoralis muscle is located more distally. In centrosaurines, the pectoralis insertion is more proximal, and the smaller proximal head is distinctly narrower in outline proximally than it is distally.

Acknowledgments

B. Strilisky and J. Gardner provided access to specimens at the Royal Tyrrell Museum, and B. Strilisky provided specimen data. J. Campbell photographed the sacrum of TMP 2009.080.001. C. Kennedy and S. Swann expertly remounted CMN 344. K. Shepherd and M. Currie provided collections assistance at the Canadian Museum of Nature, and A. Murray provided photographic assistance and helpful discussions. Reviews by B. Chinnery-Allgeier and J. Mallon helped improve the manuscript.

References

Brown, B. 1917. A complete skeleton of the horned dinosaur *Monoclonius*, and a description of a second skeleton showing skin impressions. Bulletin of the American Museum of Natural History, 37:281–306.

Brown, B., and E. M. Schlaikjer. 1937. The skeleton of *Styracosaurus* with the description of a new species. American Museum Novitates, 955:1–12.

Brown, B., and E. M. Schlaikjer. 1940. The structure and relationships of *Protoceratops*. Annals of the New York Academy of Sciences, 40:133–266.

Brown, B., and E. M. Schlaikjer. 1942. The skeleton of *Leptoceratops* with the description of a new species. American Museum Novitates, 1169:1–15.

Campione, N., and R. Holmes. 2006. The anatomy and homologies of the ceratopsid syncervical. Journal of Vertebrate Paleontology, 26:1014–1017.

Chinnery, B. 2004. Morphometric analysis of evolutionary trends in the ceratopsian postcranial skeleton. Journal of Vertebrate Paleontology, 24:591–609.

Currie, P. J., and D. A. Russell. 2005. The geographic and stratigraphic distribution of articulated and associated dinosaur remains, p. 537–569. *In* P. J. Currie and E. Koppelhus (eds.), Dinosaur Provincial Park: A Spectacular Ancient Ecosystem Revealed. Indiana University Press, Bloomington.

Currie, P. J., W. Langston, Jr., and D. H. Tanke. 2008. A new species of *Pachyrhinosaurus* (Dinosauria, Ceratopsidae) from the Upper Cretaceous of Alberta, Canada, p. 1–108. *In* P. J. Currie, W. Langston, Jr, and D. H. Tanke (eds.), A New Horned Dinosaur from an Upper Cretaceous Bone Bed in Alberta, Canada. National Research Council Press, Ottawa.

Dodson, P., and J. O. Farlow. 1997. The forelimb carriage of ceratopsid dinosaurs, p. 393–398. *In* D. L. Wolberg, E. Stump, and G. D. Rosenberg (eds.), Dinofest International. Academy of Natural Sciences, Philadelphia.

Dodson, P., C. Forster, and S. Sampson. 2004. Ceratopsidae, p. 494–513. *In* D. Weishampel, P. Dodson, and H. Osmólska (eds.), The Dinosauria, Second Edition. University of California Press, Los Angeles.

Fujiwara, S.-I. 2009. A reevaluation of the manus structure in *Triceratops* (Ceratopsia: Ceratopsidae). Journal of Vertebrate Paleontology, 29:1136–1147.

Giffen, F. 1995. Functional interpretations of spinal cord anatomy in living and fossil amniotes, p. 235–248. *In* J. J.

Table 1. Selected postcranial measurements (in mm) of *Styracosaurus albertensis*.

	Centrum length (max.)	Centrum width (max.)	Vertebra height (max.)
CMN 344			
Syncervical (1–3)	265	111	247
Cervical 4	67	115	254
Cervical 5	66	117	254
Cervical 6	64	114	274
Cervical 7	63	111	287
Cervical 8	63	106	300
Cervical 9	62	100	308
Thoracic 1	66	94	338
Thoracic 2	65	94	338
Thoracic 3	65	92	348
Thoracic 4	67	90	358
Thoracic 5	72	92	386
Thoracic 6	68	92	392
Thoracic 7	67	90	381
Thoracic 8	76	92	384
Thoracic 9	68	95	362
Thoracic 10	68	92	378
Thoracic 11	67	100	339
Thoracic 12	69	92	339
Caudal 1	65	80	252
Caudal 5	48	85	220
TMP 1989.097.001			
Cervical 5	–	97	161
Cervical 8	–	102	198
Cervical 9	–	97	193
Thoracic 5	–	98	326

	CMN 344		TMP 1989.097.001	
	Left	Right	Left	Right
Pectoral Girdle and Forelimb				
Scapula length	770	800	–	660
Scapula width (max.)	260	260	–	200
Coracoid length	–	360	–	210
Sternal plate length	–	340	–	–
Humerus length	595	630	510	500
Radius length	380	390	–	–
Metacarpal I	–	81	–	–
Metacarpal IV	105	–	–	–
Pelvic Girdle and Hind Limb				
Ilium length	–	1050	–	660
Ischium max. linear length	795	830	–	800
Prepubis length	–	–	–	350
Femur length	840	810	685	690
Tibia length	610	610	–	460
Fibula length	572	–	–	–
Metatarsal II	175	–	–	186

Thomason (ed.), Functional Morphology in Vertebrate Paleontology. Cambridge University Press, Cambridge, UK.

Gilmore, C. W. 1917. *Brachyceratops*, a ceratopsian dinosaur from the Two Medicine Formation of Montana. United States Geological Survey Professional Paper, 103:1–45.

Hatcher, J. B., O. C. Marsh, and R. S. Lull. 1907. The Ceratopsia. United States Geological Survey Monograph, 49:1–300.

Holmes, R., M. J. Ryan, and A. M. Murray. 2005. Photographic atlas of the postcranial skeleton of the type specimen of *Styracosaurus albertensis* with additional isolated cranial elements from Alberta. Syllogeus, 75:1–75.

Hone, D. W. E. 2012. Variation in the tail length of non-avian dinosaurs. Journal of Vertebrate Paleontology, 32:1082–1089.

Kozisek, J., and K. Derstler. 2004. Scapular facets on the dorsal ribs of sauropods and neoceratopsian dinosaurs. Journal of Vertebrate Paleontology, 24(supplement to number 3):80A.

Lambe, L. 1913. A new genus and species of Ceratopsia from the Belly River Formation of Alberta. Ottawa Naturalist, 27:109–116.

Larson, P., and C. Ott. 2004. Triceresies—a bold new look at *Triceratops*. Journal of Vertebrate Paleontology, 24(supplement to number 3):82A.

Lehman, T. M. 1989. *Chasmosaurus mariscalensis*, sp. nov., a new ceratopsian dinosaur from Texas. Journal of Vertebrae Paleontology, 9:137–162.

Lehman, T. M. 1998. A gigantic skull and skeleton of the horned dinosaur *Pentaceratops sternbergi* from New Mexico. Journal of Paleontology, 72:894–906.

Lull, R. S. 1933. A revision of the Ceratopsia or horned dinosaurs. Memoires of the Peabody Museum of Natural History, 3:1–175.

Maidment, S. C. R., and P. M. Barrett. 2011. A new specimen of *Chasmosaurus belli* (Ornithischia: Ceratopsidae), a revision of the genus, and the utility of postcrania in the taxonomy and systematics of ceratopsid dinosaurs. Zootaxa, 2963:1–47.

Mallon, J. C., and R. B. Holmes. 2006. A reevaluation of sexual dimorphism in the postcranium of the chasmosaurine ceratopsid *Chasmosaurus belli* (Dinosauria: Ornithischia). Canadian Field Naturalist, 120:403–412.

Mallon, J. C., and R. Holmes. 2010. Description of a complete and fully articulated chasmosaurine postcranium previously assigned to *Anchiceratops* (Dinosauria: Ceratopsia), p. 189–202. *In* M. J. Ryan, D. A. Eberth, and B. J. Chinnery-Allgeier (eds.), New Perspectives on Horned Dinosaurs: The Royal Tyrrell Museum Ceratopsian Symposium. Indiana University Press, Bloomington.

Ostrom, J. H., and P. Wellnhofer. 1986. The Munich specimen of *Triceratops* with a revision of the genus. Zitteliana, 14:111–158.

Ryan, M. J., and D. C. Evans. 2005. Ornithischian dinosaurs, p. 312–348. *In* P. J. Currie and E. B. Koppelhus (eds.), Dinosaur Provincial Park. A Spectacular Ancient Ecosystem Revealed. Indiana University Press, Bloomington.

Ryan, M. J., R. Holmes, and A. P. Russell. 2007. A revision of the late Campanian centrosaurine ceratopsid genus *Styracosaurus* from the Western Interior of North America. Journal of Vertebrate Paleontology, 27:944–962.

Ryan, M. J., D. C. Evans, P. J. Currie, C. M. Brown, and D. Brinkman. 2012. New leptoceratopsids from the Upper Cretaceous of Alberta, Canada. Cretaceous Research, 35: 69–80.

Sampson, S., M. A. Loewen, A. A. Farke, E. M. Roberts, C. A. Forster, J. A. Smith, and A. L. Titus. 2010. New horned dinosaurs from Utah provide evidence for intracontinental dinosaur endemism. PLoS One, 5(9):1–11.

Sternberg, C. M. 1927. Horned dinosaur group in the National Museum of Canada. Canadian Field Naturalist, 41:67–73.

Sternberg, C. M. 1951. Complete skeleton of *Leptoceratops gracilis* Brown from the Upper Edmonton Member on the Red Deer River, Alberta. Bulletin of the National Museum of Canada, 123:225–255.

Thompson, S., and R. Holmes. 2007. Forelimb stance and step cycle in *Chasmosaurus irvinensis* (Dinosauria: Neoceratopsia). Palaeontologia Electronica, 10(1):5A:17.

Tsuihiji, T., and P. Makovicky. 2007. Homology of the neoceratopsian cervical bar elements. Journal of Paleontology, 81:1132–1138.

You, H., and P. Dodson. 2010. Basal Ceratopsia, p. 478–493. *In* D. B. Weishampel, P. Dodson, and H. Osmolska (eds.), The Dinosauria, Second Edition. University of California Press, Berkeley and Los Angeles, CA.

Wiman, C. 1930. Über Ceratopsia aus der Oberen Kreide in New Mexico. Nova Acta Regeae Societas Scientarum Upsaliensis, 7:1–19.

KIRTLANDIA
The Cleveland Museum of Natural History

March 2013 *Number 58:38–41*

BONE "TAXON" B: REEVALUATION OF A SUPPOSED SMALL THEROPOD DINOSAUR FROM THE MID-CRETACEOUS OF MOROCCO

BRADLEY McFEETERS
Dept. of Earth Sciences
Carleton University, Ottawa, Ontario, Canada, K1S 5B6
bmcfeete@connect.carleton.ca

ABSTRACT

Two cervical vertebrae from the Kem Kem beds of Morocco have been referred to "Bone 'Taxon' B," representing a small theropod of indeterminate affinity. Reexamination of the vertebrae indicates that they are both probably from immature individuals and cannot be reliably referred to the same taxon; neither conclusively represents a small, adult theropod dinosaur. CMN 50810 has one apomorphic character, but it can only be referred to Saurischia *incertae sedis*. CMN 50811 is reinterpreted as representing an abelisauroid theropod, possibly a noasaurid.

Introduction

The early Cenomanian Kem Kem beds of southeastern Morocco have produced a famously diverse assemblage of large-bodied theropod dinosaurs (Russell, 1996; Sereno et al., 1996; McGowan and Dyke, 2009), but smaller theropod material is comparatively poorly known. Russell (1996) briefly described two cervical vertebrae as "Bone 'Taxon' B," hypothesized to represent a "small theropod" of indeterminate affinity. This material is reevaluated here.

Description

CMN 50810

CMN (Canadian Museum of Nature, formerly NMC) 50810 (Figure 1) is an axis missing the odontoid, axial intercentrum, and both postzygapophyses. The centrum is elongate (length >2.5 times height) and does not have a ventral keel. Its posterior articular surface is concave. A large, flat parapophysis is preserved on the right side. Pneumatic foramina are positioned on the anterior half of the centrum, and the foramen on the left side is split by a lamina. The interior pneumatic architecture of the centrum is camerate. The round prezygapophyses face dorsolaterally above the neural canal. A pair of tablike processes project anteriorly in front of the prezygapophyses. Pendant diapophyses and postzygodiapophyseal laminae are present. The neural spine is low and transversely narrow, without a spine table. A large spinopostzygapophyseal fossa occurs ventral to the neural spine posteriorly. There is no hyposphene.

Russell (1996:376) concluded from the closure of the neurocentral sutures that CMN 50810 represents a small-bodied theropod taxon, but Fowler et al. (2011) considered neurocentral closure to be an inconsistent and unreliable indicator of maturity in theropods. The neurocentral sutures of CMN 50810, though firmly attached, are readily discernible and thus not fully closed (Brochu, 1996). Although the anterior end of the axis is damaged, the presence of an oval depression for the missing odontoid indicates that this element had not fused to the axis. CMN 50810 is here reinterpreted as an immature specimen representing a taxon of unknown adult size. Comparisons to published measurements of well-known theropods suggest a total body length of approximately 4 m at the time of death.

No characters were stated in the original description to justify the referral of CMN 50810 to Theropoda (Russell, 1996). Pneumatic cervical vertebrae are present in three groups of Cretaceous archosaurs: theropods, sauropods, and pterosaurs. CMN 50810 is unlikely to be a pterosaur because it has features not seen in other pterosaur axes (distinct parapophysis, pneumatic foramina of the centrum split by an accessory lamina), and lacks other features expected in a large Cretaceous pterosaur (postexapophyses). A sauropod identity is more difficult to satisfactorily reject, in part because sauropod axes are highly variable, yet little phylogenetic pattern has been recognized in this variation (Wilson and Mohabey, 2006:477). Most of the variable characters in sauropod cervical vertebrae listed by Wilson and Mohabey (2006:Table 3) parallel those observed in theropods. The early ontogeny of the sauropod axis is also poorly understood. The elongate axial centrum of CMN 50810 resembles the condition in many sauropods, in contrast to the typically compact theropod axis (excluding coelophysids, ornithomimids and therizinosaurids). However, none of the character states observed in CMN 50810 are reported to occur exclusively in sauropods or theropods, so the most conservative referral pending further work is to Saurischia *incertae sedis*.

If CMN 50810 is a theropod, the presence of a sheet-like neural spine that projects farther anteriorly than the prezygapophyses is a character of coelophysoids and ceratosaurs (Tykoski and Rowe, 2004), while the relatively dorsal position of the prezygapophyses with respect to the neural canal is also indicative of a non-tetanuran affinity. Charaeters excluding CMN 50810 from Abelisauroidea include the absence of additional pairs of fossae

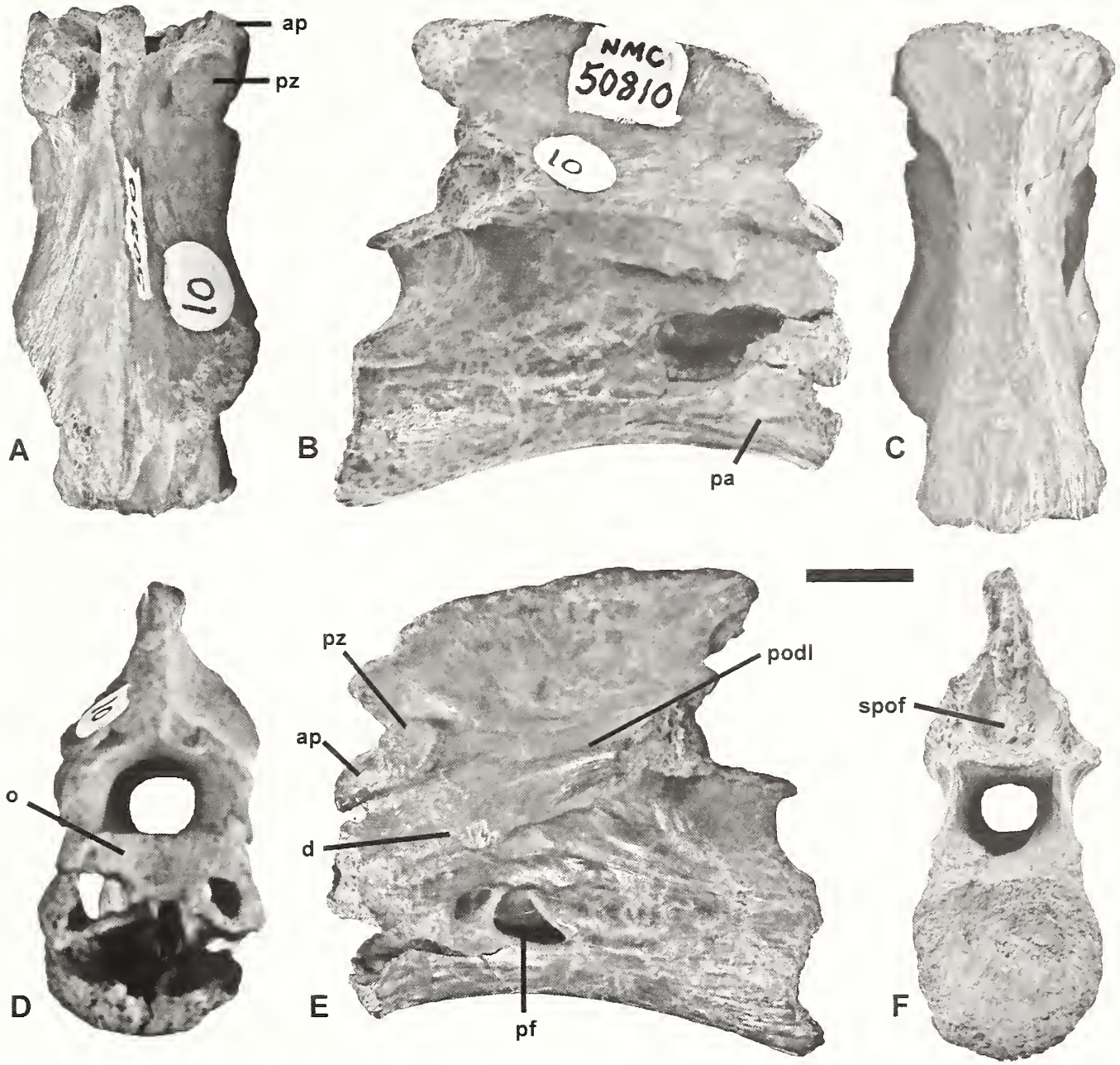

Figure 1. CMN 50810, Saurischia indet., axis. A, dorsal, B, right lateral, C, ventral, D, anterior, E, left lateral, and F, posterior views. Scale bar: 1 cm. Abbreviations: *ap*, tablike process anterior to prezygapophysis; *d*, diapophysis; *o*, oval depression for odontoid process; *pa*, parapophysis; *pf*, pneumatic foramen; *podl*, postzygodiapophyseal lamina; *pz*, prezygapophysis; *spof*, spinopostzygapophyseal fossa.

posteroventral to the postzygodiapophyseal laminae and posterior to the neural spine (O'Connor, 2007; Carrano et al., 2011). Elongate postaxial cervical centra are known in basal ceratosaurs (Carrano and Sampson, 2008), but no basal ceratosaur axis has been described. It is possible that CMN 50810 is a juvenile of the giant, gracile basal ceratosaur *Deltadromeus*, but this idea cannot be tested because CMN 50810 does not overlap with known material of that taxon (Sereno et al., 1996).

Regardless of the true phylogenetic position of CMN 50810, the tablike processes anterior to the prezygapophyses are an autapomorphic feature of this specimen.

CMN 50811

CMN 50811 (Figure 2) is an hourglass-shaped cervical centrum. The anterior articular surface is flat and the posterior articular surface is concave. The ventral surface is flat along the midline and lacks a keel. The pneumatic foramina of the centrum are expressed asymmetrically, with an anterior foramen present on both sides and a posterior foramen present on the left side only. The rugose neurocentral suture was completely open. No foramina are present in the neural canal.

This specimen was included in CMN (NMC) 50810 by Russell (1996:377), but there is no evidence that it represents the same

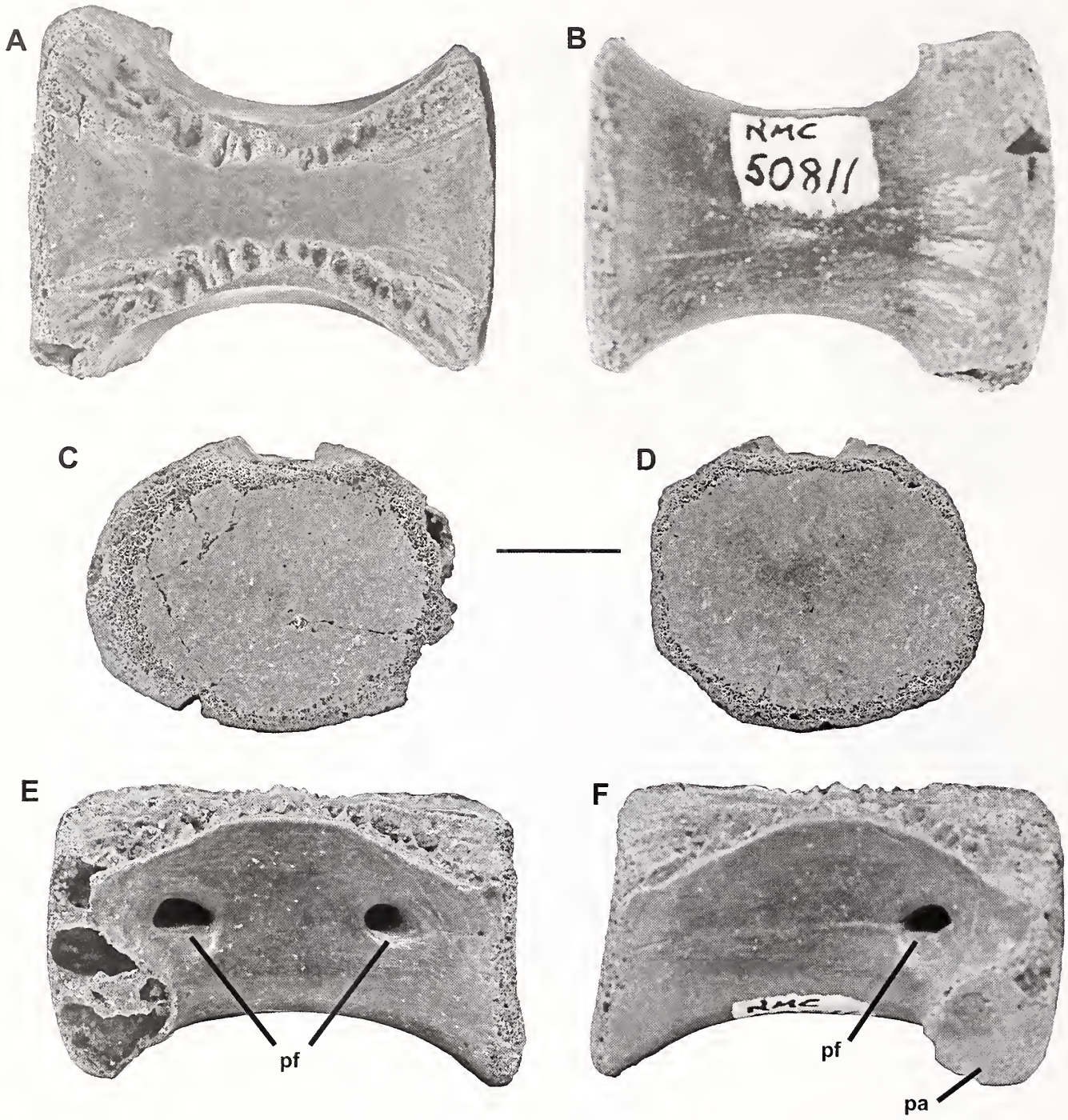

Figure 2. CMN 50811, Abelisauroidea indet., posterior cervical centrum. A, dorsal, B, dorsal, C, anterior, D, posterior, E, left lateral, and F, right lateral views. Scale bar: 1 cm. Abbreviations as in Figure 1.

individual. The presence of separate anterior and posterior pneumatic foramina on the left side identifies CMN 50811 as a ceratosaur (Tykoski and Rowe, 2004). The overall morphology and size of the specimen is consistent with representing an individual of Abelisauroidea, a ceratosaurian clade previously recognized in the Kem Kem beds on the basis of skull material (Russell, 1996; Mahler, 2005). Russell (1996:377) referred to CMN 50811 as belonging to the mid-cervical region, but it more closely resembles the most posterior cervical vertebrae of other abelisauroids in the completely flat anterior surface and lack of dorsoventral offset between anterior and posterior articulations (O'Connor, 2007; Carrano et al., 2011). The modestly elongate shape of the centrum resembles noasaurids such as *Laevisuchus* (Novas et al., 2004) and *Masiakasaurus* (Carrano et al., 2011). CMN 50811 has no recognized autapomorphies, and like other described Kem Kem abelisauroid material it is here considered indeterminate at the generic level.

Discussion

The specimens originally described as "Bone 'Taxon' B" (Russell, 1996) are not supported as a single taxon, nor as

definitive evidence of a small-bodied adult theropod in the Kem Kem assemblage. The axis CMN 50810 is interpreted as autapomorphic, but likely immature (*contra* Russell, 1996), and insufficient evidence was found to conclusively decide between a theropod (basal ceratosaur) or sauropod affinity for this specimen. The centrum CMN 50811 is reinterpreted as representing a posterior cervical vertebra of a skeletally immature abelisauroid theropod, possibly a noasaurid.

Other small theropod bones described by Russell (1996) may be uncertain indicators of total body size (distal humerus, Bone "Taxon" H), or were interpreted as the immature form of a larger taxon (femur, Bone "Taxon" M). A small dorsal vertebra described as avialan by Riff et al. (2004) was considered comparable to *Rahonavis*, a taxon variously assigned to Dromaeosauridae (Turner et al., 2012) or basal Avialae (Agnolin and Novas, 2011). Rauhut et al. (2012) recently suggested that some isolated teeth referred to Dromaeosauridae, such as those described from the Kem Kem beds (Amiot et al., 2004; Richter et al., in press), may instead belong to immature individuals of large-bodied basal tetanurans. The supposed small or medium-sized Kem Kem theropod "*Kemkemia auditorei*" (Cau and Maganuco, 2009) has been recently reidentified as a crocodyliform (Lio et al., 2012). With the reinterpretation of "Bone 'Taxon' B," it is possible that no unquestionable material of a small-bodied adult non-avialan theropod has yet been described from the Kem Kem beds.

Acknowledgements

I thank Michael Ryan for encouraging this project and inviting the contribution to this volume, Kieran Shepherd and Margaret Currie of the Canadian Museum of Nature for access to the material, and Matthew Carrano and Matt Lamanna for reviewing the manuscript.

References

Agnolin, F. L., and F. E. Novas. 2011. Unenlagiid theropods: Are they members of Dromaeosauridae (Theropoda, Maniraptora)? Anais da Academia Brasileira de Ciencias, 83:117–162.

Amiot, R., E. Buffetaut, H. Tong, L. Boudad, and L. Kabiri. 2004. Isolated theropod teeth from the Cenomanian of Moroceo and their palaeobiogeographical significance. Revue de Paléobiologie, Genève Vol. spéc., 9:143–149.

Brochu, C. A. 1996. Closure of neurocentral sutures during crocodilian ontogeny: implications for maturity assessment in fossil archosaurs. Journal of Vertebrate Paleontology, 16:49–62.

Carrano, M. T., and S. D. Sampson. 2008. The phylogeny of Ceratosauria (Dinosauria: Theropoda). Journal of Systematic Palaeontology, 6:183–236.

Carrano, M. T., M. A. Loewen, and J. J. W. Sertich. 2011. New materials of *Masiakasaurus knopfleri* Sampson, Carrano, and Forster, 2001, and implications for the morphology of the Noasauridae. Smithsonian Contributions to Paleobiology, 95:1–53.

Cau, A., and S. Maganuco. 2009. A new theropod dinosaur, represented by a single unusual caudal vertebra, from the Kem Kem Beds (Cretaceous) of Morocco. Atti della Società Italiana di Scienze Naturali e del Museo Civico di Storia Naturale di Milano, 150:239–257.

Fowler, D. W., H. N. Woodward, E. A. Freedman, P. L. Larson, and J. R. Horner. 2011. Reanalysis of "*Raptorex kriegsteini*": a juvenile tyrannosaurid dinosaur from Mongolia. PLoS ONE, 6:e21376, 1–7.

Lio, G., F. Agnolin, A. Cau, and S. Maganuco. 2012. Crocodyliform affinities for *Kemkemia auditorei* Cau and Maganuco, 2009, from the Late Cretaceous of Morocco. Atti della Società Italiana di Scienze Naturali e del Museo di Storia Naturale di Milano, 153:119–126.

Mahler, L. 2005. Record of Abelisauridae (Dinosauria: Theropoda) from the Cenomanian of Morocco. Journal of Vertebrate Paleontology, 25:236–239.

McGowan, A. J., and G. D. Dyke. 2009. A surfeit of theropods in the Moroccan Late Cretaceous? Comparing diversity estimates from field data and fossil shops. Geology, 37:843–846.

Novas, F. E., F. L. Agnolin, and S. Bandyopadhyay. 2004. Cretaceous theropods from India: A review of specimens described by Huene and Matley (1933). Revista del Museo Argentino de Ciencias Naturales n.s., 6:67–103.

O'Connor, P. M. 2007. The posteranial axial skeleton of *Majungasaurus crenatissimus* (Theropoda: Abelisauridae) from the Late Cretaceous of Madagascar. Society of Vertebrate Paleontology Memoir, 8:127–162.

Rauhut, O. W. M., C. Foth, H. Tischlinger, and M. A. Norell. 2012. Exceptionally preserved juvenile megalosauroid theropod dinosaur with filamentous integument from the Late Jurassic of Germany. Proceedings of the National Academy of Sciences, 109:11746–11751.

Richter, U., A. Mudroch, and L. G. Buekley. In press. Isolated theropod teeth from the Kem Kem Beds (Early Cenomanian) near Taouz, Morocco. Paläontologische Zeitschrift. DOI 10.1007/s12542-012-0153-1:1–19.

Riff, D., B. Mader, A. W. A. Kellner, and D. A. Russell. 2004. An avian vertebra from the continental Cretaceous of Morocco, Africa. Arquivos do Museo Nacional, Rio de Janeiro, 62:217–223.

Russell, D. A. 1996. Isolated dinosaur bones from the Middle Cretaceous of the Tafilalt, Morocco. Bulletin du Muséum national d'Histoire naturelle, Paris, 4e sér., 18:349–402.

Sereno, P. C., D. B. Dutheil, M. Iarochene, H. C. E. Larsson, G. H. Lyon, P. M. Magwene, C. A. Sidor, D. J. Varricchio, and J. A. Wilson. 1996. Predatory dinosaurs from the Sahara and Late Cretaceous faunal differentiation. Science, 272: 986–991.

Turner, A. H., P. J. Makovicky, and M. A. Norell. 2012. A review of dromaeosaurid systematics and paravian phylogeny. Bulletin of the American Museum of Natural History, 371:1–206.

Tykoski, R. S., and T. Rowe. 2004. Ceratosauria, p. 47–70. *In* Weishampel, B., Dodson, P., and Osmólska, H. (eds.) The Dinosauria, Second Edition. University of California Press, Berkeley.

Wilson, J. A., and D. M. Mohabey. 2006. A titanosauriform (Dinosauria: Sauropoda) axis from the Lameta Formation (Upper Cretaceous: Maastrichtian) of Nand, Central India. Journal of Vertebrate Paleontology, 26:471–479.

KIRTLANDIA
The Cleveland Museum of Natural History

March 2013 *Number 58:42–53*

NEW LATE MIOCENE FOSSIL PECCARIES FROM CALIFORNIA AND NEBRASKA

DONALD R. PROTHERO
Department of Vertebrate Paleontology
Natural History Museum, 900 Exposition Blvd., Los Angeles, California 90007
donaldprothero@att.net

AUDRIANNA POLLEN
Department of Geology
Occidental College, Los Angeles, California 90041
pollen@oxy.edu

ABSTRACT

We describe two new genera and species of peccaries from the late Miocene of the western United States. Both of these new taxa are referable to the *Macrogenis-Tayassu* clade, but form their own clade united by the presence of a zygomatic wing whose anterior edge protrudes laterally at right angles to the snout. Numerous nearly complete skulls and jaws from Blackhawk Ranch (Green Valley Formation, latest Clarendonian, about 9.0–9.5 Ma) pertain to a new genus and species, *Woodburnehyus grenaderae*. *W. grenaderae* is distinguished from similar taxa by its wide dentary and broad, bulbous cheek teeth. In addition, it is distinct from other species in lacking a contact between the maxillary and the suborbital bulla. Its suborbital bulla is narrows anteriorly, and it has a narrow tympanic process. A second new genus and species, *Skinnerhyus shermerorum*, is based on material from the late Clarendonian Merritt Dam Member, Ash Hollow Formation, north-central Nebraska. It has remarkable laterally flaring wing-like zygomatic processes, and it is distinguished from other members of the *Macrogenis-Tayassu* clade by having an anterior atrial aperture medial to M1, and the anterior palatine foramen medial to M1. The high diversity of peccaries at this time is largely a function of their disparate array of zygomatic crests in male skulls.

Introduction

The peccaries or javelinas (family Tayassuidae) are a group of suiform artiodactyls with a long history in the New World. Although they look somewhat similar to pigs, the tayassuids are a separate family that split off from true pigs (family Suidae) more than 37 million years ago. Since then, they underwent a long evolutionary history in North America before spreading to South America in the late Miocene. Today peccaries are found largely in Central and South America, although they also occur in the southwestern deserts of the United States. Three species still survive: *Dicotyles tajacu*, the collared peccary; *Tayassu pecari*, the white-lipped peccary; and *Catagonus wagneri*, the Chacoan peccary. This last species was known only from fossils until living populations were discovered in the Gran Chaco of Paraguay in 1975. However, peccaries were much more diverse over the past 37 million years, with at least 20 genera and an unknown number of valid species represented in the fossil record of North America.

Despite their abundant fossil record in North America, and large new collections with excellent skulls in many museums (especially the Frick Collection in the American Museum of Natural History in New York), there has not been a significant published description of most of these fossils yet. Prothero (2009) published a revision of the early radiation of North American Eocene-Oligocene peccaries, but that study did not deal with the Miocene forms. In 1983, David B. Wright did his master's thesis at the University of Nebraska on some late Miocene peccaries, and in 1991 he completed a doctoral dissertation on Neogene peccaries at the University of Massachusetts. Except for a few short peripheral papers (e.g., Wright, 1993), and a short summary chapter that provided no detailed descriptions or new names (Wright, 1998), none of Wright's work has been published, and it has been more than 20 years since he left the profession. Because no one else has taken up the task of finishing Wright's work and properly naming and describing these new fossils, we have begun to do so in this paper. Most of Wright's descriptions were sound, but they are not widely available to the scientific community since they remain in unpublished theses. Thus, we have re-described the fossils as much as possible, or when necessary, paraphrase from Wright's unpublished theses, since we are in agreement with most of his conclusions.

Materials and Methods

This study began as a student research project by Pollen and was presented at the 2011 Society of Vertebrate Paleontology

meeting in Las Vegas (Prothero and Pollen, 2011). It is published separately here, but it is part of a much larger complete monographic revision of the Tayassuidae currently being written (Prothero in prep.). Specimens were measured with digital calipers and data entered and statistically analyzed using Excel spreadsheets. The photos were taken with a Nikon 5700 camera, and edited in Photoshop.

Museum Abbreviations: AMNH, American Museum of Natural History, New York, New York, including the Frick Collection (F:AM); UCMP, University of California Museum of Paleontology, Berkeley, California.

Systematic Paleontology

Class MAMMALIA Linneaus 1858
Order ARTIODACTYLA Owen 1848
Family TAYASSUIDAE Palmer 1897
Woodburnehyus n. gen.
Figures 1–4, Tables 1–2

Type and only species

W. grenaderae.

Diagnosis

Same as for *W. grenaderae*.

Etymology

In honor of Dr. Michael O. Woodburne, for his many contributions to the understanding of fossil peccaries and Miocene localities such as Blackhawk Ranch, plus *-hyus*, Greek for "pig".

Type and only locality

Blackhawk Ranch Quarry, UCMP locality V3310, Green Valley Formation, Contra Costa County, California; late Clarendonian in age (see Prothero and Tedford, 2001).

Description

Same as for *W. grenaderae*.

Discussion

Wright (1983, 1991, 1998) recognized the distinctiveness of the Blackhawk Ranch peccary specimens, but never published a description of that material, nor did he give it a taxonomic name even though he recognized that it was clearly a new genus and species. In those publications (especially his 1998 summary chapter) it was just referred to as the "Blackhawk Ranch species", but no adequate justification was given for his taxonomic decisions. Wright (1983) refers to this species as "Species F" in his unpublished master's thesis. In the UCMP data base, the published literature, and in online faunal lists of the locality, this material is incorrectly referred to *Prosthennops*, which is a wastebasket taxon for late Miocene peccary taxa with teeth which are low-crowned and bunodont (Wright, 1998; Prothero in prep.).

Woodburnehyus grenaderae n. sp.

Diagnosis

A peccary from the *Macrogenis-Tayassu* clade distinguished from all other members of that clade (including *Skinnerhyus*) by its relatively broad and robust dentary and wide, bulbous cheek teeth. It also lacks a contact between the maxillary and the suborbital bulla, and the auditory bulla and tympanic process are relatively narrow. The facial crest or zygomatic wing is quite short and blunt, with the anterior edge protruding laterally and perpendicularly from the facial region, and extending anteriorly over the rostral muscle fossa. These features distinguish it from *Skinnerhyus, Macrogenis*, and other peccaries.

Etymology

In honor of Jessica Grenader, for her contributions to peccary paleontology.

Type specimen

UCMP 74812, partial skull with right and left P2-M3, lacking rostrum anterior to P2 and region posterior to orbit (Figure 1A–C).

Distribution

From type locality only.

Referred material

UCMP 39470 (Figure 2A–B), partial skull with left and right canines, P2-M3; UCMP 77675, partial skull with right P4-M2 (Figure 2C); UCMP 33738, right maxillary fragment with dP4-M1; UCMP 125191, right dp3; UCMP 47325 and 125290, left P3; UCMP 58535, right P3; UCMP125283 and 125287, left P4; UCMP 125293, right P4; UCMP 33739 and 125285, left M2; UCMP 90144, 125281, right M2; UCMP 64413, left M3; UCMP 125286, right M3; UCMP 36471, partial jaw with left p2-4, m2-3,. right p3-m2; UCMP 34638, right ramus lacking symphysis or condyle, m1-3 present (Figure 3A–B); UCMP 33737, left ramus with p2-m2 (premolars erupting)(Figure 3C–D); UCMP 34665, left ramus with p3-m3; UCMP 49865, right ramus with p4-m3; UCMP 65217, left ramus fragment with m2; UCMP 34639, left lower canine; UCMP 125288, right dp3; UCMP 125289, right p2; UCMP 90155, right p3; UCMP 125284, right p4; UCMP 90156 and 125282, left m1; UCMP 34672 and 90142, left m3; UCMP 90143 and 125292, right m3. Over 66 specimens of this taxon are listed on the UCMP online catalogue, so there are many additional specimens not included here.

Description

There are four partial skulls that give a reasonable picture of the complete skull anatomy of *W. grenaderae*: UCMP 33736, 39470, 74812, and 77675 (Figures 1–2). The description below is modified from the unpublished work of Wright (1983, pp. 174–175), and represents a composite description based on these four skulls and additional material in the Blackhawk Ranch collection.

In lateral view (Figure 1C, 2C), the frontal bones slope anteriorly as in most Clarendonian peccaries. On UCMP 74812 (Figure 1A–C), there are large canine buttresses as well as a large canine, which is presumed to represent a male individual. However, UCMP 39470 (Figure 2A–B) has much smaller canines and buttresses, so it probably represents a female specimen. Similar sexually dimorphic canines and canine buttresses are widely observed in the peccaries (Wright, 1983), and can be seen in living peccary populations. *W. grenaderae* has relatively short premaxillae compared to other species from the Clarendonian. There is a strong buccinator ridge on the snout, particularly well shown on UCMP 74812.

The zygomatic wings or facial crests of *W. grenaderae* are distinct from those of any other peccary known, and distinctive enough from *Macrogenis, Skinnerhyus*, and other genera that a

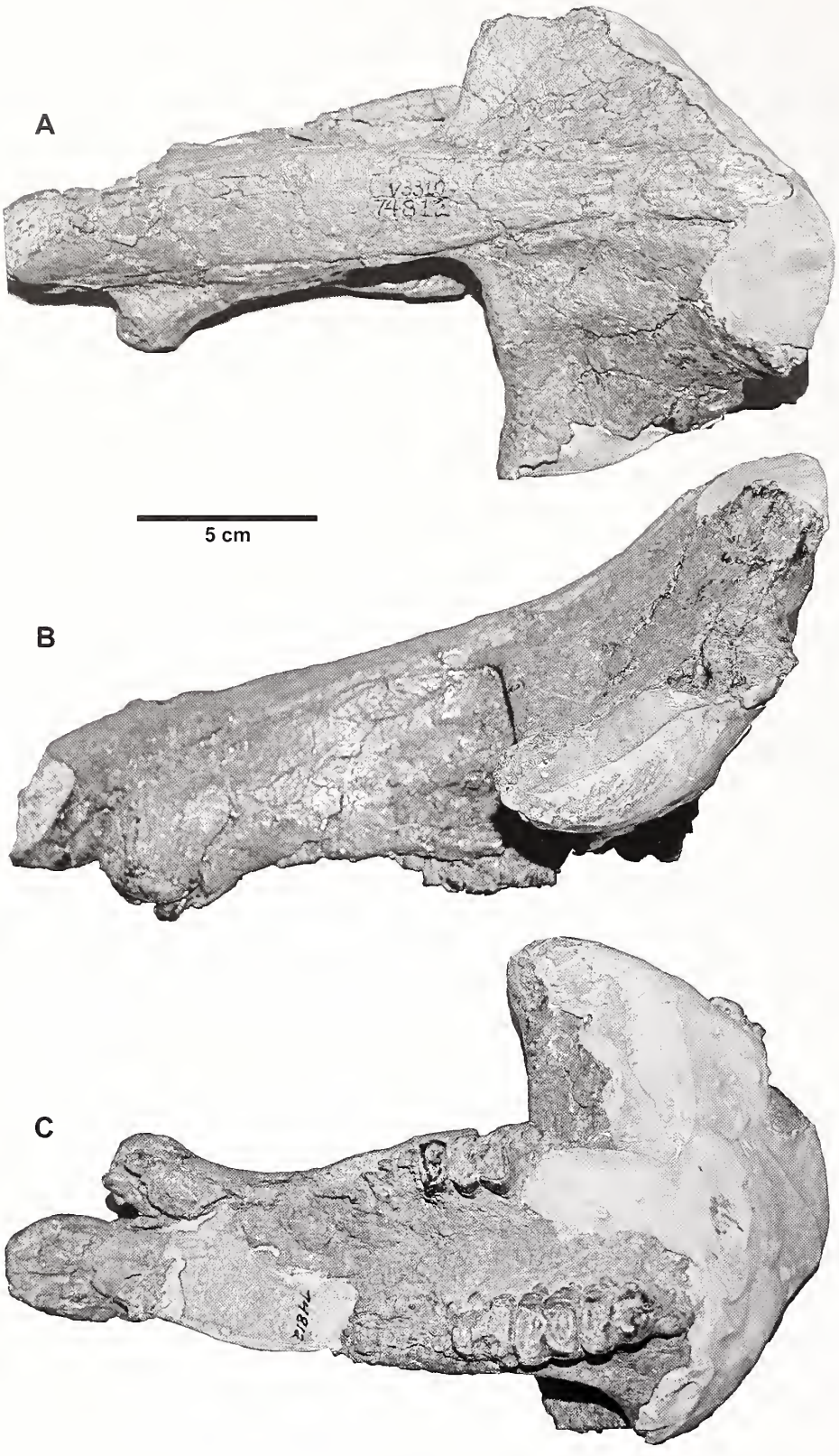

Figure 1. *Woodburnehyus grenaderae,* UCMP 74812, type specimen. A, dorsal, B, left lateral, and C, ventral views. Scale bar equals 5 cm.

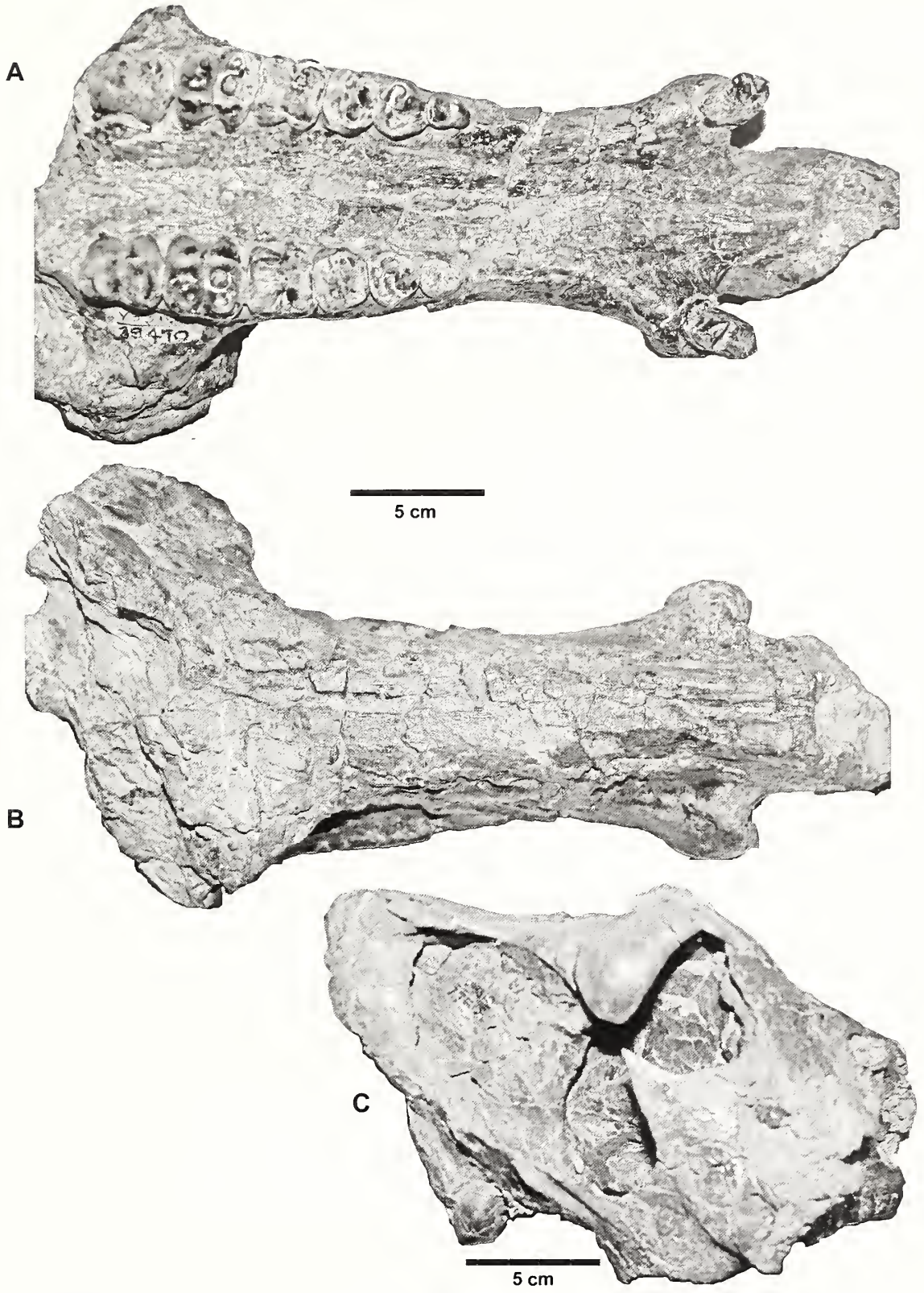

Figure 2. *Woodburnehyus grenaderae.* UCMP 39470, referred female skull. A, ventral, and B, dorsal views. C, UCMP 77675, referred partial skull in right lateral view. Scale bar equals 5 cm.

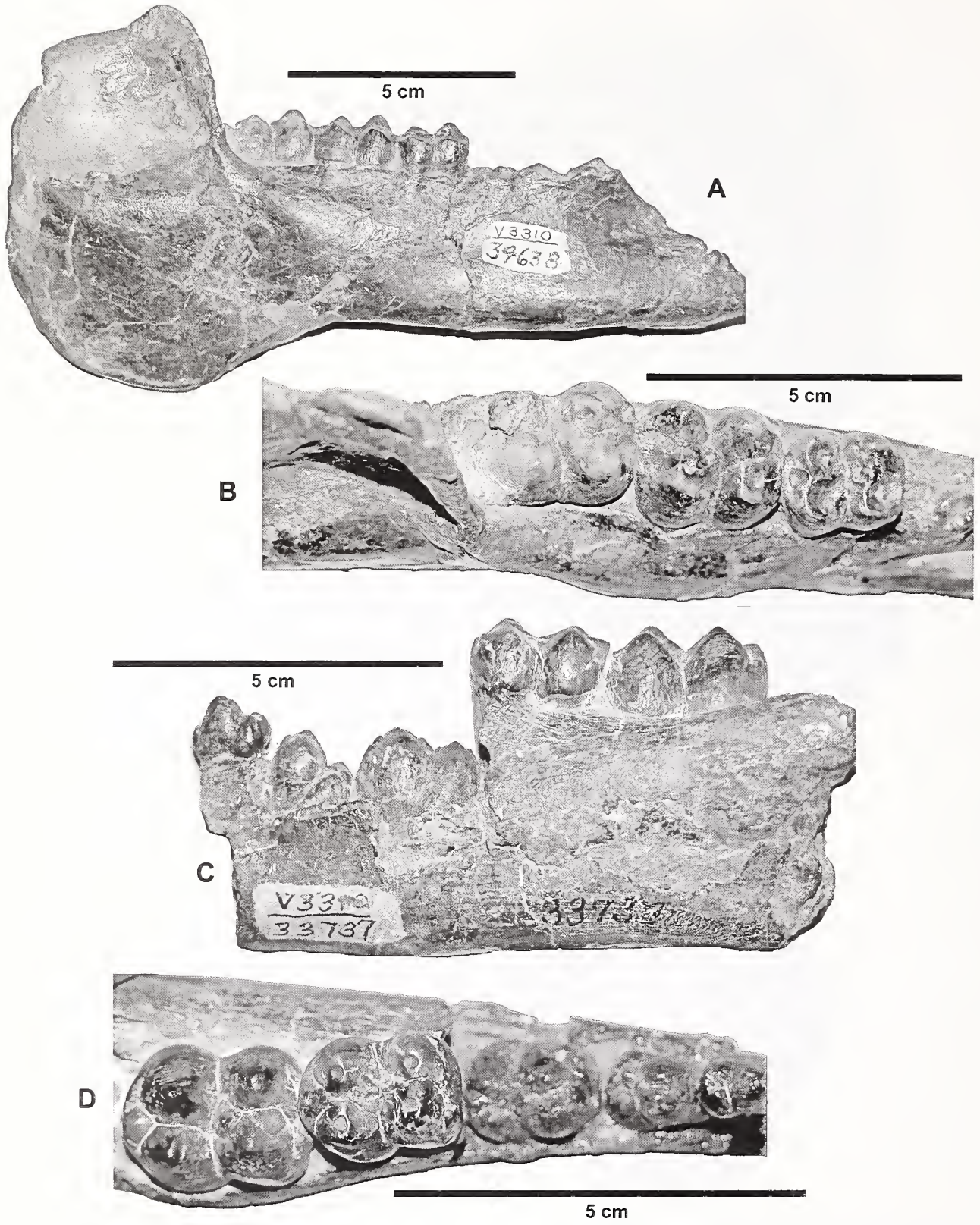

Figure 3. *Woodburnehyus grenaderae.* UCMP 34638, adult ramus. A, right lateral, and B, occlusal views. UCMP 33737, adult ramus with p2-4 still erupting in C, left lateral, and D, occlusal views. Scale bar equals 5 cm.

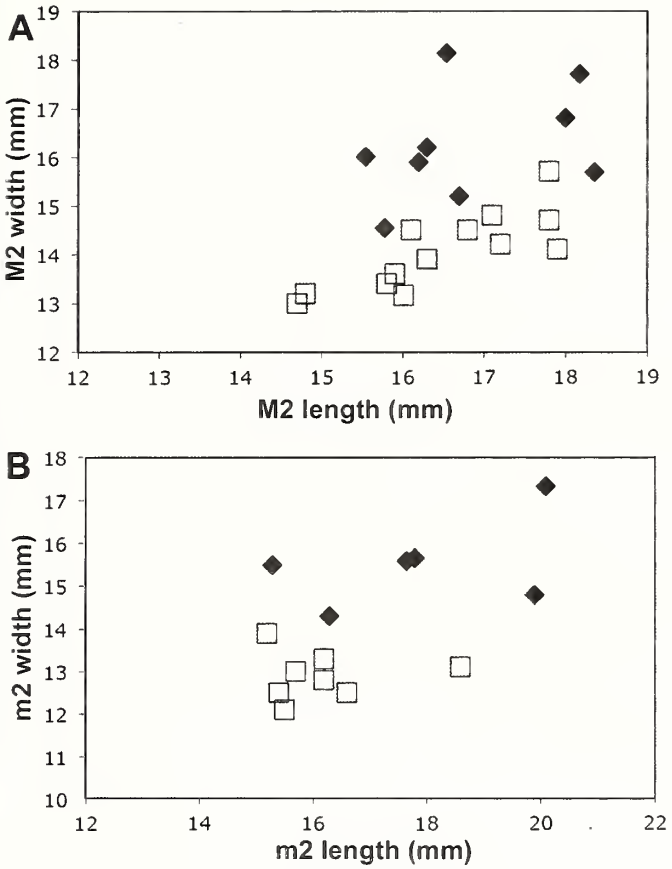

Figure 4. Plot of specimens of *Woodburnehyus grenaderae* versus other peccaries, showing that the lower molars are significantly wider in *W. grenaderae* than in other taxa. A, Comparison of M2 dimensions. B, Comparison of m2 dimensions. Open squares are *S. shermerorum*, solid diamonds are *W. grenaderae*. In every plot, the *W. grenaderae* specimens are broader in tooth dimensions, with no overlap, or only slight overlap with the *S. shermerorum* specimens.

new genus is justified. In nearly all UCMP specimens, the distal portion of the zygoma is broken, but the proximal portion is known from three different skulls. The anterior edge of the zygomatic wing narrows in the spot where it merges with the dorsal surface of the rostrum right above P4 and M1. The large rostral muscle fossa extends beneath the anterior edge of the zygomatic wing, as in *Skinnerhyus shermerorum*. The anterior edge of the zygoma thickens dorsoventrally about 45 mm distal to its origin on the rostrum. Thus, the proximal portion of the zygoma is very similar to the condition seen in *S. shermerorum*.

There is a deep palatine fossa, which is especially well developed on UCMP 77675. The broad pterygoid processes of the alisphenoid flare laterally and meet the palatine bone at an angle of about 130–140°. There is also a large orbitosphenoid bulla, similar in size and proportions to the condition seen in *S. shermerorum*. There is a well-developed glenoid fossa that extends laterally to the edge of the tympanic wing, as seen in *Macrogenis crassigenis* and other Clarendonian peccaries. Most of the specimens lack a well-preserved auditory bulla, but where the bulla is preserved, it seems to have a narrow cross-section, as in many other Miocene peccaries. There is a fragment of juvenile maxilla (UCMP 33738) that preserves the lateral cancellous inflation above dP4 and M1.

The first and second upper incisors are not preserved on any of the skulls known, but their alveoli suggest that the incisors are similar to those of other Clarendonian peccaries. As discussed above and by Wright (1983), the canines show strong sexual dimorphism in both their size and curvature, and also in the size of the canine buttresses from which they protrude.

Most of the dP3 and dP4 specimens in the collection are highly worn, but they are similar to those in other Clarendonian peccaries. All known specimens of *W. grenaderae* have highly worn P2s (Figures 1–2). The P2 has a large protocone, with a smaller metacone posterior to the paracone. The protocone is posterolingual to the paracone. P3 has a trapezoid-like shape in crown view, with the protocone lingual to the paracone as in P2. A crest off the protocone extends anterolabially to join the anterior cingulum. There is a small metaconule, which is surrounded lingually by the hypocone as it fuses with the lingual cingulum. There is a fusion of the two lingual roots on P3. P4 is very similar to the condition in P3, with a large cusp-shaped metaconule fused with the posterior cingulum. Unlike P3, however, the lingual roots appear not to be fused in P4.

The upper molars of *W. grenaderae* are known primarily from very worn teeth, especially M1. In most features, the unworn molars (Figures 1–2) are typical of other Clarendonian peccaries, and their cusp pattern is generalized and non-diagnostic. The most striking feature is that they are relatively wide laterally compared to any other known peccary, and the lower jaw itself is wide and robust compared to those of other peccaries as well (Figure 4). The broad, robust upper and lower cheek teeth and lower jaw is a diagnostic feature for this species.

As was the case for the upper cheek teeth, nearly all the lower cheek teeth are broader and more bulbous than seen in any other peccary (Figure 3). The p2 is like that of most peccaries except that it has a broad, bulbous heel, and a fused protoconid. The robust p3 bears a metaconid with a posterolabial process and a small anterior cusp. The p3 has a distinct, low anteroconid, and its broad heel bears three cusps in unworn specimens (such as the juvenile jaw with the premolars still in their crypts and undergoing eruption, UCMP 33737—Figure 3C–D). The p4 bears a posterolabial process on the metaconid, and most specimens have a cusp on the anterior side of the metaconid as well. The heel of the p4 is very broad, and may bear two large partially fused cusps in unworn specimens, or two large cusps with a smaller cusp in the hypoconulid position, or a large hypoconid and entoconid separated by two smaller cusps. This high variability of cusps in peccaries is why most diagnoses do not rely to heavily on cusp patterns to define species (Colbert, 1938; Simpson, 1949; Wright, 1991, 1998). The molars are much like those of most other Clarendonian peccaries except that they are broader and more bulbous. On the m3, the third lobe bears a single large cusp.

Skinnerhyus n. gen.
Figures 5–7, Tables 1–2

Type and only species

S. shermerorum.

Type locality

Machaerodus Quarry, Merritt Dam Member, Ash Hollow Formation, Cherry County, Nebraska; late Clarendonian (just beneath an ash dated 9.95 ± 0.8 Ma) (Skinner and Johnson, 1984, p. 315). In some references (e.g., Wright, 1983), the holotype is attributed to "Kat Quarry," although according to Skinner and Johnson (1984, p. 315), *Machaerodus* Quarry is a separate quarry

Table 1. Comparisons of skull jaw dimensions in the peccary specimens described in this paper. All numbers beginning with 113 are F:AM numbers of specimens of *S. shermerorum*. The other numbers are UCMP catalogue numbers of specimens of *W. grenaderae*. All measurements in mm.

Measurement	113317	113316	113263	39470	74812	77675
Condylobasal length	324					
Premaxilla length	44.5			37.5	33	
Postcanine diastema	53	58	57	45	39	
Palate posterior to M3	43					30.5
Canine buttress width	78.9			57.1		
Palate width at M1	26.4			24.1	24.9	
Zygomatic width	295					
Parietal width	125					
Width at glenoid fossa	131.5					
Occiput height	147					135
Tympanic wing width	126					
Occipital condyle height	24					18.5
Occipital condyle width	49.1					48
Foramen magnum height	18.5					
Foramen magnum width	20.6					

Lower jaws	113266	113192	113265	113264	113266	113286	113291	34638	33737
Symphysis length	83.5		81	82.8		87.7	81		
Symphysis width	25.6	21.3	25.6	24		22	27.8		
Diastema length	62.5		64.9	66.1	54.3	62.3	67		
Ramus depth							52.9	31.8	23.5
Ramus width							25.7		23.8

channel within the Xmas Channel-Kat Channel Quarry system, not the same as "Kat Quarry" itself.

Etymology

In memory of Morris Skinner, who discovered the specimen, plus *-hyus*, Greek for "pig".

Diagnosis

Same as for *S. shermerorum*.

Description

Same as for *S. shermerorum*.

Discussion

Wright (1983, 1991, 1998) recognized the distinctiveness of the *Machaerodus* Quarry peccary, but never published a description or a name for this species. In those publications (especially his 1998 summary chapter) Wright referred to as the "*Machaerodus* Quarry species" or "Kat Quarry species", or to his "Species A" (Wright 1983), but no adequate justification was given for his taxonomic decisions. The holotype specimen from *Machaerodus* Quarry (F:AM 113317) and unassociated jaw from Emry Quarry (F:AM 113264) are currently on display in the AMNH fossil mammal hall under the incorrect name *Macrogenis crassigenis*.

Skinnerhyus shermerorum n. sp.

Type specimen

F:AM 113317, male skull (Figure 5).

Referred material

All from quarries in the Merritt Dam Member, Ash Hollow Formation, Cherry County, Nebraska, late Clarendonian (Skinner and Johnson, 1984).

Table 2. Statistics of tooth dimensions in samples of *W. grenaderae* and *S. shermerorum*. N = number of samples; SD = standard deviation.

	W. grenaderae			*S. shermerorum*		
Dimension	N	Mean	SD	N	Mean	SD
P2L	2	9.4	0.8	3	10.1	0.5
P2W	2	7.8	1.1	3	8.6	0.4
P3L	6	10.8	1.1	6	11.3	0.6
P3W	6	10.7	0.8	6	10.4	1.5
P4L	8	12.3	0.6	8	12.7	0.6
P4W	8	12.6	0.5	8	11.8	1.4
M1L	5	13.9	0.8	9	14.2	0.9
M1W	5	14.5	1.1	9	12.6	0.9
M2L	9	16.8	1.1	13	16.8	0.8
M2W	9	16.2	1.1	13	14.2	0.7
M3L	5	17.8	1.2	5	19.3	0.8
M3W	5	14.5	0.9	5	13.5	1.1
M1-3	4	48	3	1	38.4	—
P2-4	2	31.8	4.4	1	52.4	—
P2-M3	2	79.5	9.5	1	87.3	—

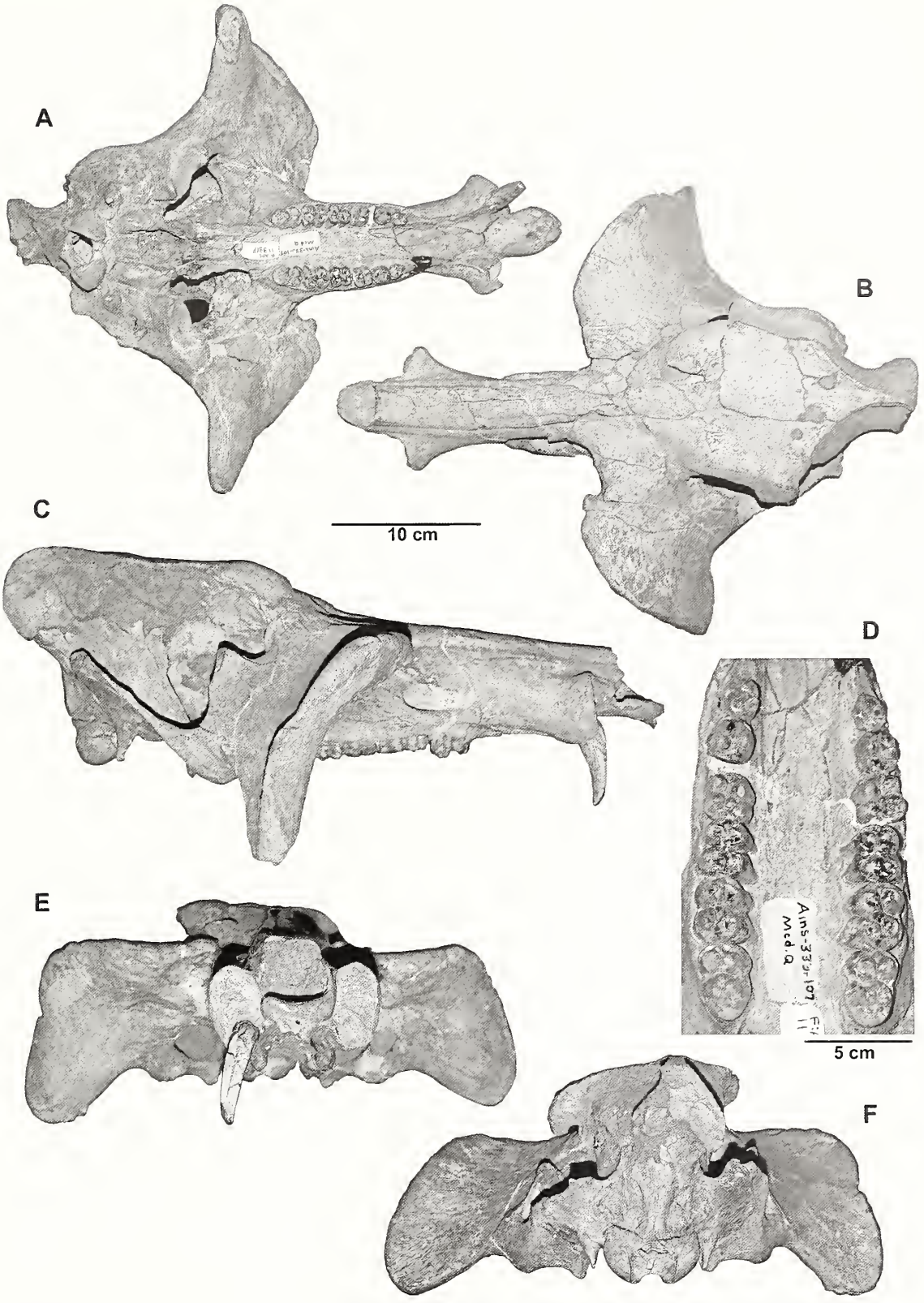

Figure 5. *Skinnerhyus shermerorum*, F:AM 113317, holotype specimen. A, ventral, B, dorsal, and C, right lateral views. D, close-up of upper cheek teeth. E, anterior view showing zygomatic flanges. F, posterior view. Scale bar equals 10 cm.

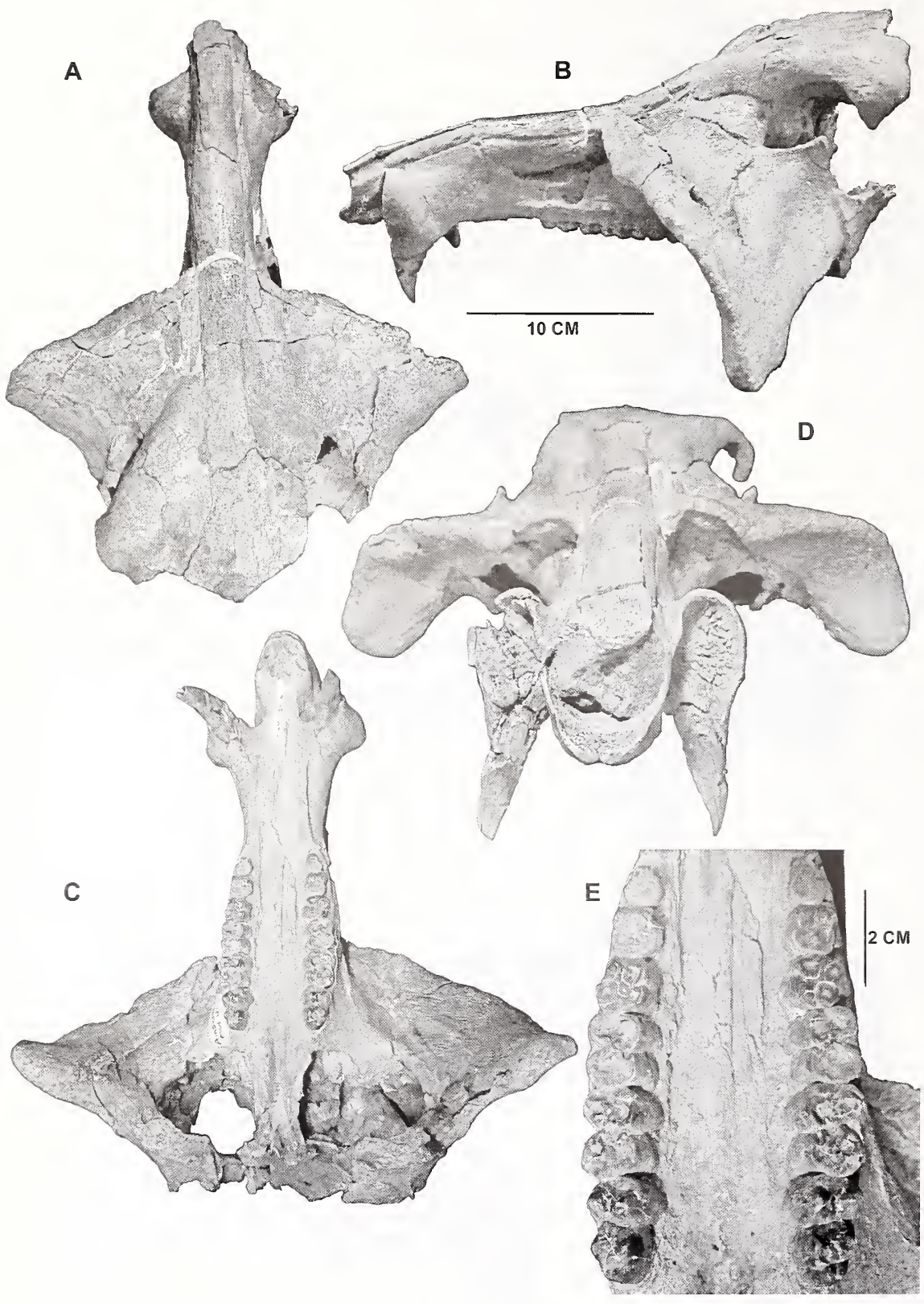

Figure 6. *Skinnerhyus shermerorum*, F:AM 113316, referred specimen. A, dorsal, B, left lateral, C, ventral, and D, anterior views. E, A close-up of upper cheek teeth. Scale bars: (A-D) equals 10 cm; E equals 2 cm. (Photos by Alana Gishlick).

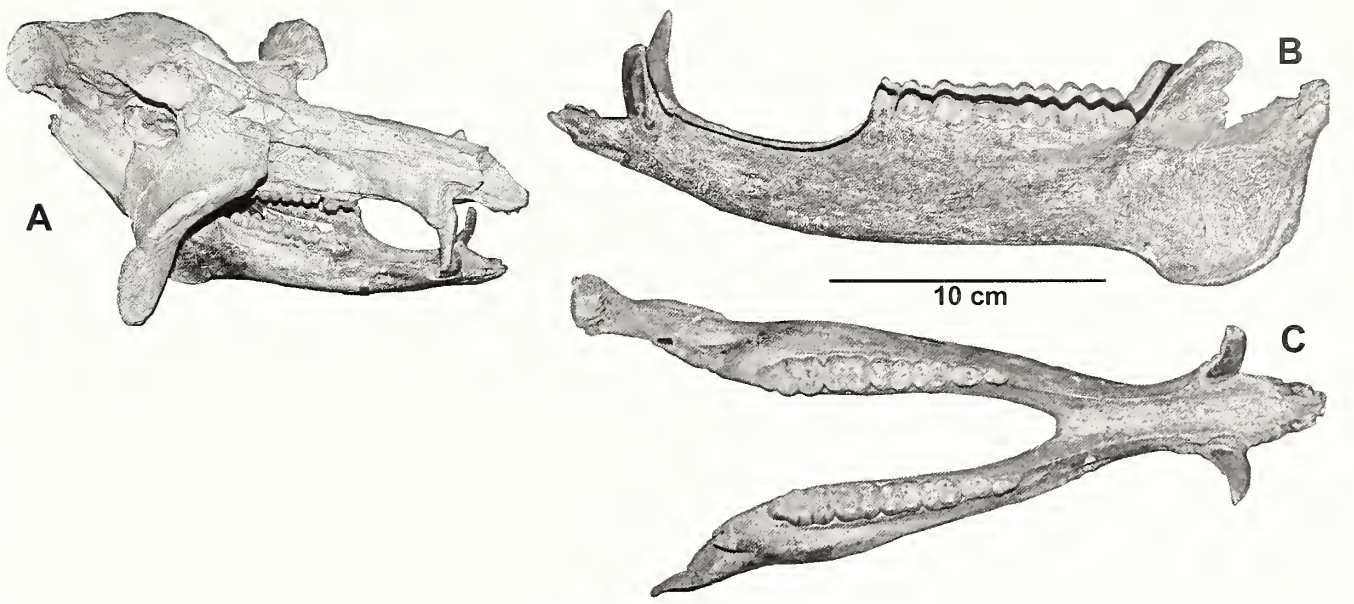

Figure 7. *Skinnerhyus shermerorum*. A, Oblique anterior view of F:AM 113317 (skull) and F:AM 113264 in articulation as they are mounted on display at the AMNH. F:AM 113264, referred lower jaw in B, left lateral, and C, crown views. Scale bar (B and C) equals 10 cm.

From Kat Quarry: F:AM 113316 (Figure 6), partial skull missing basicranial and occipital regions, with left and right canines, P2-M3;

From Emry Quarry: F:AM 113264, lower jaw (Figure 7); F:AM 113259, left maxilla; F:AM 113260, right maxilla; F:AM 113263, partial skull; F:AM 113264, mandible; F:AM 113265, mandible, F:AM 113266, mandible; F:AM 113267, partial symphysis;

From Egger Quarry, F:AM 113193, maxilla; F:AM 113195, maxilla; F:AM 113198, canine; F:AM 113197, dP4; F:AM 113192, partial symphysis; F:AM 113194, left ramus; F:AM 113199, right M2; F:AM 113200, right M1; F:AM 113201, left P4; F:AM 113213, right ramus; F:AM 113214 left ramus; F:AM 113407, right M1; F:AM 143935, left M2;

From Wade Quarry, F:AM 113282, canine; F:AM 113283 canine; F:AM 113284, canine; F:AM 113286, mandible; F:AM 113287, right ramus; F:AM 113288, right ramus; F:AM 113289, right ramus; F:AM 113291, symphysis; F:AM 143934; right P4;

From Xmas Quarry: F:AM 113176, partial palate with left P4-M3; F:AM 113175, partial mandible with left p2-m3, right p3; F:AM 113179, partial left ramus with p4-m3; F:AM 113174, partial right ramus with c1, dp2-4, p4-m2; F:AM 113178, partial right ramus with dp2-4, m1 in crypt.

Etymology—In honor of Dr. Michael Shermer and his daughter Devin Shermer.

Diagnosis

(Modified from Wright, 1983, p. 121): Broad fan-like zygomatic wings that flare outward and upward; deep rostral muscle fossa beneath the anterior edge of the zygomatic wing; glenoid fossa not extending lateral to tympanic wing; no contact between maxilla and lateral edge of orbitosphenoid bulla; narrow auditory bulla; cancellous suprapalatine inflation, with deep dorsal palatine sulcus; moderate-sized premaxilla, about 45 mm in length; nearly spherical occipital condyles compared to other tayassuines; long upper post-canine diastema (greater than 50 mm); cheek teeth without broad, bulbous shape seen in *Macrogenis*; P2 with protocone, metacone; P3, P4 submolarized.

Description

(Modified from Wright, 183, p. 122–123): *S. shermerorum* differs from *Macrogenis, Woodburnehyus*, and virtually all other peccaries in the unique shape of its broadly fan-like zygomatic wings, which extend wider laterally and are more oriented dorsoventrally than in any other tayassuine. On this basis alone, it is clearly a distinct genus, and cannot be referred to any other genus of tayassuid. *S. shermerorum* also has a longer rostrum than that of *Macrogenis, Woodburnehyus*, or other peccaries, with large canines and canine buttresses in presumed male skulls (e.g., F:AM 113317, F:AM 113316—Figures 5, 6). The front edge of the zygomatic wing meets the rostrum above M1-2 and ventral to the supraorbital canal. The proximal front edge of the zygomatic wing appears to be straight in dorsal view, and lies perpendicular to the sagittal plane. When viewed from the anterior, the front edge of the zygomatic wing is arched slightly dorsally in F:AM 113317 and markedly so in F:AM 113316, where it forms the dorsal edge of the rostral muscle fossa. On the lateral side of the rostral muscle fossa, the front edge of the zygomatic wing curves posteriorly and ventrally. The distal part of the wing curves in the dorsal direction, especially in F:AM 113317. One feature unique to this species is found in the distal tip of the zygomatic wing, which protrudes ventrally to a position about 3 cm below the glenoid fossa.

When the skull is viewed from the ventral side (Figure 5), the areas of origin for the rostral and masseteric muscles are delimited by sharp crests. The lacrimal foramen is small in F:AM 113317, but in most other specimens it is about the size typical of *Macrogenis* and other late Miocene peccaries. In F:AM 113317, the lateral edges of the palatine bones are parallel, but they converge posteriorly in F:AM 113316. There is a trough-shaped

Figure 8. Restoration of *Skinnerhyus shermerorum* by Pat Linse.

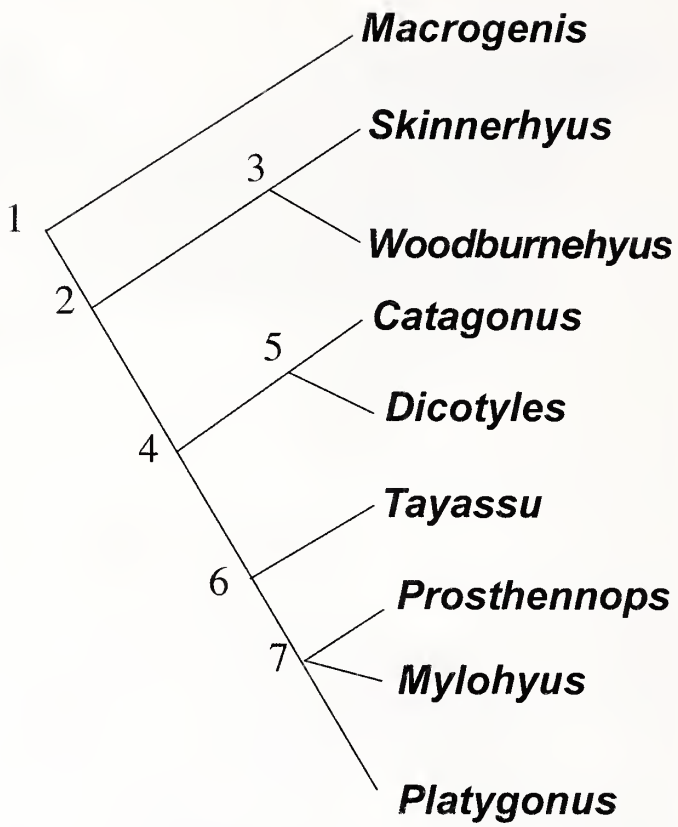

Figure 9. Cladogram of the peccaries discussed in this paper (modified from Wright 1993, 1998). Characters at nodes: 1, *Macrogenis-Tayassu* clade: pneumatic zygomatic arch; anterior palatine foramen lies anterior to M1; I3 absent; p3 lacking paraconid, and with large talonid cusps; 2, facial crest of zygoma extends anteriorly and dorsal to P4; 3, *Woodburnehyus-Skinnerhyus* clade: anterior edge of zygomatic wing is straight and extends perpendicularly from facial region; 4, *Catagonus-Tayassu* clade: tectum of maxillopalatine labyrinth meets nasal septum dorsal to floor of nasal cavity; atrium of maxillpalatine labyrinth subangular in cross-section; P4 with entoconid, hypoconulid; P2 protocone lingual to paracone; p2 with metaconid; dp2 with metaconid; 5, *Catagonus-Dicotyles* clade: pterygoid processes of alisphenoid converge medially at choanal margin; posterior palatine foramen opens within nasal cavity, anterior to sphenopalatine foramen; zygodonty present in some specimens; large suborbital bulla having sharp lateral crest; 6, *Platygonus-Tayassu* clade: deep nasal incision, which is pointed posteriorly; 7, *Prosthennops-Mylohyus-Platygonus* clade: atrium of maxillopalatine labyrinth having posterior aperture; dP2 with protocone.

palatine fossa, which has flat surfaces on each side. The angle between the pterygoid wings of the alisphenoid is about 155°. The pterygoid fossa is elongate, much like that in other late Miocene peccaries. There are no preserved orbitosphenoid bullae in F:AM 113317, but they are large in F:AM 113316, and extend laterally to the level of labial sides of the cheek teeth.

Compared to *M. crassigenis*, the glenoid fossae of *S. shermerorum* are not as far laterally from the tympanic wing. There is a concave posterior surface on the squamosal just dorsal to the glenoid fossa. Compared to *Macrogenis* and *Woodburnehyus*, the auditory bullae are not as broad. The occipital condyles are more spherical than is seen in any other tayassuine. The dorsoventral width of the articular surface of the condyle is greater than the lateral width, while the opposite is the case in most other tayassuines.

F:AM 113317 and 113316 have two upper incisors, with I1 being much larger than I2, as in most Miocene tayassuines. The canines show sexual dimorphism in size and shape, as documented by Wright (1993). There is a long canine to P2 diastema. P2 is composed of a distinct protocone and metacone posterior to the paracone, with a thick posterior cingulum. The lingual roots of P3 are fused. P3 also has a small metaconule, and there is a swelling of the posterior cingulum of the hypcone lingual to the metaconule. The paracone, metacone, and protocone of P4 are roughly equal in size. There is a distinct cusp for the hypocone as well, although it is partially joined to the posterior cingulum. The molars of *S. shermerorum* show the stereotypical pattern of *Macrogenis, Woodburnehyus*, and other late Miocene species.

The lower jaw, as shown by F:AM 113264 (Figure 7) shows the typical morphology of most late Miocene peccaries. The lower incisors, i1 and i2, are small, peg-like, and pointed anterodorsally, and there are large canines which are even larger in males. The long curved post-canine diastema terminates in a cheek-tooth series with the classic bunodont pattern of nearly all Miocene tayassuines. The coronoid process is short and pointed strongly posterodorsally, with a short rounded articular process behind it. The angular region of the jaw has the robust ridge along the posteroventral edge for the attachment of the strong temporalis and masseteric muscles.

When the type skull (F:AM 113317) and referred lower jaw (F:AM 113264) are articulated and viewed in anterior oblique orientation, the truly remarkable shape of the zygomatic flanges becomes even more apparent (Figure 7A).

A restoration of *Skinnerhyus shermerorum* is shown in Figure 8.

Discussion

As Wright (1993, 1998) pointed out, the late Clarendonian was a time of great diversification of peccaries, primarily due to the dramatic development of their zygomatic flanges and facial crests. Although the sample size is small in most taxa, we can be confident that these features are not solely due to sexual dimorphism, since there are several quarry samples where we have the zygomatic crests and flanges associated with both diagnostically male and female canines. According to Wright (1983), the sample of *Macrogenis crassigenis* shows this particularly well. In addition, we have the male skulls of *S. shermerorum* (F:AM 113316, 113317) versus the female skull (F:AM 113263). Thus, there appears to be regional diversification of tayassuid species in the late Clarendonian: *Woodburnehyus grenaderae* in California, *Skinnerhyus shermerorum* in the Plains, plus several species of *Macrogenis* in the Plains, and a new genus and species from Love Bone Bed in Florida that is still unnamed and undescribed (Wright, 1993, 1998).

The phylogenetic relationships of these peccaries and their nearest relatives are shown in Figure 9 (modified from Wright, 1993, 1998). As Wright noted, the *Macrogenis-Tayassu* clade is a monophyletic group of nearly all the higher peccaries. The next most derived clade on this cladogram is the node of the *Woodburnehyus-Skinnerhyus* clade, which is differentiated from more primitive *Macrogenis* by the distinctive facial crest of the zygoma extending anteriorly and dorsal to the P4. The *Woodburnehyus-Skinnerhyus* clade can be distinguished from all other peccaries by their distally angular, wing-like zygomatic flanges, whose anterior edges are straight and protrude perpendicularly from the faeial region of the snout (rather than sloping posteriorly back from the snout, as in nearly all other peccaries with flaring zygomatic arches, like *Macrogenis* and *Catagonus brachydontus*). Both *Woodburnehyus* and *Skinnerhyus* are distinct genera that cannot be referred to *Macrogenis* or any other existing taxon of peccaries due to the diagnostic combination of characters listed above, especially since their zygomatic flanges are so different in shape from each other and from all other known peccaries.

Acknowledgments

We thank Meng Jin and Judy Galkin for aceess to the AMNH specimens, and Ruth O'Leary and Alana Gishlick for cataloguing and curating them. We thank Jessica Grenader for help with measuring and photographing the AMNH specimens, and the Carl Mehling of the AMNH for helping us remove specimens from display. We thank Pat Holroyd for access to the UCMP collections. We thank Alana Gishlick for additional photographs, and Pat Linse for Photoshopping the illustrations and drawing Figure 8. We thank M. Mihlbachler for lodging while Prothero visited the AMNH. We thank the late Morris F. Skinner and the Frick Lab crews for their discoveries, and David Wright for his pioneering unpublished work in peccaries. Prothero thanks his former undergraduate professor Mike Woodburne not only for his teaching and inspiration, but also for helping me begin my peccary research where he and Ruben Stirton left off. We thank Spencer G. Lucas and an anonymous reviewer for helpful comments. DRP was funded for this research by a Faculty Research Grant from Occidental College.

References

Colbert, E. H. 1938. Pliocene peccaries from the Pacific Coast region of North America. Carnegie Institute of Washington Publication, 487:241–269.

Prothero, D. R. 2009. The early evolution of North American peccaries (Tayassuidae). Museum of Northern Arizona Bulletin, 65:509–542.

Prothero, D. R., and A. Pollen. 2011. A new species of peccary from the late Clarendonian (late Miocene) Blackhawk Ranch locality, Contra Costa County, California. Journal of Vertebrate Paleontology, 31(supplement to 3):177.

Prothero, D. R., and R. H. Tedford. 2000. Magnetic stratigraphy of the type Montediablan Stage (Late Miocene), Black Hawk Ranch, Contra Costa County, California: implications for regional correlations. Paleobios, 20(3):1–10.

Simpson, G. G. 1949. A fossil deposit in a cave in St. Louis. American Museum Novitates, 1408:1–46.

Skinner, M. F., and F. W. Johnson. 1984. Tertiary stratigraphy and the Frick Collection of fossil vertebrates from north-central Nebraska. American Museum of Natural History Bulletin, 178:215–368.

Wright, D. B. 1983. Late Miocene Tayassuidae (Artiodactyla, Mammalia) of North America. Unpublished. M.A. thesis, University of Nebraska, Lincoln, NE.

Wright, D. B. 1991. Cranial morphology, systematics and evolution of Neogene Tayassuidae (Mammalia). Unpublished Ph.D. dissertation. University of Massachusetts, Amherst, MA.

Wright, D. B. 1993. Evolution of sexually dimorphic characters in peccaries (Mammalia, Tayassuidae). Paleobiology, 19:52–70.

Wright, D. B. 1998. Tayassuidae. p. 389–401. *In* C. M. Janis, K. M. Scott, and L. L. Jacobs (eds.), Evolution of Tertiary Mammals of North America. Volume 1: Terrestrial Carnivores, Ungulates, and Ungulatelike Mammals. Cambridge University Press, Cambridge.

KIRTLANDIA
The Cleveland Museum of Natural History

March 2013 *Number 58:54–60*

PECCARIES (MAMMALIA, ARTIODACTYLA, TAYASSUIDAE) FROM THE MIOCENE-PLIOCENE PIPE CREEK SINKHOLE LOCAL FAUNA, INDIANA

DONALD R. PROTHERO
Department of Vertebrate Paleontology
Natural History Museum, 900 Exposition Blvd., Los Angeles, California 90007
donaldprothero@att.net

HOPE A. SHEETS
Department of Biology
Trine University, One University Ave., Angola, Indiana 46703
hasheets@gmail.com

ABSTRACT

The Pipe Creek Sinkhole local fauna from near Swayzee, Grant County, Indiana, yields an interesting mixture of both plant and animal fossils, including previously unidentified peccaries. The fossil mammals suggest either a latest Hemphillian (latest Miocene-Pliocene) or earliest Blancan (earliest Pliocene) age for the assemblage. The peccaries can be assigned to two taxa: *Catagonus brachydontus*, a large species with brachydont, bunodont cheek teeth, found in the latest Miocene of Mexico, Florida, and Oklahoma, which is related to the living Chacoan peccary *C. wagneri*, and *Platygonus pollenae*, a newly described latest Miocene taxon. The latter is the smallest and most primitive species known from the lineage which culminated with the flat-headed peccaries (*Platygonus compressus*) common in the Pleistocene. Both of these species are unknown from the early Blancan, and support (along with the rhinos and other taxa) a latest Hemphillian age for the fauna.

Introduction

The Pipe Creek Sinkhole biota was discovered in an ancient sinkhole deposit eroded into the underlying Silurian limestones near Swayzee, Indiana (Farlow et al., 2000). It yields a rich flora and fauna that has been described by Farlow et al. (2000, 2006). Shunk et al. (2009) analyzed the paleoclimate of the assemblage, and Farlow et al. (2010) described the coprolites. Farlow et al. (2000), Martin et al. (2002), and Dawson et al. (2008) published a faunal list and described some of the mammals. According to these authors, the lagomorphs suggest an earliest Blancan age for the assemblage, and the carnivorans are early Blancan or older. However, the rodents (Martin et al., 2002) and the presence of the rhinoceros *Teleoceras* suggests a latest Hemphillian age (Prothero, 1998), although there are some claims that rhinos survived in North America until the earliest Blancan (Prothero, 2005; Gustafson, pers. commun. to DRP).

Farlow et al. (2000) mentioned the presence of an "unidentified large peccary" in the fauna, but made no further comments on the specimens. In the course of Prothero's ongoing revision of the North American Tayassuidae beginning in 2007 (first installment published in Prothero, 2009), we learned of these specimens. Farlow loaned them to HAS so they could be compared to specimens in the American Museum of Natural History (AMNH) and properly identified. When we first studied them in the AMNH in January 2009, the systematics of North American late Miocene-Pliocene peccaries had not been resolved well enough to make a reliable comparison with valid taxa. Since then, Prothero and co-authors (Prothero and Grenader, 2012; Prothero, in prep.) have updated the systematics of these taxa, and now the Pipe Creek specimens can be compared to valid taxa and properly identified.

Materials and Methods

This study began in 2008 as a graduate student research project by Sheets. It is published separately here, but it is part of a much larger complete monographic revision of the Tayassuidae currently being written (Prothero, in prep.).

All measurements were made with digital calipers, and recorded in Excel spreadsheets. All statistics and plots were done in Excel. Photos were taken with a Nikon 5700 camera, and then edited in Photoshop.

Abbreviations: AMNH, American Museum of Natural History, New York, including the Frick Collection (F:AM); INSM, Indiana State Museum; TMM, Texas Memorial Museum, Austin.

Systematic Paleontology

Class MAMMALIA Linneaus 1858
Order ARTIODACTYLA Owen 1848
Family TAYASSUIDAE Palmer 1897

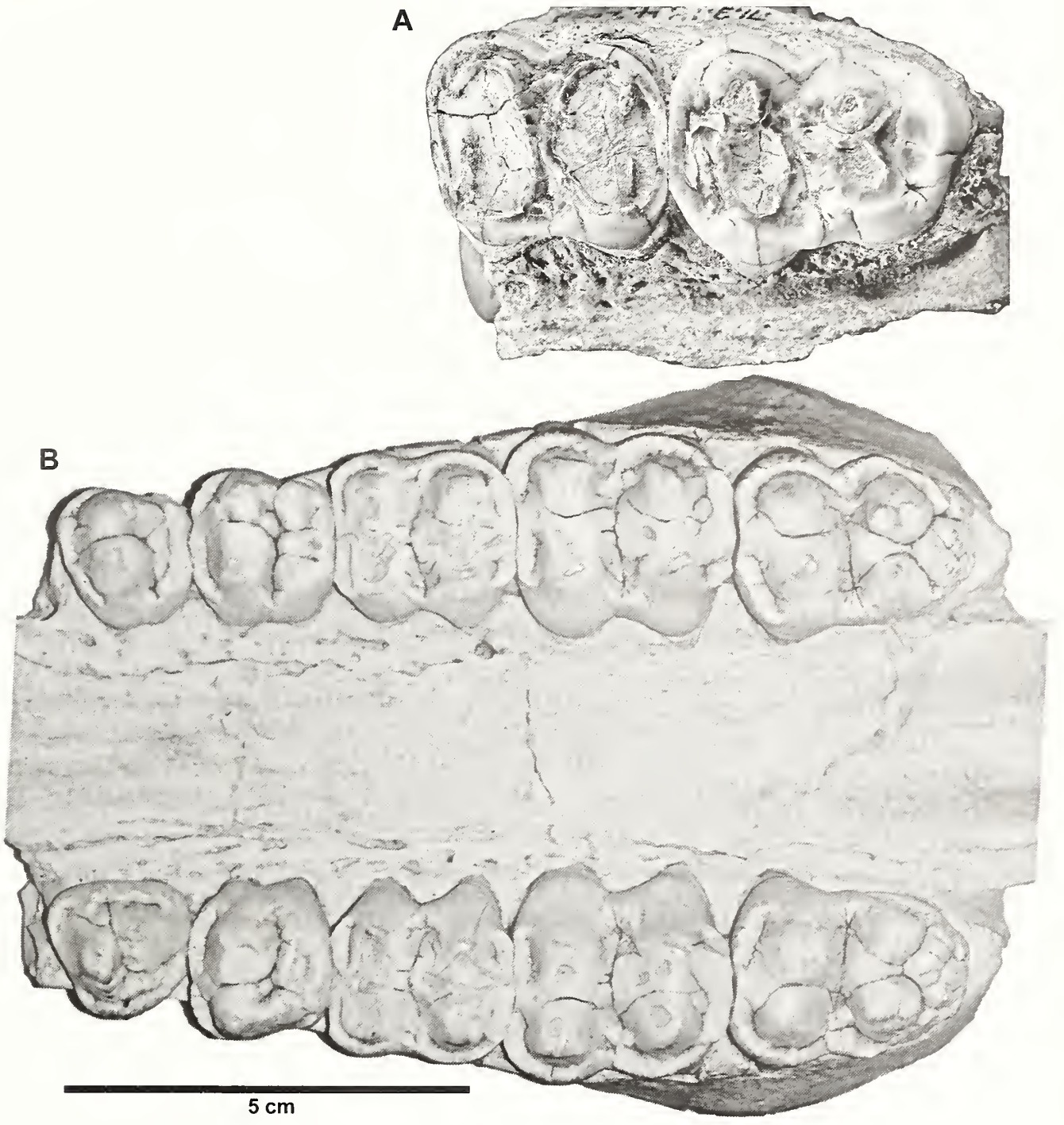

Figure 1. A, *Catagonus brachydontus*, INSM 71.3.144.2003, M2-3. B, cast of AMNH 101932, a palate of *C. brachydontus* from the Bone Valley Formation, Florida, for camparison. Scale bar equals 5 cm. Photo by Jim Whitcraft, courtesy J. O. Farlow.

Catagonus Ameghino 1904
Desmathyus brachydontus Dalquest and Mooser 1980
Catagonus brachydontus Wright, 1983
Figures 1–2, Table 1

Type specimen

TMM 41685-13, a left m3 from the late Hemphillian Rancho el Ocote fauna (Dalquest and Mooser, 1980, Figure 4).

Referred material

INSM 71.3.144.2003, maxillary fragment with right M2-3 (Figure 1).

Description

INSM 71.3.144.2003 consists of two upper molars, M2 and M3, which show a high degree of wear, so that the cusps are deeply worn into lakes or fossettes. M2 is the more worn of the two teeth

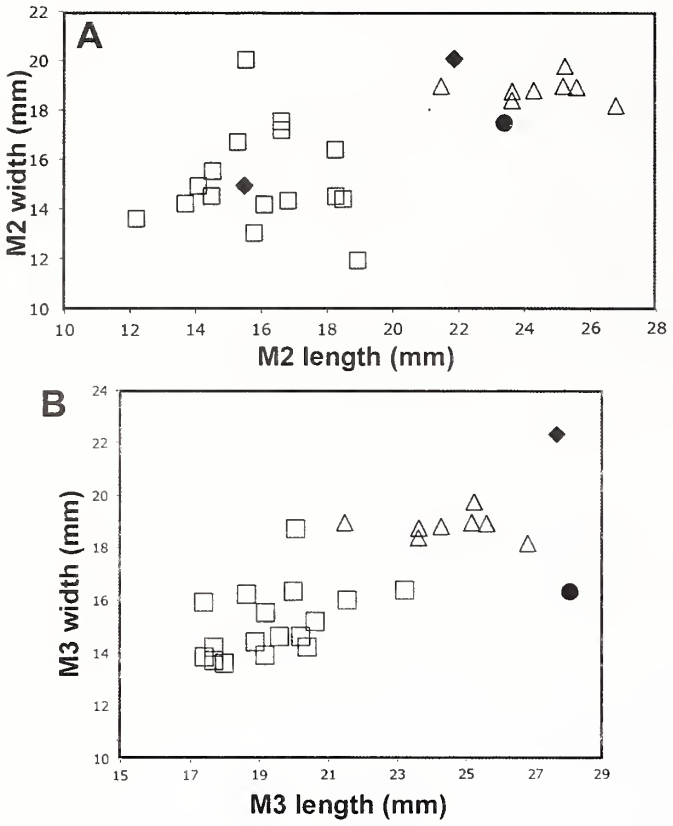

Figure 2. Graph of upper teeth dimensions from Pipe Creek Sinkhole compared to known peccary samples. A, plot of M2 dimensions. B, plot of M3 dimensions. Symbols: open square equals *P. pollenae* from Edson Quarry, Kansas; open diamonds equals *C. brachydontus* from the Bone Valley Formation, Florida; solid circle equals holotype of *P. rex*; larger solid diamond equals INSM 71.3.144.2003; smaller solid diamond equals INSM 71.3.144.2007.

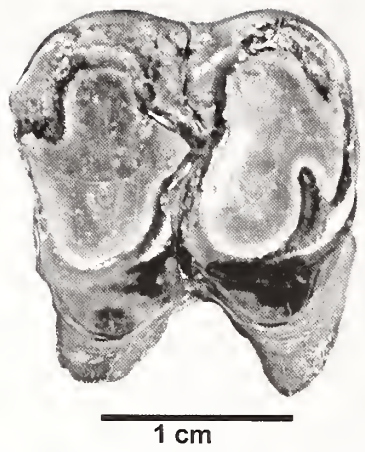

Figure 3. INSM 71.3.144.2007. Right upper M2 in occlusal view. Scale bar equals 1 cm. Photo by Jim Whitcraft, courtesy J. O. Farlow.

(since it erupts earlier than M3), and nearly all the crown pattern has been worn away. The paracone and protocones have worn down to a large transversely oval-shaped fossette with slight enamel ridges where the anterior cingula have been joined to the cusp fossettes due to wear. There is a distinct lingual cingulum on the tooth that forms a bridge between the anterior and posterior fossettes, but no labial cingulum. The posterior fossette has a more rounded shape than does the anterior fossette, with slight crenulations in the surrounding ridge of enamel where the metacone was separated from the metaconule, and where the posterior cingulum has merged with the worn basin of the metacone-metaconule. The rounded shape of this fossette and the enamel ridges suggest that prior to wear this tooth bore discrete bunodont cusps as in *Catagonus*, not lophodont or zygolophodont cusps as in *Platygonus*.

M3 of INSM 71.3.144.2003 is also highly worn down into fossettes surrounded by ridges, but not as worn as M2. There is a strong anterior cingulum that wraps around the worn bases of the paracone and protocone, each of which is marged by a round or oval enamel ridge within the anterior fossette, the worn base of a rounded or oval bunodont cusp. The oval base of the paracone fossette is much smaller than that of the protocone fossette. There is a strong labial cingulum that wraps into the intervallum between the anterior and posterior fossette. There is a distinct but weak lingual cingulum, which forms a weak and discontinuous ridge in the lingual intervallum between the anterior and posterior fossettes. The posterior fossette on the M3 still bears the remnant of a highly worn metacone, which was clearly conical and bunodont in shape before wear. There was also a discrete conical metaconule connected directly to the lingual side of the metacone, now represented by a loop of enamel within the fossette. There may have been a third cusp anterior to the metacone and metaconule, since the loops of worn enamel suggest such a cusp, and cusp variability is very high in peccaries (Simpson, 1949; Slaughter, 1966; Guilday et al., 1971; Wright, 1991). At the posterior end of the crown is a worn pair of cusps connected to

Table 1. Statistics of tooth dimensions. First three columns are INSM 171.3.144.2003, INSM 171.3.144.3010, and INSM 171.3.144.2007 respectively. N = number of samples; SD = standard deviation.

				P. polleni			*C. brachydontus*		
Dimension	2003	**3010**	**2007**	**N**	**Mean**	**SD**	**N**	**Mean**	**SD**
P2L	—	8.1	—	18	9.92	0.71	6	12.28	0.85
P2W	—	8.9	—	18	8.66	0.65	6	11.58	1.52
P3L	—	11.6	—	18	11.69	0.75	8	13.62	0.87
P3W	—	13.2	—	18	10.54	0.84	8	13.38	0.82
M2L	21	—	15.5	18	15.97	1.93	8	20.3	0.72
M2W	20	—	14.9	18	14.87	1.65	8	18.39	1.28
M3L	27.6	—	—	16	19.4	1.58	8	24.5	1.62
M3W	22.2	—	—	16	15.12	1.33	8	18.78	0.47

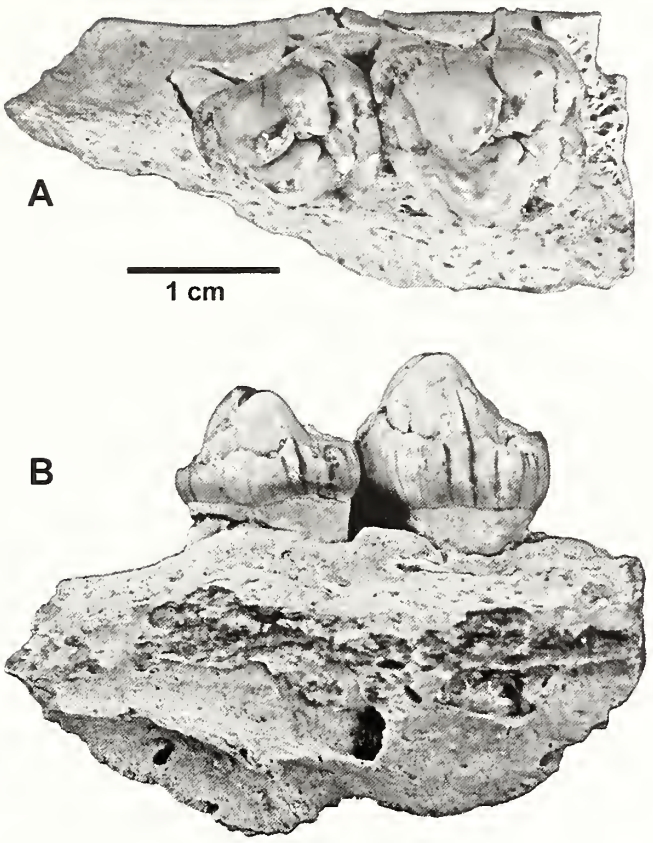

Figure 4. INSM 71.3.144.3010. Maxilla with P2 and P3, referred to *P. pollenae*. A, crown, and B, lateral views. Scale bar equal 1 cm. Photo by Jim Whitcraft, courtesy J. O. Farlow.

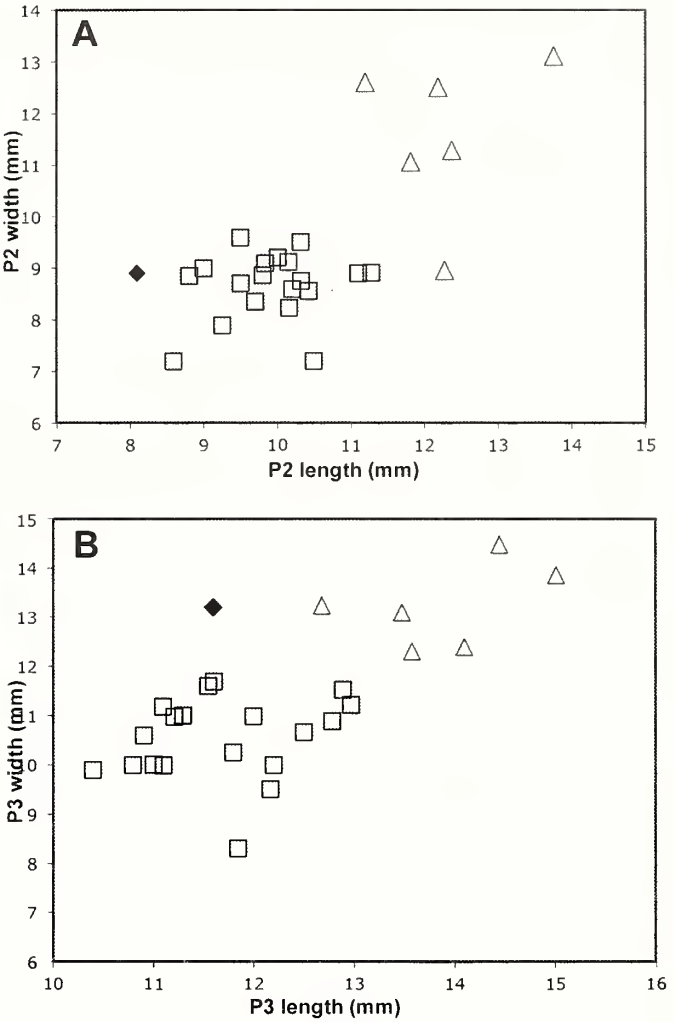

Figure 5. Plot of INSM 71.3.144.3010 (solid diamond), compared to known peccary samples. A, P2 dimensions. B, P3 dimensions. Symbols: open square equals *P. pollenae* from Edson Quarry, Kansas; open diamonds equals *C. brachydontus* from the Bone Valley Formation, Florida.

the posterior cingulum, which are now represented by a pair of enamel loops that once formed their base. Finally, the lingual, posterior, and labial cingulum forms a continuous ridge around the outside of the tooth, but these cingula are not as strong nor discrete as they are on the M2.

Discussion

The sample from Pipe Creek Sinkhole does not appear to come from a single species of peccary, but at least two. Specimen INSM 71.3.144.2003 is clearly a very large species, whereas the remaining tooth specimens seem to pertain to a smaller species.

Comparing INSM 71.3.144.2003 to the available sample at the AMNH, it seems clear that the most likely assignment is with *Catagonus brachydontus* Wright, 1983. Dalquest and Mooser (1980) first described this taxon as "*Desmathyus*" *brachydontus*. It is a mark of how long peccary systematics have been in a state of confusion that their specimens were assigned to the early Miocene (late Arikareean-Hemingfordian) genus *Desmathyus* simply on the basis of its primitive bunodont cusp morphology. This is despite the fact that the Rancho el Ocote material is much larger than any known specimen of *Desmathyus*, and from beds at least 10 million years younger than this early Miocene genus.

Wright (1983) recognized the true affinities of "*D.*" *brachydontus*, and re-assigned it to *Catagonus*, which today is represented by the living Chacoan peccary, *C. wagneri*. First described in 1975 (Wetzel et al., 1975), *C. wagneri* is a remarkable case of an animal that was first described as a tooth fossil by Florentino Ameghino in 1904, then discovered to be alive almost 70 years later. Wright (1983) described a large number of specimens from the late Hemphillian of Florida (Bone Valley Formation), Oklahoma (Buis Ranch local fauna), and Mexico (Rancho el Ocote local fauna), which clearly showed that "*D.*" *brachydontus* was referable to *Catagonus*, and not to a much older and smaller early Miocene taxon. These include specimens with complete undistorted skull and jaws, and abundant jaws and teeth, as well.

Comparison of INSM 71.3.144.2003 with samples of other peccaries (Figures 1B, 2) shows that its M2 is within the size distribution of *C. brachydontus* from the Bone Valley Formation, Florida. The M3 of INSM 71.3.144.2003, however, appears to be larger than the Bone Valley material (Figures 1B, 2B), but it still falls within the size range of the sample from the topotypic locality, Rancho el Ocote (Dalquest and Mooser, 1980, Table 3).

The only other possible match for such a large peccary is *Platygonus rex* Marsh 1894 whose type specimen (YPM 11870) probably came from the Hemphillian Rattlesnake Formation of Oregon. However, *P. rex* is slightly smaller (Figure 2) and has a

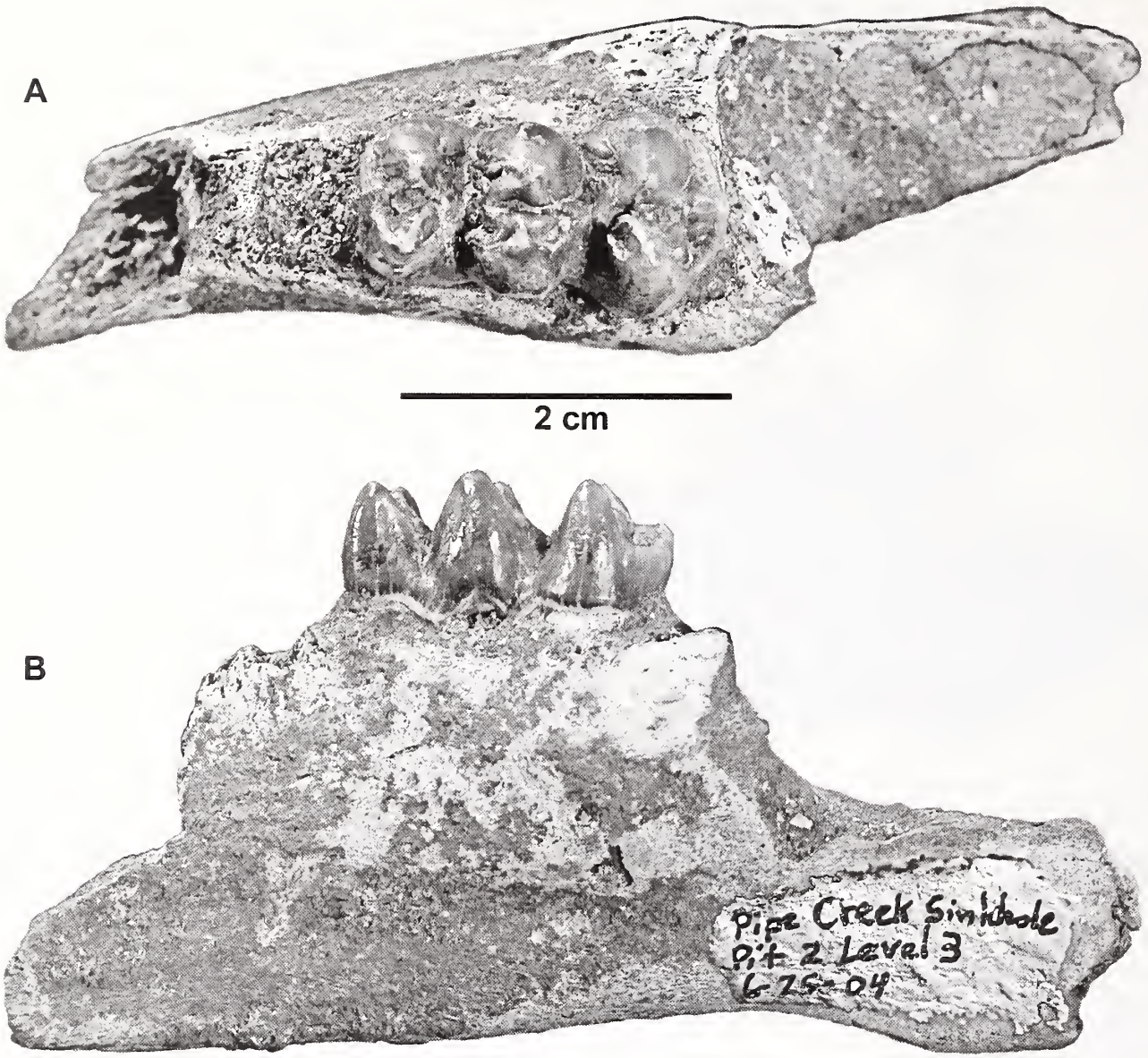

Figure 6. INSM 71.3.144.3004. Left ramal fragment with isolated deciduous premolar in, A, crown and B, lateral view. Scale bar equals 2 cm. Photo by Jim Whitcraft, courtesy J.O. Farlow.

much more zygolophodont dentition than INSM 71.3.144.2003. The *Platygonus* species known from the Pliocene (*P. bicalcaratus, P. texanus, P. pearcei*) are within the size range of INSM 71.3.144.2003, but they all have much more lophodont or zygolophodont teeth than INSM 71.3.144.2003F.

Thus, in its relatively brachydont cusp morphology but large size, INSM 71.3.144.2003 is assigned to *C. brachydontus*, a taxon known only from the late Hemphillian.

Platygonus Le Conte, 1848
Platygonus pollenae Prothero and Grenader, 2012
Figures 3–6, Table 1

Type specimen

AMNH 17582, fragmentary skull and palate; from the latest Hemphillian ZX Bar local fauna, Johnson Member of the Snake Creek Formation, Sioux County, Nebraska (Skinner et al., 1977).

Referred material

INSM 71.3.144.2007, INSM 71.3.144.3010, and possibly other small tooth fragments from Pipe Creek Sinkhole (Figures 3, 4).

Description

INSM 71.3.144.2007 (Figure 3) is a highly worn isolated upper right M2 with roots exposed. Both the paracone-protocone and metacone-metaconule cusps are so worn that they form elongate oval-shaped fossettes. The paracone-protocone fossette bears slight enamel ridges where the anterior cingulum has merged with the cusps due to wear. No other traces of the original cusps remain. However, the shape of the base of those cusps, and the parallel flat sides in the transverse axis (rather than convexly curved sides) of the fossette suggest that the tooth was zygolophodont or lophodont, as confirmed by the well-developed intervallum between them. The metacone-metaconule fossette

is also parallel-sided in the transverse axis, but bears convexly rounded bulges of the surrounding enamel ridge where the hypocone would have been, and another protruding into the intervallum between the ridges. The enamel outlines suggests that this part of the tooth was not as lophodont or zygolophodont as the other, but still much more so than the condition seen in the M2 of INSM 71.3.144.2003. When plotted with M2s from other Hemphillian peccaries (Figure 2), it falls completely within the *P. pollenae* size cluster.

INSM 71.3.144.3010 is a portion of an upper left maxilla with P2 and P3 preserved (Figures 4, 5). Both are relatively unworn with well-developed cusps, in contrast to INSM 71.3.144.3007 and INSM 71.3.144.2003. P2 has a small conical metacone, an anteriolingually displaced paracone, and a large protocone, forming a triangle with the apex oriented anteriorly. There is a discrete posterior cingulum with an intervallum separating it from the main cusps, and in lateral view (Figure 4B) one can see the weak lingual and posterior cingula that wrap around the crown of the tooth. P3 is considerably larger than P2, but has a similar arrangement of cusps: a small labial metacone, a larger anteromedially shifted paracone, and a large protocone, with posterior and lingual cingula wrapping around. These teeth have the typical simple crown patterns seen in most peccary teeth, and since peccary premolars are known to have high intrapopulational variability (Simpson, 1949; Slaughter, 1966; Guilday et al., 1971; Wright, 1991), they are not very diagnostic taxonomically.

The remaining tooth material is less diagnostic. INSM 71.3.144.3004 is a right ramal fragment with portions of deciduous premolars preserved (Figure 6). Deciduous premolars are very rarely preserved in most peccary specimens, and where they are known they are highly variable and non-diagnostic (Simpson, 1949; Slaughter, 1966; Guilday et al., 1971; Wright, 1991). INSM 71.3.144.3005 is an upper right maxillary fragment, again with a portion of a deciduous premolar that is not very useful taxonomically. INSM 71.3.144.3007 is a fragment of a premolar crown that cannot be identified beyond the fact that it came from a peccary. INSM 71.3.144.3008, INSM 71.3.144.3009, and INSM 71.3.144.3006 are fragments of the crown of a tooth showing a single cusp, again non-diagnostic beyond "Tayassuidae". Based on overall size, all these fragments could belong to the smaller taxon at Pipe Creek Sinkhole, although they are too poorly preserved to be certain of this.

Discussion

As described above, the smaller material from Pipe Creek Sinkhole consists of a single right M2 (INSM 71.3.144.2007) and a maxillary fragment with P2 and P3 (INSM 71.3.144.3010), as well as other tooth fragments. INSM 71.3.144.2007 is very highly worn, but clearly shows some sort of bilophodonty or zygolophodonty, which makes it referable to *Platygonus*. Although they are not highly diagnostic, the premolar morphology of INSM 71.3.144.3010 seems to be a good match for the premolars of *Platygonus* as well. Prothero and Grenader (2012) described a new, very primitive species of *Platygonus, P. pollenae*, currently known only from the latest Hemphillian of Nebraska (ZX Bar local fauna, Snake Creek Formation), Kansas (Edson local fauna), Colorado (Wray local fauna), and Texas (Coffee Ranch local fauna). In size and morphology, INSM 71.3.144.2007 and INSM 71.3.144.3010 are good matches for the known sample of *P. pollenae* (Figures 3–5, Table 1). They are clearly too small to pertain to the larger species of *Platygonus*, such as *P. rex* and the Blancan species mentioned above, so *P. pollenae* is the only reasonable referral. In its size and morphology, *P. pollenae* is a very distinctive peccary not easily mistaken for any other species in the Hemphillian and Blancan. It is known only from the late Hemphillian.

Conclusions

Two taxa of peccary are represented at Pipe Creek Sinkhole: the large bunodont species *Catagonus brachyodontus*, and the small zygolophodont species *Platygonus pollenae*. Both are currently known only from the late Hemphillian and have no record in the Blancan. Thus, they support the idea that at least part of the Pipe Creek Sinkhole fauna is latest Miocene, not Pliocene.

Acknowledgments

We thank Meng Jin and Judy Galkin for access to the AMNH specimens, and Ruth O'Leary and Alana Gishlick for cataloguing and curating them. We thank Jim Farlow from IPFW for the loan of the Indiana collections, and for providing the photos taken by Jim Whitcraft. We thank Pat Linse for Photoshopping the illustrations. We thank Richard Stucky, Jim Farlow, and an anonymous reviewer for helpful comments. A Faculty Research Grant from Occidental College funded part of the research by DRP.

References

Ameghino, F. 1904. Nuevas especies de mamiferos cretaeos y terciarios de la Republica Argentina (continuacion). Annales Sociedad Cientificas Argentina, 58:182–192.

Dalquest, W. W., and O. Mooser. 1980. Late Hemphillian mammals of the Ocote local fauna, Guanojuato, Mexico. Pearce-Sellards Series, 32:1–25.

Dawson, M. R., J. O. Farlow, and A. Argast. 2008. *Hypolagus* (Mammlia, Lagomorpha, Leporidae) from the Pipe Creek Sinkhole, Grant County, Indiana, p. 5–10. *In* G. H. Farley and J. R. Choate (eds.), Unlocking the Unknown: Papers Honoring Dr. Richard J. Zakrzewski. Fort Hays State University, Hays, Kansas.

Farlow, J. O., J. A. Sunderman, J. J. Havens, A. L. Swinehart, J. A. Holman, R. L. Richards, N. G. Miller, R. A. Martin, R. M. Hunt, Jr., G. W. Storrs, B. B. Curry, R. H. Fluegeman, M. R. Dawson, and M. E. T. Flint. 2001. The Pipe Creek Sinkhole biota, a diverse late Tertiary continental faunal assemblage from Grant County, Indiana. American Midland Naturalist, 145:367–378.

Farlow, J. O., and A. Argast. 2006. Preservation of fossil bone from the Pipe Creek Sinkhole (late Neogene, Grant County, Indiana, U.S.A.). Journal of the Paleontological Society of Korea, 22:51–75.

Farlow, J. O., K. Chin, A. Argast, and S. Poppy. 2010. Coprolites from the Pipe Creek Sinkhole (Late Neogene, Grant County, Indiana, U.S.A.). Journal of Vertebrate Paleontology, 30:959–969.

Guilday, J. E., H. W. Hamilton, and A. D. McCrady. 1971. The Welsh Cave peccaries (*Platygonus*) and associated fauna, Kentucky Pleistocene. Annals of the Carnegie Museum, 43(9): 249–320.

Marsh, O. C. 1894. Description of Tertiary artiodactyls. American Journal of Science, 48:259–274.

Martin, R. A., H. T. Goodwin, and J. O. Farlow. 2002. Late Tertiary (late Hemphillian) rodents from the Pipe Creek Sinkhole, Grant County, Indiana. Journal of Vertebrate Paleontology, 22:137–151.

Prothero, D. R. 1998. Rhinocerotidae, p. 595–605. *In* C. Janis, K. M. Scott, and L. Jacobs (eds.), Evolution of Tertiary Mammals of North America, Cambridge Univ. Press, Cambridge.

Prothero, D. R. 2005. The Evolution of North American Rhinoceroses. Cambridge University Press, Cambridge. 218 p.

Prothero, D. R. 2009. The early evolution of North American peccaries (Tayassuidae). Museum of Northern Arizona Bulletin, 65:509–542.

Prothero, D. R., and J. Grenader. 2012. A new primitive species of *Platygonus* (Mammalia: Tayassuidae) from the late Miocene-Pliocene of the High Plains. Journal of Paleontology, 86:1021–1031.

Shunk, A. J., S. G. Driese, J. O. Farlow, M. S. Zavada, and M. K. Zobaa. 2009. Late Neogene paleoclimate and paleoenvironment reconstruction from the Pipe Creek Sinkhole, Indiana, U.S.A. Palaeogeography, Palaeoecology, Palaeoclimatology, 274:173–184.

Simpson, G. G. 1949. A fossil deposit in a cave in St. Louis. American Museum Novitates, 1408:1–46.

Slaughter, B. H. 1966. *Platygonus compressus* and associated faunas from Laubach Cave of Texas. American Midland Naturalist, 75(2): 475–494.

Wetzel, R. M., R. E. Dubos, R. L. Martin, and P. Meyers. 1975. *Catagonus*, an "extinct" peccary, alive in Paraguay. Science, 189:379–381.

Wright, D. B. 1983. Phylogenetic relationships of *Catagonus wagneri*: sister taxa from the Tertiary of North America. Advances in Neotropical Mammalogy, 1989:281–308.

Wright, D. B. 1991. Cranial morphology, systematics and evolution of Neogene Tayassuidae (Mammalia). Unpublished Ph.D. dissertation. University of Massachusetts, Amherst, MA.

Wright, D. B. 1998. Tayassuidae. p. 389–401. *In* C. M. Janis, K. M. Scott, and L. L. Jacobs (eds.), Evolution of Tertiary Mammals of North America. Cambridge University Press, Cambridge.

KIRTLANDIA
The Cleveland Museum of Natural History

March 2013 *Number 58:61–72*

RECONSTRUCTING PALEODIET IN GROUND SLOTHS (MAMMALIA, XENARTHRA) USING DENTAL MICROWEAR ANALYSIS

NICHOLAS A. RESAR
Department of Geology
Kent State University, 221 McGilvrey Hall, Kent, Ohio 44242

JEREMY L. GREEN
Kent State University at Tuscarawas, 330 University Drive NE,
New Philadelphia, Ohio 44663

AND **ROBERT K. McAFEE**
Department of Biological and Allied Health Sciences
Ohio Northern University, 525 S. Main Street, Ada, Ohio 45810

ABSTRACT

Understanding the paleoecology of extinct xenarthrans, such as ground sloths, is complicated because they lack living analogues. Previous studies have applied functional morphology and biomechanical analyses to reeonstruct the diet and lifestyle of ground sloths, yet the application of dental microwear as a proxy for feeding ecology in extinct xenarthrans remains understudied. Here, we hypothesize that dental microwear patterns are statistically different among extinct ground sloths, thereby providing new evidence of feeding ecology in these animals. In a blind study, the dental microwear patterns in three extinct taxa representing two clades [*Megalonyx wheatleyi* and *Acratocnus odontrigonus* in Megalonychidae, *Thinobadistes segnis* in Mylodontidae] were quantitatively analyzed using scanning electron microscopy at 500× magnification. Two independent observers recovered similar relative trends in microwear patterns between *M. wheatleyi*, *A. odontrigonus*, and *T. segnis*, with mean number of scratches and feature width being the most informative variables among taxa. Microwear patterns in *M. wheatleyi* correspond most closely with living selective xenarthran herbivores (i.e., *Bradypus*), with a low number of scratches but a high feature width. *T. segnis*, in contrast, has an unusually high number of scratches but low feature width, which is unlike any patterns exhibited by living xenarthrans and indicates possible grazing habits. *A. odontrigonus* falls between these two extremes, which we interpret as a more generalized browser, similar to *Choloepus*. Microwear patterns among living and extinct sloths sampled to date seem to fall along a continuum of herbivorous feeding strategies, with grazing and selective browsing representing the two extremes. Although we only examine three taxa, our results (stemming from a blind analysis that accounts for observer error) support the feasibility of using high-magnification dental microwear to examine feeding ecology in extinct ground sloths.

Introduction

Xenarthrans form a major clade of placental mammals (Delsuc et al., 2002) that include extant armadillos, tree sloths, and anteaters, as well as the extinct ground sloths, pampatheres, and glyptodonts (McKenna and Bell, 1997). Among other specialized traits, such as xenarthrous articulations of the spinal column and the articulation between the transverse processes of the proximal caudal vertebrae with the ischium (Vizcaíno and Loughry, 2008), xenarthrans are differentiated from other mammals by the absence of enamel on their adult teeth (Hillson, 2005). Although several clades of placental mammals have evolved partial or complete enamel loss on their teeth (Hillson, 2005; Green, 2009a; Ungar, 2010), xenarthrans are unique in the almost universal enamel loss within the clade (Vizcaíno, 2009). The orthodentine that composes the surface of xenarthran dentition is a softer tissue than enamel (Hillson, 2005; Kalthoff, 2011), which causes their teeth to wear much faster compared to the enamel-covered teeth of other mammals. This wear is compensated for by the presence of an open root, which allows for continuous growth of the tooth throughout the life of the animal. Because dentition functions mainly to process food, the unique, soft, simple-shaped morphology of xenarthran teeth begs the question as to what food items

extinct members of this group consumed. Although ground sloth taxa are numerous in the Cenozoic fossil record in North and South America (McDonald and De Iuliis, 2008), understanding the paleoecology of these extinct mammals is complicated because they lack exact living ecological analogues.

Ground sloths inhabited a wide range of environments, stretching from Alaska to Argentina (McDonald and De Iuliis, 2008), including the Caribbean islands (White, 1993) and possibly Antarctica (Vizcaíno and Scillato-Yane, 1995; MacPhee and Regeuro, 2010). Hypothesized eating habits ranged from grazing (Webb, 1989, Shockey and Anaya, 2011) and forest browsing (McDonald, 1995; Hoganson and McDonald, 2007) to aquatic feeding (Muizon et al., 2004), and ground sloths could have reached large sizes (approximately1000–6000 kg in some taxa; Fariña et al., 1998). Their closest living relatives, the extant tree sloths, however, are limited to arboreal habitats in tropical climates (Vizcaíno et al., 2008) and are relatively small compared to ground sloths (Gaudin and McDonald, 2008). Previous studies have applied functional morphology and biomechanical analyses to reconstruct life history in ground sloths (Naples, 1989; Vizcaíno et al., 2006; Bargo et al., 2006a, b; Shockey and Anaya, 2011). As noted by Smith and Redford (1990), anatomy may not always be an accurate predictor of feeding ecology in extant xenarthrans. Therefore, it is important to pursue as many independent lines of evidence when examining diet in extinct xenarthrans.

One recent, new line of analysis that is being used to help better understand paleodiet in xenarthrans is dental microwear. Dental microwear refers to the microscopic scarring of the occlusal surface of teeth due to tooth-on-food or tooth-on-tooth interactions during mastication and can take the form of scars, such as scratches and pits of various widths, lengths, and orientations (Teaford, 1991). The type and density of microwear features depends on several factors, including, but certainly not limited to, the amount of oral processing and the frequency of abrasives in the diet. The longer an animal chews its food (i.e., oral processing), the more microwear features should be deposited on the chewing surface of the tooth (Teaford, 1991). The toughness of food particles also directly affects microwear, as tougher, more abrasive foods (e.g., grasses) are correlated with higher levels of tooth scarring (Ungar et al., 2008). For this reason, browsers (herbivores that consume tender leaves, fruits, etc.) should exhibit a lower density of microwear features than grazers (herbivores that primarily eat tough, abrasive grasses), as the grazer will use more oral processing to break down tougher foods (Solounias et al., 1988; Teaford, 1991; Ungar, 2010). Ingested grit from other sources including digging for food (such as roots or insects) or dust on low-level vegetation is also a major contributor to microwear formation (Williams and Kay, 2001). It is also possible that the acidity of fruits in an animal's diet will partially erase microwear (i.e., acid etching; Teaford, 1988). Analysis of microwear patterns can be done either qualitatively (describing overall texture or complexity), or quantitatively by measuring the size and density of features (Teaford, 1991). When applied to living organisms, it is possible to correlate specific diets with unique microwear patterns; this data can be used as a foundation for reconstructing the paleodiet of extinct taxa (e.g., Solounias et al., 1988; Solounias and Semprebon, 2002; Green et al., 2005).

While dental microwear is a well-established proxy for feeding patterns in mammals with enamel-covered teeth, the significance of microwear on softer orthodentine has received comparably less attention, until recently (Oliveira, 2001; Green, 2009b, 2009c; Green and Resar, 2012). Initial microwear studies on xenarthrans (Oliveira, 2001; Green, 2009b; Green and Resar, 2012) show that these enigmatic mammals do record scars on their teeth that are similar in size and appearance to those observed in other mammals with enamel. Further, orthodentine microwear patterns in these animals can be statistically differentiated between taxa with different diets, although the resolution is not as high as that found in enamel studies that apply the same methodology (Green, 2009b; Green and Resar, 2012). These initial findings support the use of dental microwear as a proxy for xenarthran paleoecology. Most recently, Green and Resar (2012) examined microwear patterns in five extant species, each grouped into one of four dietary categories. Folivores consisted of *Bradypus variegatus* (Linnaeus, 1758), whieh consumes leaves from a narrow range of plant species (Chiarello, 2008). Frugivore-folivores were represented by *Choloepus didactylus* (Linnaeus, 1758) and *C. hoffmanni* (Peters, 1858), which eat a more variable mixture of fruits, leaves, and flowers (Chiarello, 2008). Among armadillos, insectivores were represented by *Dasypus novemcinctus* (Linnaeus, 1758), which primarily consumes insects, although some opportunistic omnivory does occur is this group (McDonough and Loughry, 2008). Carnivore-omnivores were represented by the armadillo *Euphractus sexcinctus* (Linnaeus, 1758), which has a more variable omnivorous diet relative to other cingulates (McDonough and Loughry, 2008). The authors concluded that relative differences in the number of scratches and width of scar features was useful in statistically differentiating not only xenarthrans living in distinct habitats (i.e., semi-fossorial armadillos versus arboreal tree sloths), but also taxa living in the same habitat (e.g., two-toed tree sloths versus three-toed tree sloths; Green and Resar, 2012). On average, insectivorous armadillos had a lower scratch count and higher feature width than armadillos classified as carnivore-omnivores. Likewise, folivorous three-toed sloths consistently had lower scratch density with a greater feature width than frugivore-folivorous two-toed sloths (Green and Resar, 2012).

Using data from Green and Resar (2012) as a foundation, we hypothesize that dental microwear patterns can be differentiated among extinct ground sloths, thereby providing new evidence of feeding ecology in this group. We test this hypothesis by quantifying and statistically comparing microwear patterns in three extinct ground sloth species with microwear in living tree sloths (with the latter taken from Green and Resar, 2012), using the same methodological approach as Green and Resar (2012). Originally, we sampled six extinct taxa for this study (see Appendix). However, post-taphonomic screening sample sizes for three of the taxa (*Hapalops*, *Octodontotherium*, *and Scelidotherium*) were insufficient to provide objective information about paleodiet, yet the data from these few specimens can still help identify methodological error in our analysis. Microwear patterns in the remaining three taxa (*Acratocnus*, *Megalonyx*, *and Thinobadistes*) were analyzed in detail, and we use data from these three species to test our hypothesis. We directly compared ground sloth microwear with data from Green and Resar (2012) for extant xenarthrans to aeeomplish this goal. The hypothesized paleoecology for the three primary study taxa is summarized below.

Megalonyx wheatleyi is a North American species of the clade Megalonychidae and includes several species with a wide geographic distribution from Mexico to the Yukon, including both east and west coasts (McDonald, 1995; Hoganson and

McDonald, 2007). Across its wide geographic distribution, *M. wheatleyi* has been reconstructed as a forest-dwelling browser (McDonald, 1995; Kohn et al, 2005; Hoganson and McDonald, 2007). *M. wheatleyi* specimens for this study come from the McLeod Limerock Mine in Levy County, Florida, which is middle Pleistocene (Irvingtonian) in age (Hulbert, 2001). As a hypothesized strict browser, we predict that *M. wheatleyi* should have a lower density of microwear features on its teeth relative to other ground sloths, an observation supported by data from living tree sloths (Green and Resar, 2012).

Acratocuus odontrigouus is also a member of Megalonychidae, and is considered more closely related to extant *Choloepus* (two-toed sloths) than to *M. wheatleyi* (Gaudin, 2004). While *Acratocnus* has a distribution across a number of the Great Antilles islands, this species is known only from the Quaternary of Puerto Rico (White and MacPhee, 2001). *A. odontrigouus* has been reconstructed as at least partially arboreal (White, 1993), but at this time, no hypotheses of paleodiet have been postulated for this species. *A. odontrigonus* specimens for this study came from Cerro Hueco Cave (Quaternary) in Puerto Rico (White and MacPhee, 2001), which, based on the associated fauna, represents an arid environment, characterized by savanna grasslands and dry scrub forests (Pregill and Olson, 1981). While the bulk of *Acratocuus* finds are from cave deposits, such a locality was probably not their typical habitat, as some sites implicitly indicate a trap environment (Anthony, 1916). Given the aboveground environments, semi-arboreal habits of these sloths, and morphological similarities to the feeding apparatuses of other megalonychids of all sizes (Bargo et al. 2006a, b; McAfee, 2011), we suggest *Acratocuus* was a folivorous browser.

Thinobadistes seguis is a mylodontid sloth from the Miocene of the Gulf Coastal Plain and southern Great Plains (Webb, 1989). During the Miocene, *T. segnis* occupied a complex mixed environment including forest, river, and open country (Webb et al., 1981). Very little has been published on *T. seguis,* but it has been hypothesized that mylodontids were grazers or bulk feeders in open habitats (Moore, 1978; McDonald and De Iuliis, 2008; Shockey and Anaya, 2011), although some species have been reconstructed as intermediate mixed feeders (Naples, 1989). More specifically, the broad, flat premaxilla and the correspondingly wide predental spout of the mandible that is indicative of Mylodontinae sloths, such as *Lestodou* and *Glossotheriuu* of South America, suggests a bulk grazing strategy (Bargo et al., 2006b). This muzzle morphology is also present in *T. segnis*, a species closely aligned with *Lestodon* (Webb, 1989; Gaudin, 2004). Specimens here come from Mixson's Bone Bed in Levy County, Florida, which is late Miocene (Hemophilia) in age (Hulbert, 2001; Morgan, 2005). Brief reports of the lithology of the Mixson's site appear to reflect a woodland savanna (typical of the late Miocene environments along the Gulf Coast; Webb 1977), yet detailed paleoenvironmental information about this location is currently lacking (Leidy and Lucas, 1896; R.C. Hulbert, Jr., personal communication).

Materials and Methods

Specimen selection

Twenty-three specimens from six taxa (*Megalonyx wheatleyi* [n=6]; *Acratocuus odontrigonus* [n=4]; *Thinobadistes seguis* [n=6]; *Octodontotheriuu grandee* [n=3]; *Hapalops elongates* [n=3]; *Scelidotheriuu* sp. [n=1]) were analyzed (Appendix 1). Specimens came from the vertebrate paleontology collections at the Field Museum of Natural History, Chicago, IL (FMNH) and the American Museum of Natural History (AMNH), New York, NY. Following the approach standardized by Green and Resar (2012), we sampled only the mesial wear facet on upper second molariforms (M2; *seusu* Naples, 1982) for each taxon (Figure 1). For isolated teeth, we used direct comparison of *in situ* teeth in maxillae (available in the collections where sampling was conducted) to positively identify isolated M2s for our analysis, along with the following references: Anthony (1926); Hoffstetter (1956), McDonald (1977, 1987); Scott (1904); Webb (1989). All sample teeth for a particular species were chosen from the same locality, and while this did limit sample size, the authors felt that minimizing potential intraspecific variation in microwear patterns was necessary for this introductory study.

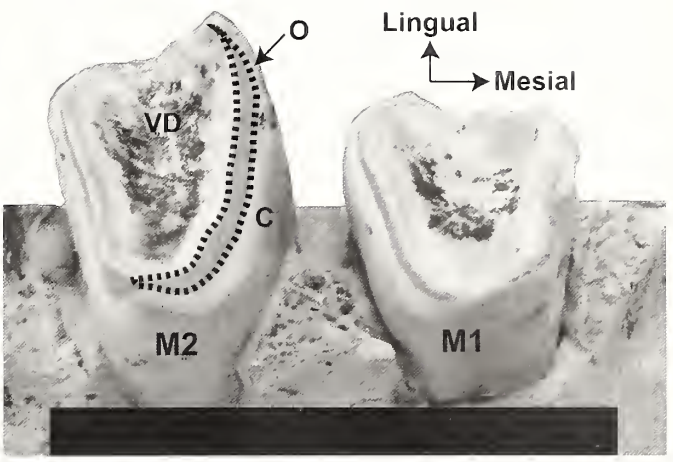

Figure 1. Representative image of upper sloth molariform (*Megalouyx*; UF 223806). Location of SEM imaging and analysis in this study was always along the orthodentine layer on the mesial facet of M2, indicated by the dashed crescent. Key: C, cementum; M1, molar 1; M2, molar 2; O, orthodentine; VD, vasodentine. Scale bar equals 3 cm.

Specimen preparation

Cleaning, molding, and casting protocols for microwear analysis followed Green and Resar (2012). Resulting casts were mounted on 25.4 mm or 12.7 mm aluminum stubs, according to tooth size, using standard carbon adhesive tabs (Electron Microscopy Sciences, Inc). A belt of colloidal silver liquid (Electron Microscopy Sciences, Inc.) was applied to the base of the specimen and the top of the aluminum stub to improve electron dispersal and overall adhesion between the stub and the cast. The final preparation step, accomplished just before imaging, was to coat the specimen with a thin layer of gold (105 s) using a SEM Coating System (Microscience Division, Bio-Rad Laboratories, Inc.).

Scanning electron microscopy

For each tooth, two digital images along the outer orthodentine band (Figure 1) on the mesial wear facet on M2s were captured at 500× (with an operating voltage of 20 kV using secondary electrons) in an Amray Model 1600 Turbo scanning electron microscope located in McGilvery Hall at Kent State University. To standardize the counting area, a 100 μm × 100 μm square was digitally constructed and centered over the area of highest density of visible microwear features in each image. This also allowed us

to select the most opportune location to sample ante-mortem microwear and to exclude areas with obvious casting artifacts. Brightness, contrast adjustments, and construction of the digital counting square were all accomplished using Adobe Photoshop CS4 and Adobe Illustrator CS4 (Adobe Systems, Inc.).

Controlling for taphonomic alteration

Since taphonomic processes can alter microwear patterns (Teaford, 1988), specimens were checked for possible false microwear by looking at non-occlusal surfaces of the tooth. Post-mortem abrasion is unlikely to affect only the chewing surface, so teeth that show similar microwear patterns on both the chewing and non-chewing surfaces were rejected due to the high likelihood of original microwear alteration (Teaford, 1988). In addition, if microwear was absent on the chewing surface of a tooth, the specimen was also considered altered and rejected, as ante-mortem microwear was most likely obliterated by taphonomic processes (King et al., 1999).

Microwear analysis

Following the methods of Green and Resar (2012), orthodentine microwear patterns on digital images were analyzed using the semi-automated custom software package Microware 4.02 (Ungar, 2002). This program was originally designed to quantify scratches and pits on enamel surfaces in mammals; however, the overall similarity of orthodentine microwear features to those in enamel (i.e., Oliveira, 2001; Green, 2009b, c; Green and Resar, 2012) supports the use of this program for this study. The Microware program involves a cursor-based user interface, where the researcher identifies endpoints of scratches and pits on the image. We focused on four variables recorded by the program: 1, number of scratches (S); 2, number of pits (P); 3, feature minor axis length, i.e., feature width (FW); and 4, degree of parallelism in feature orientation (R). Feature major axis length is automatically recorded by the program, but we did not analyze this variable because the endpoints of some scars extended beyond the 100 μm^2 counting square. We maintained a length/width ratio of 4:1 to discriminate scratches from pits.

Because the Microware program relies on human recognition of features, it is critical to account for operator error (Grine et al., 2002). Additionally, knowledge of specimen identification and dietary category assignment during analysis may lead to subconscious bias during data collection (e.g. Mihlbachler et al., 2012). As in Green and Resar (2012), we controlled for observer error in the following ways: 1) observers 1 (NAR) and 2 (JLG) independently counted microwear features on all images; 2) all images were randomly organized by an independent third-party (i.e., not an author) and the specimen number and species identity were removed prior to counting, thus creating a blind analysis. Ten randomly selected images were duplicated within the randomized image file. These duplicates were analyzed along with all other images, which allowed us to measure intraobserver error in the consistency of feature recognition by both researchers.

Eight non-parametric Wilcoxon signed-rank tests [one per variable (4) per observer (2)] were applied to determine if each observer consistently recognized the same numbers of features between iterations of the duplicate images. We did not re-analyze images more than once because repeated iterations can lead to observer familiarity with images, which can falsely deflate error measurements (Mihlbachler et al., 2012). Four Wilcoxon signed-rank tests (one per variable) were applied to test for significant differences between observer datasets, providing a measure of interobserver error in absolute values of variables. We measured the degree of correlation between observer datasets by calculating one Pearson Correlation Coefficient (PCC) per variable; this reveals whether observers recovered the same differences between species studied, regardless of absolute values (e.g., Mihlbachler et al., 2012; Green and Resar, 2012). Following Grine et al. (2002), we also calculated the Mean Absolute Percent Difference (MAPD) per microwear variable between observers, which allows us to estimate whether some variables are more error-prone relative to others.

Both observers independently acquired data from the same images using a blind experimental design, so the discovery of similar microwear patterns means that the two observers consistently found the same type of data. This in turn suggests that additional individuals should be able to reproduce these results. Therefore, we analyze both observer datasets in the same statistical manner to provide the most error-free, objective conclusions possible using this analytical technique. Descriptive statistics were computed for both observer datasets for each variable in each dietary group. We used non-parametric Mann–Whitney U tests to determine if significant interspecific differences exist in each observer's dataset.

Finally, two canonical discriminant function analyses (DFA) were conducted (one per observer) to determine which microwear variables are statistically correlated with diet among extinct ground sloths. All four variables were included in the analysis, with taxon as the grouping variable. A Wilks' Lambda test was the metric of significance for resulting functions. All statistical tests in this study were conducted in a PC environment using SPSS (Statistical Package for Social Sciences, Inc.) version 19.0.

Results

Taphonomic alteration

Of the 23 specimens examined for this study, six (FMNH P13133, FMNH P13145, FMNH P13507, FMNH P13593, FMNHP 14450 (the only specimen of *Scelidotherium*), and AMNH 99186) showed post-mortem obliteration of original microwear, as deseribed by King et al. (1999). One specimen of *M. wheatleyi* (AMNH 140855-C) had only one spot of observable microwear that was deemed genuine, so only one image was captured for this specimen, as opposed to two non-overlapping images for each of the remaining teeth. After taphonomic screening, *H. elongatus* and *O. grandae* were represented by only one specimen eaeh in our sample. Ante-mortem microwear is visible on these two remaining specimens, so we included them (along with unaltered specimens from *A. odontrigonus*, *M. wheatleyi*, and *T. segnis*) in our analysis of intra- and interobserver error to provide the most comprehensive results. However, one tooth per species does not provide enough statistically useful information to reconstruet paleodiet, as there is no measure of populational variation in microwear. Thus, *H. elongatus* and *O. grandae* were not included in our statistical analysis of interspecific microwear patterns; only data from unaltered *A. odontrigonus, M. wheatleyi*, and *T. segnis* specimens were statistically analyzed for interspecific microwear differences.

Observer error

Wilcoxon signed-rank tests for intraobserver error revealed very little difference among variables between replicate images for either observer; only R varied significantly for observer 2

Table 1. Results from Wilcoxon signed-rank tests for significant differences in variables both between and among independent observers. Significant p-values are in bold. Variable abbreviations follow the text. Key: Z, z value.

	Observer 1		Observer 2	
Microwear variable	Z	p	Z	p
Intraobserver Differences				
FW	−0.26	0.80	−0.92	0.36
R	−0.46	0.65	−2.09	**0.04**
P	−1.72	0.09	−0.56	0.57
S	−0.26	0.80	−1.26	0.21
Interobserver Differences (Observer 1 vs. Observer 2)				
FW	−0.73	0.46		
R	−1.56	0.11		
P	−3.42	**<0.01**		
S	−3.01	**<0.01**		

(Table 1). However, two out of four variables (S, P) varied significantly between observers (Table 1). PCCs for each variable revealed a high degree of correlation between observer datasets though, with three of the variables (S, FW, R) being significant below the 0.01 level (Table 2). Mean P had the highest MAPD (42%; Table 3), while mean R had the lowest (3%; Table 3).

Microwear statistics

A total of 25 images from *M. wheatleyi*, *T. segnis*, and *A. odontrigonus* were analyzed for interspecific differences in microwear using descriptive, ANOVA/Welch and DFA statistical tests to address the hypothesis that there are significant differences between taxa that can be used to differentiate feeding ecology. For both observers, *T. segnis* had the highest scratch count and lowest feature width, whereas *M. wheatleyi* had the lowest number of scratches and greatest feature width (Table 4; Figures 2–3). For both of these variables, *A. odontrigonus* had intermediate values, relative to the other species (Table 4; Figures 2–3).

Mann–Whitney U tests revealed mean S and FW as statistically different between *M. wheatleyi* and *T. segnis* (Table 5). However, neither mean S nor mean FW could statistically distinguish *A. odontrigonus* from the other two analyzed taxa (Table 5). Observer 2 found that R and P were significant in distinguishing *A. odontrigonus* from *M. wheatleyi*, but observer 1 did not corroborate this result (Table 5).

To discriminate further between these three ground sloths, two canonical functions were formed by SPSS for each observer's DFA. Function 1 explains the majority of the variance and is statistically significant for both observers, whereas function 2 is never significant (Table 6). Mean S has the highest correlation with function 1 for both observers, with mean FW also correlated with function 1 only in observer 2 (Table 7). Both observers recorded a total percent correct classification of 93.30% for all specimens analyzed (Table 8).

Table 2. Pearson Correlation Coefficients (PCC) for data sets between Observers 1 and 2, organized by microwear variable. Significant p-values are in bold. Variable abbreviations follow the text.

Microwear variable	PCC	p
FW	0.76	**<0.01**
R	0.79	**<0.01**
P	0.40	0.11
S	0.77	**<0.01**

Table 3. Mean Absolute Percentage Differences (MAPD) for all variables between observers. Variable abbreviations follow the text.

Microwear variable	Observer 1	Observer 2	Combined mean	MAPD
S	20.76	30.35	14.78	18.76%
P	2.85	6.97	4.91	41.96%
FW	2.43	2.26	2.35	3.40%
R	0.72	0.68	0.70	2.85%

Discussion

Observer error

With the exception of R for observer 2, both observers were able to consistently recognize and identify the same microwear variables on replicate images (Table 1). However, because R was not unanimously significant in diagnosing interspecific microwear in ground sloths (discussed further below; Table 5), significant observer variation in this variable does not hinder our overall analysis. Between observers, both mean S and P varied significantly (Table 1); such interobserver error is not uncommon, as similar error levels were present in the previous analysis of microwear in extant xenarthrans (Green and Resar, 2012) and have been also recorded in enamel microwear studies (e.g., Grine et al., 2002; Purnell et al., 2006; Mihlbachler et al., 2012). While S and P varied significantly between observers, it follows reason that FW and R would not vary as much. The expected average of a random sample from a population should be approximately the same as the mean of the entire population, regardless of sample size. Given that S and P are counts, they would differ significantly based on the number of features identified. However, FW and R, being averages calculated from a sample of features identified in the image, are approximate to the true mean for the entire image, even though the feature counts may differ between observers. FW and R should be similar between both observers because they are looking at the same image.

MAPD for our variables are relatively comparable with those reported in Green and Resar (2012), with the error being highest in P and S and lowest among FW and R (Table 3). However, absolute values for MAPDs in our study (with the exception of R) are higher than that of extant xenarthrans (Table 3). This increased relative error between observers may be inflated by the sheer density of microwear features in taxa such as *Thinobadistes* (Figure 3C), where number of fine-scale scratches is high, causing some inconsistency between observers.

However, even though interobserver variation is present, PCCs still revealed significant correlations for three variables (FW, S, R; Table 2). Thus, while absolute values may differ between observers, independent observers consistently identified similar relative patterns under blind conditions in our analysis. This finding, coupled with the presence of similar interobserver correlations in extant xenarthrans (Green and Resar, 2012), supports the application of high-magnification SEM microwear analysis for reconstrueting paleoecology in ground sloths.

Variable significance

To avoid subjectivity in microwear studies, reproducibility in observer data should be assessed before interpretation and, ideally, only repeated results between multiple, independent observers should be accepted. Following these criteria, we can

Table 4. Mean values of microwear variables recorded by two independent observers for five extant xenarthran species (grouped by dietary category, labeled in bold in the specimen column). Variable abbreviations follow the text. Key: AMNH, American Museum of Natural History; FMNH, Field Museum of Natural History.

	Observer 1				Observer 2			
Specimen	FW	R	P	S	FW	R	P	S
A. odoutrigonus								
AMNH 17722	1.31	0.82	1.50	19.00	1.23	0.75	8.50	27.50
AMNH 94713	2.72	0.58	3.50	25.50	2.03	0.51	13.00	40.50
AMNH 17715	3.36	0.43	4.50	12.00	3.26	0.47	11.00	18.50
Group Average (SD)	**2.46 (1.05)**	**0.61 (0.20)**	**3.17 (1.53)**	**18.83 (6.75)**	**2.17 (1.02)**	**0.58 (0.15)**	**10.83 (2.25)**	**28.83 (11.06)**
H. elongatus								
FMNH P13122	1.56	0.84	2.00	46.00	2.17	0.57	4.00	30.00
M. wheatleyi								
AMNH 140854	3.01	0.95	1.50	14.00	2.10	0.79	5.50	23.00
AMNH 140855-A	3.18	0.84	2.00	8.50	1.92	0.72	2.00	16.00
AMNH 140855-B	3.29	0.81	6.00	9.00	3.63	0.93	7.00	10.50
AMNH 140855-C	2.97	0.85	0.50	11.50	2.13	0.76	5.00	36.00
AMNH 140855-D	2.40	0.97	1.50	14.00	3.02	0.96	7.00	16.00
AMNH 99186	5.24	0.60	4.50	5.00	3.70	0.93	7.00	11.00
Group Average (SD)	**3.35 (0.98)**	**0.84 (0.13)**	**2.67 (2.11)**	**10.33 (3.52)**	**2.75 (0.81)**	**0.85 (0.10)**	**5.58 (1.96)**	**18.75 (9.58)**
O. graudae								
FMNH P13583	2.42	0.64	2.50	11.00	2.86	0.40	7.50	15.00
T. segnis								
AMNH FAM 102658	1.69	0.60	4.00	28.50	1.45	0.64	10.00	57.00
AMNH FAM 102672	1.45	0.37	1.00	36.50	1.59	0.17	13.50	46.50
FMNH 28354	1.67	0.85	2.00	30.00	1.42	0.83	4.00	47.50
FMNH 34347	1.64	0.93	10.50	47.50	1.90	0.91	9.50	57.50
FMNH 34348	1.60	0.82	1.00	18.00	1.57	0.77	3.00	36.00
Group Average (SD)	**1.67 (0.17)**	**0.65 (0.25)**	**3.08 (3.88)**	**29.58 (11.51)**	**1.73 (0.38)**	**0.62 (0.29)**	**6.83 (4.87)**	**45.33 (11.79)**

be reasonably certain that our interpretations of paleodiet from microwear are as unbiased as possible (e.g., Mihbachler et al., 2012). In our study, although there is a high degree of correlation between observer datasets, there were some mixed results from statistical tests between observers.

Both observers found that variables S and FW revealed the same significant distinction among sampled ground sloths using Mann–Whitney U tests (Tables 5–8). In contrast, when DFA results are considered, the only variable that was shared between observers for function 1 (the only significant function in both analyses; Table 6) was FW. Variable S, in addition to FW, was important to function 1 only for observer 2 (Table 7).

We conclude that both variables FW and S have the highest significance in reconstructing paleoecology from microwear in extinct ground sloths. These two variables yielded significant results between observers, although the significance of each variable is, in some cases, dependent on the nature of the statistical test. Nevertheless, significant PCCs for S and FW suggest that both observers recorded the same relative patterns between species, which supports a genuine interspecific pattern. Although observer 2 found that R and P were significant between *A. odoutrigonus* and *M. wheatleyi*, observer 1 did not corroborate this result (Table 5); this discrepancy, coupled with the presence of significant intraobserver error in R for observer 1 (Table 1) calls into question the validity of this result. Thus, R and P likely have no significance in distinguishing ground sloth taxa in our study and we do not consider these variables further in this study.

Interpretation of feeding ecology

Of the examined taxa, *Megalonyx wheatleyi* was most similar to extant xenarthran folivores (*Bradypus*) and frugivore-folivores (*Choloepus*) through the presence of lower mean S and higher mean FW values relative to other sampled taxa (Table 5, Figure 2; Green and Resar, 2012). This result supports the hypothesis that *M. wheatleyi* was a forest browser. As a hypothesized browser, we predicted that *M. wheatleyi* should have less oral processing and hence a lower density of microwear features (Ungar et al. 2008). Since oral processing (or chewing) is correlated with the formation of microwear features, more chewing usually leads to more microwear features. Browsers, herbivores that are more selective about what plants they are eating and typically feed on softer leaves, have less need to chew and therefore are predicted to have fewer microwear features than grazers, who feed more indiscriminately and on tougher vegetation (Teaford, 1991; Ungar et al., 2008). We support this prediction, reporting lower feature density in *M. wheatleyi*, relative to other ground sloths (Figure 3), which results from a significantly lower number of scratches (Tables 4–6). Consuming a large quantity of tough branches or twigs may account for relatively wider scars in *M. wheatleyi* relative to *A. odoutrigonus* and *T. segnis*. The similarity of *M. wheatleyi* to both extant sloths suggests that it may have had a more varied diet than *Bradypus*, but less varied than that of *Choloepus*. In contrast to extant sloths, however, *Megalonyx* would have been feeding at a much lower level (i.e., ground-dwelling niche; Hoganson and McDonald, 2007), so a larger and/or different selection of available browse may be reflected by microwear. Overall, our results support previous hypotheses, drawn from independent lines of evidence (e.g., Hoganson and McDonald, 2007), that *M. wheatleyi* occupied a forest browsing niche during the Quaternary in Florida and likely in other parts of its North American distribution (e.g., Kohn et al., 2005).

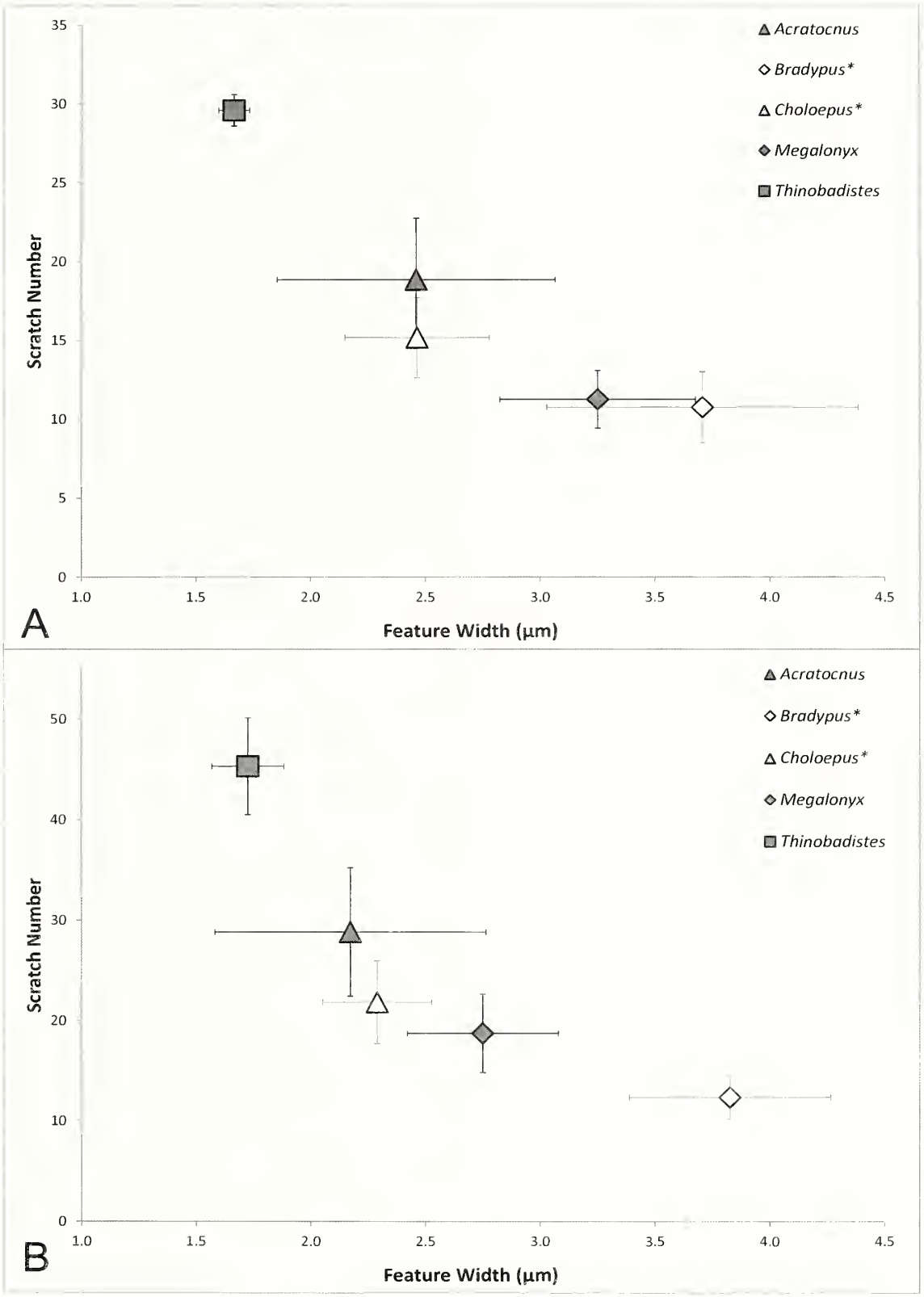

Figure 2. Graph of mean feature width (FW) vs. scratch number (S) for both observers; A, Observer 1; B, Observer 2. * denotes extant taxa (taken from Green and Resar, 2012).

Microwear in *Thinobadistes segnis* was anomalous in that we consistently observed thinner scratches in a much higher density on its teeth than any other sampled xenarthran to date, both extinct and extant (Table 4; Figures 2–3). Mylodontids are considered general grazers (Moore, 1978; McDonald and De Iuliis, 2008; Shockey and Anaya, 2011) or possibly mixed feeders (Naples, 1989), diets usually correlated with increased oral processing relative to browsers (Ungar et al., 2008). A relatively

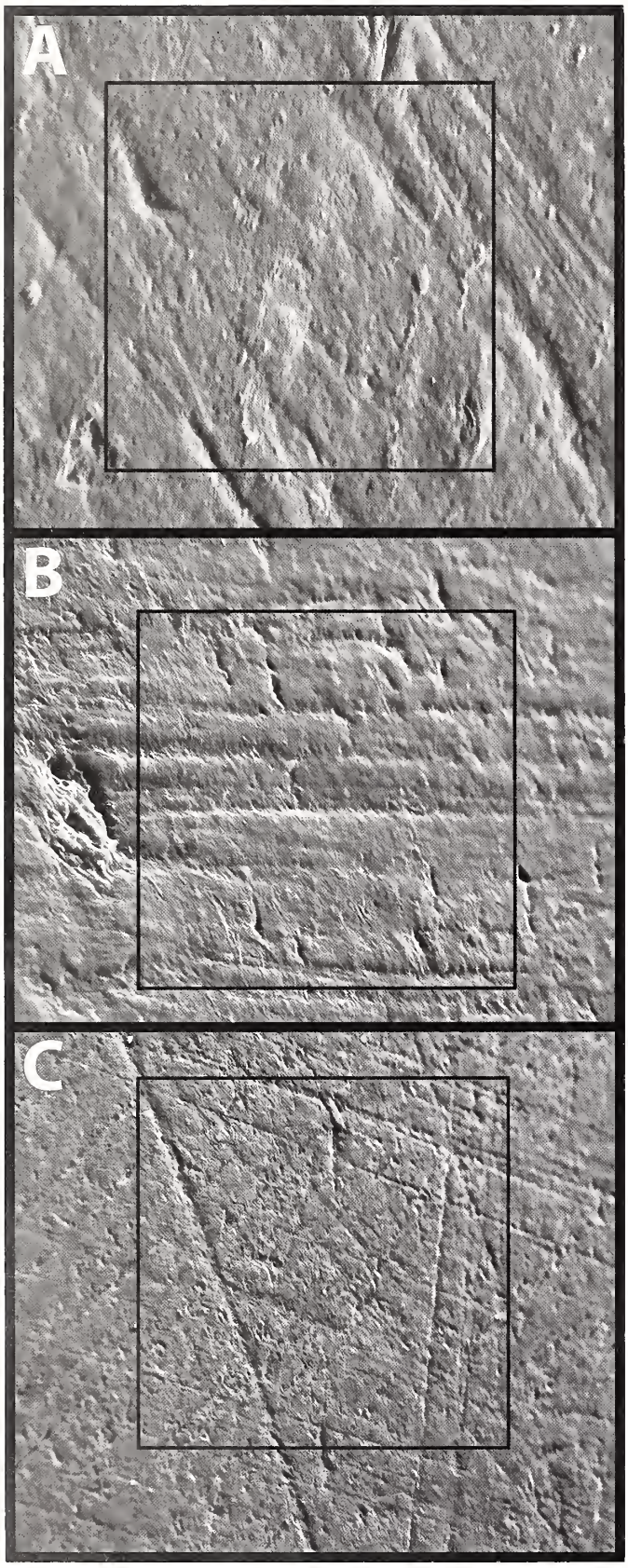

Figure 3. Examples of dental microwear on ground sloths M2s taken at 500×; black square represents the 100 μm×100 μm counting square; A, *Megalonyx wheatleyi* (AMNH 140855-A); B, *Acratocnus odontrigonus* (AMNH 17715); C, *Thinobadistes segnis* (AMNH FAM 102672).

Table 5. Mann–Whitney U tests for data from both observers. Significant p-values are in bold. Variable abbreviations follow the text. Key: Z, z value.

	Observer 1		Observer 2	
	Z	p	Z	p
Acratocnus* vs. *Megalonyx				
S	−1.82	0.07	−1.56	0.12
P	−0.40	0.70	−2.36	**0.02**
FW	−0.78	0.44	−1.03	0.30
R	−1.81	0.07	−2.07	**0.04**
Acratocnus* vs. *Thinobadistes				
S	−1.29	0.20	−1.69	0.09
P	−0.78	0.44	−1.03	0.30
FW	−0.78	0.44	−0.52	0.61
R	−0.39	0.70	−0.52	0.61
Megalonyx* vs. *Thinobadistes				
S	−2.89	**<0.01**	−2.65	**0.01**
P	−0.40	0.69	−0.32	0.75
FW	−2.88	**<0.01**	−2.40	**0.02**
R	−1.29	0.20	−1.60	0.11

high scratch density in *T. segnis* supports high amounts of oral processing (Ungar et al., 2008), which in turn suggests the possible inclusion of tough, abrasive vegetation, such as grass, in the regular diet of this taxon (Solounias et al. 1988). Therefore, it is possible that *T. segnis* occupied a mainly grazing niche in the Miocene savannas of Florida. However, we note that the correlation between high scratch density and grazing only exists in enamel-based microwear studies (Solounias et al., 1988; Teaford, 1991; Solounias and Semprebon, 2002); there are no extant grazers that have teeth composed solely of orthodentine, so it is difficult to fully test this hypothesis. As an alternate hypothesis, the high scratch density and relatively low FW could come from the consumption of high amounts of fine-scale grit, which accumulates near ground level in open habitats (Williams and Kay, 2001). The paleoenvironment of Mixson's bone bed is not as well understood as that of contemporary Miocene environments in Florida (e.g., Love Bone Bed; Hulbert, 2001), yet current evidence suggests an open, savanna-like environment (Leidy and Lucas, 1896; R.C. Hulbert, Jr., personal communication). This observation, coupled with smaller body size (about 450 kg; McDonald, 2005) that suggests low-level feeding habits (e.g., Webb, 1989), supports the inclusion of grit during feeding, and/or possibly a diet that consisted mainly of abrasive grasses and vegetation. *T. segnis* may very well have been a grazer in the Miocene grasslands, but supporting empirical evidence for grazing in this taxon is currently lacking.

Acratocnus odontrigonus most closely resembled extant frugivore-folivores (*Choloepus*) in terms of S and FW (Figure 2). The predicted lifestyle of *A. odontrigonus* is at least semi-arboreal, and may have been somewhat similar to the obligate arboreal role of living two-toed sloths (White, 1993). Among extant xenarthrans, microwear patterns are significantly different between ground-dwelling forms versus strictly arboreal taxa, thereby reflecting habitat occupancy as much as dietary differences (Green and Resar,

Table 6. Variance and significance of generated discriminant functions for each observer's DFA. Significant p-values are in bold. Key: %V, percent of total variance described by each function; df, degrees of freedom; p, p-value; WL, Wilks' Lambda value.

	Observer 1				Observer 2			
Function	%V	WL	df	p	%V	WL	df	p
1	97.30	0.14	8	**<0.01**	80.30	0.14	8	**<0.01**
2	2.70	0.88	3	0.71	19.70	0.58	3	0.12

Table 8. Probabilities from DFA classification matrix for each observer. Bold values indicate total percent correct classification per taxon.

Observer		Taxon	*A. odontrigonus*	*M. wheatleyi*	*T. segnis*
1	% Correct	*A. odontrigonus*	**100.00**	0.00	0.00
		M. wheatleyi	0.00	**100.00**	0.00
		T. segnis	16.70	0.00	**83.30**
2	% Correct	*A. odontrigonus*	**100.00**	0.00	0.00
		M. wheatleyi	0.00	**83.30**	16.70
		T. segnis	0.00	0.00	**100.00**

2012). Our results support the view of *A. odontrigonus* occupying at least a semi-arboreal habitat in the Quaternary of Puerto Rico. However, we exercise caution in assuming that *Choloepus* and *A. odontrigonus* had similar diets, because the West Indies during the Quaternary were much drier than the tropical regions where *Choloepus* resides today (Pregill and Olson 1981). It is possible that *A. odontrigonus* was herbivorous and engaged in a browsing folivorous habit akin to that of *Choloepus* due to their close phylogenetic affinity (White et al., 2001; Gaudin, 2004), and the differences perhaps reflect different amounts of grit or abrasive particles within the opposing plant matter constituting the two diets. *Neocnus*, another Caribbean meglonychid with close affinities to *Acratocnus* and *Choloepus* (White and MacPhee, 2001; Gaudin, 2004), has also been suggested as an arboreal folivore but with a feeding strategy more similar to that of *Bradypus* (McAfee, 2011), further highlighting the potential differences for dietary strategies and the need for independent lines of evidence.

Of the three taxa statistically analyzed (*M. wheatleyi*, *T. segnis*, and *A. odontrigonus*), only *M. wheatleyi* and *T. segnis* were statistically differentiable (in terms of S and FW; Table 5). This leaves *A. odontrigonus* as indistinguishable from the other two taxa (Table 5). There are two probable explanations for this occurrence. First, *A. odontrigonus* has values for S and FW in between *T. segnis* and *M. wheatleyi* (Figure 2) and thus has less of an absolute difference between its mean values and those of *T. segnis* and *M. wheatleyi*. Second, *A. odontrigonus* was represented by fewer specimens than either *T. segnis* or *M. wheatleyi* in our study (Table 4), which may obscure statistical significance.

In addition, S vs. FW plots between observers reveal a repeated trend, in that microwear patterns among xenarthrans (both living and extinct) appears to exist on a continuum (Figure 2). *Bradypus* represents one extreme of this spectrum, whereas *T. segnis* represents the other extreme, with *Acractocnus*, *Choloepus*, and *Megalonyx* occupying the middle range (Figure 2). The diet of living *Bradypus* and *Choloepus* is selectively folivorous in the former and more generalized browsing in the latter. It is possible these graphs represent a browser-grazer continuum of herbivorous feeding strategies in xenarthrans, with selective browsers (*Bradypus*) representing the lower right extreme and grazers occupying the upper left extreme. In this scenario, *T. segnis* would be a grazer, whereas *Choloepus* and *Acractocnus* (existing near the middle of the continuum) might be interpreted as more generalist browsers. *Megalonyx* always occupies the space between *Choloepus* and *Bradypus*, suggesting (under this scenario) that it was a more specialized browser than *Choloepus*, but less so than *Bradypus*. This last interpretation mirrors paleoecological reconstructions of *Megalonyx* from independent lines of evidence (e.g., Kohn et al., 2005; Hoganson and McDonald, 2007). It is also interesting to note that Figure 2 also separates the sloths into phylogenetic groupings with the megalonychids (*Acratocnus*, *Choleopus*, and *Megaloynx*) all occupying the middle range while the extremes are held by a mylodontids (*Thinobadistes*) and a bradypodid (*Bradypus*), which could indicate that portions of the feeding spectrum have their roots in phylogenetic relationships. These hypotheses remain to be tested by future microwear studies and increased analysis of paleodiet in sloths by applying this technique to a wider variety of taxa.

Table 7. Discriminant function structure matrix. Values marked with an asterisk (*) reveal the largest absolute correlation between that variable and the corresponding discriminant function. Variable abbreviations follow the text.

	Observer 1		Observer 2	
Function	1	2	1	2
FW	0.47*	−0.40	0.70*	−0.32
S	−0.50	0.66*	−0.38*	0.32
R	0.22	0.59*	−0.14	−0.72*
P	−0.34	−0.86*	−0.24	0.59*

Conclusions

To our knowledge, this is the first time that microwear patterns of multiple extinct ground sloths have been analyzed and statistically compared to data from living xenarthrans to better understand the paleoecology of this group. Our results support high-magnification orthodentine microwear analysis as a valid method of examining diet in xenarthrans, given a large enough sample size. The previously hypothesized lifestyle of *M. wheatleyi* as a forest browser (McDonald 1995; Hoganson and McDonald, 2007) is supported by a low number of scratches and wide scars, a pattern that is quantitatively identical to microwear in living folivorous three-toed sloths. Additionally, we suggest that a high number of scratches and lower scar width in *T. segnis* suggests high levels of grit in the diet, either from dust accumulating on ground level vegetation or from abrasive grasses, or possibly a mixture of these two suggestions. Our study focused on a limited number of available specimens from a narrow selection of taxa, which limits the overall conclusions that we can reasonably draw from our data. What is relevant at this time is that we must note that our respective ground sloths represent taxa from different ages, climates, and habitats (e.g., Pleistocene forests, tropical and temperate, versus Miocene savannas). Therefore, the drastic differences in microwear noted between *M. wheatleyi* and *T. segnis* may stem from intangible variation in environmental conditions, rather than strictly from diet. However, because orthodentine microwear reveals distinct feeding differences in living xenarthrans that occupy different environments (e.g., semi-fossorial armadillos versus arboreal

sloths; Green and Resar, 2012), we suggest that the differences we report here are reflective of differences in feeding ecology.

This initial work reveals that paleoecological signals should be recorded in fossil ground sloth teeth, provided post-mortem alteration has been taken into account. Future studies should look at a wider range of taxa that have more specimens available, including fossil cingulate taxa. We also suggest that future microwear studies in extinct xenarthrans examine different taxa that co-occur at the same locality, such as Rancho La Brea, rather than from chronologically different localities. Analysis of stable isotopes in xenarthran teeth may yield comparative information regarding paleodiet. Xenarthran orthodentine may be less prone to diagenetic alteration that originally assumed (MacFadden et al., 2010). However, there remain complications that need to be resolved before the geochemical signal of orthodentine can be objectively interpreted (MacFadden et al., 2010). More broadly, further investigation should be made into taxa that have been investigated with morphological methods, particularly the South American sloths (e.g., *Megatherium*, *Glossotherium*, *Mylodon*, *Hapalops, and Scelidotherium*), for which there is a large body of work (e.g., Bargo et al., 2006a, b; Vizcaíno et al., 2006). This would allow microwear analysis to be correlated against these already established methods, and would further our understanding of the usefulness of dental microwear as a tool for reconstructing feeding ecology in extinct xenarthrans.

Acknowledgements

We thank the collections staff and curators at the American Museum of Natural History (Alana Gishlick, Carl Mehling, Jin Meng, Ruth O'Leary) and the Field Museum of Natural History (K. Angielczyk, William Simpson) for permitting sampling of fossil teeth for our study. David Waugh and Merida Keatts provided technical assistance; Richard Hulbert, Jr. provided background information on Florida fossil localities; Carrie Schweitzer and Rodney Feldman allowed access to lab facilities for casting and SEM preparation; Kathryn Green helped create the blind analysis. We thank Gregory McDonald, Matthew Mihlbachler, and one anonymous reviewer for providing helpful comments on this paper. We also thank Peter Ungar for providing access to the Microware 4.02 software. The University Research Council and the Research Scholars Undergraduate Program at Kent State University provided partial funding for this project.

References

Ameghino, F. 1894. Sur les oiseaux fossiles de Patagonie; et la faune mammalogique des couches à *Pyrotherium*. Boletin del Instituto Geographico Argentino, 15:501–660.

Anthony, H. E. 1916. Preliminary report on fossil mammals from Porto Rico, with descriptions of a new genus of ground sloth and two new genera of hystricomorph. Annals of the New York Academy of Sciences, 27:193–203.

Anthony, H. E. 1926. Mammals of Porto Rico, living and extinct – Rodentia and Edentata. Scientific Survey of Porto Rico and the Virgin Islands, Publication of the New York Academy of Sciences, 9:97–241.

Bargo, M. S., G. De Iuliis, and S. F. Vizcaíno. 2006a. Hypsodonty in Pleistocene ground sloths. Acta Palaeontologica Polonica, 51:53–61.

Bargo, M. S., N. Toledo, and S. F. Vizcaíno. 2006b. Muzzle of South American Pleistocene ground sloths (Xenarthra, Tardigrada). Journal of Morphology, 267:248–263.

Chiarello, A. G. 2008. Sloth ecology: an overview of field studies, p. 269–280., *In* S. F. Vizcaíno and W. J. Loughry (eds.), The Biology of the Xenarthra. University Press of Florida, Gainesville.

Cope, E. D. 1871. Preliminary report on the vertebrata discovered in the Port Kennedy Bone Cave. American Philosophical Society, 12:73–102.

Delsuc, F., M. Scally, O. Madsen, M. J. Stanhope, W. W. de Jong, F. M. Catzeflis, M. S. Springer, and E. J. P. Douzery. 2002. Molecular phylogeny of living xenarthrans and the impact of character and taxon sampling on the placental tree rooting. Molecular Biology and Evolution, 19:1656–1671.

Fariña, R. A., S. F. Vizcaíno, and M. S. Bargo. 1998. Body mass estimations in Lujanian (late Pleistocene-early Holocene of South America) mammal megafauna. Mastozoología Neotropical, 5:87–108.

Gaudin, T. J. 2004. Phylogenetic relationships among sloths (Mammalia, Xenarthra, Tardigrada): the craniodental evidence. Zoological Journal of the Linnean Society, 140:255–305.

Gaudin, T. J., and H. G. McDonald. 2008. Morphology-based investigations of the phylogenetic relationships among extant and fossil xenarthrans, p. 24–36., *In* S. F. Vizcaíno and W. J. Loughry (eds.), The Biology of the Xenarthra. University Press of Florida, Gainesville.

Green, J. L. 2009a. Enamel-reduction and orthodentine in Dicynodontia (Therapsida) and Xenarthra (Mammalia): an evaluation of the potential ecological signal revealed by dental microwear. Ph.D. dissertation, North Carolina State University, Raleigh.

Green, J. L. 2009b. Dental microwear in the orthodentine of the Xenarthra (Mammalia) and its use in reconstructing the paleodiet of extinct taxa: the case study of *Nothrotheriops shastensis* (Xenarthra, Tardigrada, Nothrotheriidae). Zoological Journal of the Linnean Society, 156:201–222.

Green, J. L. 2009c. Intertooth variation of orthodentine microwear in armadillos (Cingulata) and tree sloths (Pilosa). Journal of Mammalogy, 90:768–778.

Green, J. L., and N. A. Resar. 2012. The link between dental microwear and feeding ecology in tree sloths and armadillos. Biological Journal of the Linnean Society, 107:277–294.

Green, J. L., G. M. Semprebon, and N. Solounias. 2005. Reconstructing the palaeodiet of Florida *Mammut americanum* via low-magnification stereomicroscopy. Palaeogeography, Palaeoclimatology, Palaeoecology, 222:34–48.

Grine, F. E., P. S. Ungar, and M. F. Teaford. 2002. Error rates in dental microwear quantification using scanning electron microscopy. Scanning, 24:144–153.

Hay, O. P. 1919. Descriptions of some mammalian and fish remains from Florida of probably Pleistocene age. Proceedings of the United States National Museum, 56:103–112.

Hillson, S. 2005. Teeth, 2nd ed. Cambridge University Press, Cambridge, United Kingdom 388p.

Hoffstetter, R. 1956. Contribution a l'étude des Orophodontoidea, gravigrades cuirasses de la Patagonie. Annales de Paléontologie, 42:27–64.

Hoganson, J. W., and H. G. McDonald. 2007. First Report of Jefferson's ground sloth (*Megalonyx jeffersonii*) in North Dakota: paleobiographical and paleoecological significance. Journal of Mammalogy, 88:73–80.

Hulbert, R. C. 2001. The Fossil Vertebrates of Florida. University Press of Florida, Gainesville.

Kalthoff, D. C. 2011. Microstructure of dental hard tissues in fossil and recent xenarthrans (Mammalia: Folivora and Cingulata). Journal of Morphology, 272:641–661.

King, T., P. Andrews, and B. Boz. 1999. Effect of taphonomic processes on dental microwear. American Journal of Physical Anthropology, 108:359–373.

Kohn, M. J., M. P. McKay, and J. L. Knight. 2005. Dining in the Pleistocene - Who's on the menu? Geology, 33:649–652.

Leidy, J., and F. A. Lucas. 1896. Fossil vertebrates from the Alachua Clays of Florida. Wagner Free Institute of Science, Philadelphia. 61 p.

Linnaeus, C. 1758. Tomus I. Systema naturae per regna tria naturae, secundum classes, ordines, genera, species, cum characteribus, differentiis, synonymis, locis. 10th edition, reformated. Laurentii Salvii, Holmiae. 824 p.

MacFadden, B. J., L. R. G. DeSantis, J. L. Hochstein, and G. D. Kamenov. 2010. Physical properties, geochemistry, and diagenesis of xenarthran teeth: prospects for interpreting the paleoecology of extinct species. Palaeogeography, Palaeoclimatology, Palaeoecology, 291:180–189.

MacPhee, R. D. E., and M. A. Reguero. 2010. Reinterpretation of a Middle Eocene Record of Tardigrada (Pilosa, Xenarthra, Mammalia) from La Meseta Formation, Seymour Island, West Antarctica. American Museum Novitates, 3689:1–21.

McAfee, R. K. 2011. Feeding mechanics and dietary implications in the fossil sloth *Neocnus* (Mammalia: Xenarthra: Megalonychidae) from Haiti. Journal of Morphology, 272:1204–1216.

McDonald, H. G. 1977. Description of the osteology of the extinct gravigrade edentate, *Megalonyx*, with observations on its ontogeny, phylogeny and functional anatomy. M.S. thesis, Department of Zoology, University of Florida, Gainesville.

McDonald, H. G. 1987. A systematic review of the Plio-Pleistocene scelidotherine ground sloths (Mammalia: Xenarthra: Mylodontidae). Ph.D. dissertation, University of Toronto, Toronto.

McDonald, H. G. 1995. Gravigrade Xenarthrans from the early Pleistocene Leisey Shell Pit 1A, Hillsborough County, Florida. Bulletin of the Florida Museum of Natural History, 37: 345–373.

McDonald, H. G. 2005. Paleoecology of extinct xenarthrans and the great American biotic interchange. Bulletin of the Florida Museum of Natural History, 45:313–333.

McDonald, H. G., and G. De Iuliis. 2008. Fossil history of sloths, p. 39–55., *In* S. F. Vizcaíno and W. J. Loughry (eds.), The Biology of the Xenarthra. University Press of Florida, Gainesville.

McDonough, C. M., and W. J. Loughry. 2008. Behavioral ecology of armadillos, p. 281–293, *In* S. F. Vizcaíno and W. J. Loughry (eds.), The Biology of the Xenarthra. University Press of Florida, Gainesville.

McKenna, M. C., and S. K. Bell. 1997. Classification of mammals above the species level. Columbia University Press, New York.

Mihlbachler, M. C., B. L. Beatty, A. Caldera-Siu, D. Chan, and R. Lee. 2012. Error rates and observer bias in dental microwear analysis using light microscopy. Palaeontologia Electronica, 15.1.12A:1–22.

Morgan, G. S. 2005. The Great American Biotic Interchange in Florida. Bulletin of the Florida Museum of Natural History, 45:271–311.

Moore, D. M. 1978. Post-glacial vegetation in the south Patagonian territory of the giant ground sloth, *Mylodon*. Botanical Journal of the Linnaean Society, 77:177–202.

Muizon, C. de., H. G. McDonald, R. Salas, and M. Urbina. 2004. The evolution of feeding adaptations of the aquatic sloth *Thalassocnus*. Journal of Vertebrate Paleontology, 24:398–410.

Naples, V. L. 1982. Cranial osteology and function in the tree sloths, *Bradypus* and *Choloepus*. American Museum Novitates, 2739:1–41.

Naples, V. L. 1989. The feeding mechanism in the Pleistocene ground sloth, *Glossotherium*. Contributions in Science, Natural History Museum of Los Angeles County, 415:1–23.

Oliveira, E. V. 2001. Micro-desgaste dentario em alguns Dasypodidae (Mammalia, Xenarthra) [Dental microwear in some Dasypodidae]. Acta Biologica Leopoldensia, 23:83–91.

Peters, W. 1858. Hr. Peters theilte der Akademie. Monatsberichte der Königlichen Preuss. Akademie der Wissenschaften zu Berlin, 1858:128 p.

Pregill, G. K., and S. L. Olson. 1981. Zoogeography of West Indian vertebrates in relation to Pleistocene climate cycles. Annual Review of Ecology and Systematics, 12:75–98.

Purnell, M. A., P. J. B. Hart, D. C. Baines, and M. A. Bell. 2006. Quantitative analysis of dental microwear in threespine stickleback: a new approach to analysis of trophic ecology in aquatic vertebrates. Journal of Animal Ecology, 75:967–977.

Scott, W. B. 1904. Mammalia of the Santa Cruz beds, Volume 5, p. 1–364., *In* W. B. Scott (ed.), Reports of the Princeton University Expedition to Patagonia, 1896–1899. Princeton University, E. Schweizerbart'sche Verlagshandlung (E. Nägele), Stuttgart.

Shockey, B. J., and F. Anaya. 2011. Grazing in a new Late Oligocene mylodontid sloth and a mylodontid radiation as a component of the Eocene-Oligocene faunal turnover and the early spread of the grasslands/savannas in South America. Journal of Mammalian Evolution, 18:101–115.

Smith, K. K., and K. H. Redford. 1990. The anatomy and function of the feeding apparatus in two armadillos (Dasypoda): anatomy is not destiny. Journal of Zoology, 222:27–47.

Solounias, N., and G. Semprebon. 2002. Advances in the reconstruction of ungulate ecomorphology with application to early fossil equids. American Museum Novitates, 3366:1–49.

Solounias, N., M. Teaford, and A. Walker. 1988. Interpreting the diet of extinct ruminants: The case of a non-browsing giraffid. Paleobiology, 14:287–300.

Teaford, M. F. 1988. Scanning electron microscope diagnosis of wear patterns versus artifacts on fossil teeth. Scanning Microscopy, 2:1167–1175.

Teaford, M. F. 1991. Dental microwear: what can it tell us about diet and dental function, p. 341–356., In M. A. Kelley and C. S. Larsen (eds.), Advances in Dental Anthropology, Wiley-Liss Inc, New York.

Ungar, P. S. 2002. Microware software. Version 4.02. A semi-automated image analysis system for the quantification of dental microwear. Unpublished: Fayetteville, Arkansas.

Ungar, P. S. 2010. Mammal Teeth: Origin, Evolution, and Diversity. The Johns Hopkins University Press, Baltimore, Maryland.

Ungar, P. S., R. S. Scott, J. R. Scott, and M. Teaford. 2008. Dental microwear analysis: historical perspectives and new approaches, p. 389–425., *In* J. D. Irish and G. C. Nelson (eds.), Technique and Application in Dental Anthropology. Cambridge University Press, Cambridge.

Vizcaíno, S. F. 2009. The teeth of the "toothless": novelties and key innovations in the evolution of Xenarthrans (Mammalia, Xenarthra). Paleobiology, 35:343–366.

Vizcaíno, S. F., and G. J. Scillato-Yane. 1995. An Eocene tardigrade (Mammalia, Xenarthra) from Seymour Island, West Antarctica. Antarctic Science, 7:407–408.

Vizcaíno, S. F., and W. J. Loughry. 2008. The Biology of the Xenarthra. University Press of Florida, Gainesville.

Vizcaíno, S. F., M. S. Bargo, and G. S. Cassini. 2006. Dental occlusal surface area in relation to body mass, food habits and other biological features in fossil xenarthrans. Ameghiniana, 43:11–26.

Vizcaíno, S. F., M. S. Bargo, and R. A. Fariña. 2008. Form, function, and paleobiology in xenarthrans, p. 86–99., *In* S. F. Vizcaíno and W. J. Loughry (eds.), The biology of the Xenarthra. The University Press of Florida, Gainesville.

Webb, S. D. 1977. A history of savanna vertebrates in the New World. Part I: North America. Annual Review of Ecology and Systematics, 8:355–380.

Webb, S. D. 1989. Osteology and relationship of *Thinobadistes segnis*, the first mylodont sloth in North America, p. 496–532., *In* K. H. Redford and J. F. Eisenberg (eds.), Advances in Neotropical Mammalogy. Sandhill Crane Press, Gainesville.

Webb, S. D., B. J. MacFadden, and J. A. Baskin. 1981. Geology and paleontology of the Love Bone Bed from the late Miocene of Florida. American Journal of Science, 281:513–544.

White, J. L. 1993. Indicators of locomotor habits in Xenarthrans: evidence for locomotor heterogeneity among fossil sloths. Journal of Vertebrate Paleontology, 13:230–242.

White, J. L., and R. D. MacPhee. 2001. The sloths of the West Indies: a systematic and phylogenetic review, p. 201–235., *In* C. A. Woods and F. E. Sergile (eds.), Biogeography of the West Indies: Patterns and Perspectives. CRC Press, New York.

Williams, S. H., and R. F. Kay. 2001. A comparative test of adaptive explanations for hypsodonty in ungulates and rodents. Journal of Mammalian Evolution, 8:207–229.

Appendix 1. Listing of all specimens sampled in this study, organized by species (with taxonomic authority). Institutional Abbreviations: AMNH = American Museum of Natural History, New York; FMNH = Field Museum of Natural History, Chicago.

Species	Specimen number	Locality
Acratocnus odontrigonus	AMNH 17715	Puerto Rico
(Anthony, 1916)	AMNH 17722	Puerto Rico
	AMNH 94713	Puerto Rico
	AMNH 94714	Puerto Rico
Hapalops elongatus	FMNH P13122	Santa Cruz Fm., Santa Cruz, Argentina
Ameghino, 1894	FMNH P13133	Santa Cruz Fm., Santa Cruz, Argentina
	FMNH P13145	Santa Cruz Fm., Santa Cruz, Argentina
Megalonyx wheatleyi	AMNH 140854	Smith Pit, Levy Co., Florida
(Cope, 1871)	AMNH 140855	Smith Pit, Levy Co., Florida
	AMNH 140855 A	Smith Pit, Levy Co., Florida
	AMNH 140855 C	Smith Pit, Levy Co., Florida
	AMNH 140855 D	Smith Pit, Levy Co., Florida
	AMNH 99186	Smith Pit, Levy Co., Florida
Octodontotherium grandae	FMNH 13512	Santa Cruz Fm., Argentina
Ameghino, 1894	FMNH P13507	Santa Cruz Fm., Argentina
	FMNH P13583	Santa Cruz Fm., Argentina
Scelidotherium sp.	FMNH P14450	Aravcano Fm., Corral Quemado, Argentina
Thinobadistes segnis	AMNH FAM 102658	Mixson's Bone Bed, Levy Co., Florida
(Hay, 1919)	AMNH FAM 102659	Mixson's Bone Bed, Levy Co., Florida
	AMNH FAM 102672	Mixson's Bone Bed, Levy Co., Florida
	AMNH FAM 102679	Mixson's Bone Bed, Levy Co., Florida
	AMNH FAM 102681	Mixson's Bone Bed, Levy Co., Florida
	AMNH FAM 102698	Mixson's Bone Bed, Levy Co., Florida

KIRTLANDIA

Kirtlandia: The Scientific Publication of The Cleveland Museum of Natural History
Michael J. Ryan, Editor

Instructions For Authors

Authors are invited to submit manuscripts on topics that fall within the sphere of natural history. Specimen-based research, especially that based on Cleveland Museum of Natural History specimens, is most welcome.

All manuscripts and correspondence regarding manuscripts should be directed to Michael J. Ryan, editor of *Kirtlandia*, at: mryan@cmnh.org; surface mail: Cleveland Museum of Natural History, 1 Wade Oval Drive, Cleveland, Ohio 44106-1796, USA.

Submission of manuscripts:

We encourage you to contact the editor regarding your submission to discuss the appropriateness of your manuscript for the journal and the availability of space in upcoming volumes. Once the editor has agreed to review your manuscript for submission you will be assigned a specific FTP folder that will be used for all files submissions (text, images, tables, etc.) and subsequent editorial changes.

ALL MANUSCRIPTS, INCLUDING ALL TEXT AND FIGURES, MUST BE FORMATTED FOR PUBLICATION FOR KIRTLANDIA FOLLOWING THE INSTRUCTIONS BELOW. MANUSCRIPTS THAT FAIL TO FOLLOW THIS DIRECTIVE WILL NOT BE CONSIDERED FOR PUBLICATION.

Each submitted file will have a file name that includes the first author's last name and some modifier that will identify each file (e.g., RyanFig1.doc)

Text Files:

All text files will be submitted as WORD docs using the suffix (*.doc). Manuscripts will be formatted for a standard 8.5x11 inch page with 1 inch margins. Text will be double spaced, with only one space after each period. Use Times Roman font, 12pt. only.

Abstracts should be concise and convey the main points and conclusions of the paper. Main headings should be centered and bold.

Headings, as well as citations in text and in the references, should follow the style used in the most recent issue of the journal.

Citations should be cited in text as follows: Krebs (1994) or (Krebs, 1994); Krebs et al. (2002) or (Krebs et al., 2002); Teraguchi and Lublin (1999) or (Teraguchi and Lublin, 1999). If specific details from a book or article are cited, or if material is quoted or paraphrased, provide page citations as in these examples: (Miller, 1989, p. 261), or Teraguchi and Lublin (1995, p. 4–5). References should be cited in the text in chronological order, e.g.: Krebs, 1994; Teraguchi and Lublin, 1999; Krebs et al., 2002.

Figures:

Figures are to be black and white, and high quality 600 dpi grayscale images (photographs) and 600 dpi for bitmap lineart (maps, illustrations, etc), and submitted as TIF files only. Please do not submit Adobe Illustrator or Corel Draw files.

Submitted images must be formatted for publication size; either full page (2 column, 7.1/8 inches) or one-half page (one column, 3.5 inches) width only. Maximum page depth is 10 inches. Do not leave excess empty space in a figure.

All figures are to be numbered sequentially and referenced in the text (e.g., Figure 1, Figure 2, etc.). Subfigures are indicated alphabetically, and labeled as A, B, C, etc. Figure font is Arial. The final type size should not be smaller than 8 points.

Figure legends should be written following the style below (example refers to a two-part figure):

Figure 1. Tubercled blossom, *Epioblasma torulosa torulosa* (Rafinesque, 1820), currently extirpated from Ohio; A, shell exterior; B, shell interior. Scale bar equals 1 cm.

Italicize genus and species names, and give species authority and year of description when species are first mentioned in the text. If a long table or appendix of taxa is presented, authorities and years may be excluded from the text but must be reported in the table. For papers dealing with systematics, give the original reference describing the taxa presented.

Unless a large number of taxa are noted, list the works naming species in the references at the end of your manuscript.

Tables:

Tables will be submitted as separate (not part of the manuscript) Excel files or as tables built using the 'Tables' function in WORD. Long tables should be submitted as appendices. Tables should be concise and convey information not repeated in text.

Other Formatting Guidelines:

Other questions about formatting can be found in the guidelines for Allen Press available here: http://allenpress.com/resources/library

A PDF of the "Guide to Manuscript Submission" from Allen Press ean be downloaded from here: http://allenpress.com/system/files/pdfs/library/apmk_manuscript_sub.pdf

Page Charges and Reprints:

Kirtlandia does not change for publication in the journal. However, scientists with grants or other funding sources covering the research to be published in Kirtlandia are encouraged to contribute $100/page. Reprint charges will be determined by the editor, but each author will receive a PDF of their published paper at no cost.

References:

Follow the examples provided here:

Krebs, C. J. 1994. Ecology: The Experimental Analysis of Distribution and Abundance. Fourth Edition. Harper Collins, New York. 801 p.

Krebs, R. A., H. M. Griffith, and M. J. S. Tevesz. 2002. A study of the Unionidae of Tinkers Creek, Ohio. Kirtlandia, 53:9–25.

Miller, B. B. 1989. Screen-washing unconsolidated sediments for small macrofossils, p. 260–263. *In* R. M. Feldmann, R. E. Chapman, and J. T. Hannibal (eds.), Paleotechniques. Paleontological Society Special Publication, No. 4.

Teraguchi, S. E., and K. J. Lublin. 1999. Checklist of the moths of Pallister State Nature Preserve, Ashtabula County, Ohio (1988–1992) with analyses of abundance. Kirtlandia, 51:3–18.

Cleveland Museum of
NATURAL HISTORY